

Involvement of cytochromes P450 (CYP)
and other haem associated enzymes in
the bioreduction of AQ4N, an antitumour
prodrug.

S M. Raleigh

PhD.

1998

**Involvement of cytochromes P450 (CYP) and other haem associated
enzymes in the bio-reduction of AQ4N, an antitumour prodrug.**

Stuart Martin Raleigh BSc

A thesis submitted in partial fulfilment of the requirement for the degree of
Doctor of Philosophy at De Montfort University

July 1998

To Catherine and Hannah

Involvement of cytochromes P450 (CYP) and other haem associated enzymes in the bio-reduction of AQ4N, an antitumour prodrug.

Stuart M Raleigh

Abstract

The anthraquinone di-*N*-oxide AQ4N is a prodrug designed to be excluded from cell nuclei until metabolised in hypoxic tumour regions to AQ4, a DNA binder and potent inhibitor of topoisomerase II. The antitumour effects of AQ4N in rodent neoplasms are well characterised but the identity of enzymes responsible for the metabolism are unknown. The aims of the present work were to identify Cytochrome P450 (CYP) enzymes responsible for AQ4N metabolism in rat and human tissue and to conduct a preliminary investigation into the *in vivo* metabolism of AQ4N in tumour bearing rodents.

AQ4N was found to undergo a two electron reduction to the mono-*N*-oxide AQM followed by a subsequent two electron reduction to cytotoxic AQ4. The process occurred in the microsomes of rat and human liver, was cofactor dependent and was inhibited by air. In rats, CYPs 2B and 2E were found to anaerobically metabolise both AQ4N and AQM. Kinetically, AQ4N metabolism conformed to a Michaelis-Menten model whereas the metabolism of AQM was better described by a sigmoidal relationship. In addition, both semi purified Cytochrome P450 reductase (CPR) and purified Nitric oxide synthase (NOS) were both able to anaerobically metabolise AQ4N. Both enzymes required NADPH and CPR mediated metabolism was dependent on the presence of exogenous haem.

In humans, the anaerobic metabolism of both AQ4N and AQM correlated with CYP 3A activity and not with the activities of CYP 1A/ 2C and 2D. AQM metabolism correlated also with the activity of CYP 2A. The involvement of CYP 3A was confirmed by the use of CYP specific inhibitors and by the use of cDNA transfected cell microsomes. Human kidney and colonic tumours were found to anaerobically metabolise AQ4N and tumour metabolism was inhibited by the CYP inhibitor carbon monoxide (CO). Finally, the *in vivo* metabolism of AQ4N was studied in C3H tumour bearing mice. Metabolites of AQ4N were found in all tissues studied but the AQ4/ AQ4N ratio was highest in the tumours.

Collectively, these findings have identified the enzymes responsible for the metabolism of AQ4N and its mono-*N*-oxide. Differences exist between the CYP isoforms responsible for metabolism in rodents and in man, in humans, CYP 3A enzymes predominantly metabolise AQ4N and this subfamily of CYP are known to be well expressed in a broad spectrum of human cancers. With this in mind, AQ4N based therapy should be considered as a rational treatment regime for patients bearing solid tumour burdens.

Acknowledgements

I would like to express my gratitude to the following people:

Professor Laurence H Patterson for constant supervision over the last few years.

Professor M Danny Burke for the kind donation of human livers for use throughout this work and for detailed discussions on enzyme kinetics.

Mr E. Wanogho (Wan) for excellent technical assistance and help with statistical analysis.

Dr P. Whiting for proofreading the manuscript.

Dr G I Murray and members of the academic and technical staff of the University of Aberdeens Department of Biomedical Sciences, for the donation of human tumours.

The technical staff of De Montfort University's Department of Pharmaceutical Sciences and the MRC's Radiobiology Unit, Chilton, Didcot, UK.

Finally, I would like to thank Catherine for her endless support and encouragement.

List of contents	
Abstract	iii
Acknowledgments	iv
List of figures	xiii
List of tables	xviii
Abbreviations	xx
 Chapter 1: Introduction	 1
1.1 Cancer	2
1.2 Conventional cancer treatments	2
1.2.1 Stem cell model of tumour growth and Gompertzian kinetics	3
1.3 Tumour hypoxia	6
1.3.1 Hypoxic cells and radio/chemoresistance	7
1.3.2 Hypoxia inducible factor 1 (HIF-1)	10
1.4 Tumour hypoxia as a target for bioreductive drugs	10
1.4.1 Nitroheterocyclics	12
1.4.2 Heterocyclic <i>N</i> -oxides	13
1.4.3 Quinones	15
1.4.4 The development of AQ4N, a novel anthraquinone di- <i>N</i> -oxide and structural analogue of mitoxantrone	17
1.5 Enzymology of bioreductive drug activation	21
1.5.1 Aldehyde oxidase (AO)	22
1.5.2 NADH cytochrome b ₅ reductase	22

1.5.3	Xanthine dehydrogenase/xanthine oxidase	23
1.5.4	NAD(P)H quinoneoxidoreductase (DT diaphorase or NQO)	24
1.5.5	NADPH cytochrome P450 reductase	28
1.5.6	Cytochrome P450	29
1.5.6.1	The catalytic cycle of CYP	32
1.5.6.2	The CYP 1A subfamily	33
1.5.6.3	The CYP 1B subfamily	34
1.5.6.4	The CYP 2B subfamily	34
1.5.6.5	The CYP 2C subfamily	35
1.5.6.6	The CYP 2D subfamily	35
1.5.6.7	The CYP 2E subfamily	36
1.5.6.8	The CYP 3A subfamily	37
1.5.6.9	The CYP 4A subfamily	38
1.5.7	CYP expression in cancer	38
1.6	Enzymes with the potential to activate bio-reductive agents	39
1.6.1	Nitric oxide synthase (NOS)	39
1.6.2	The cytochrome P450 reductase (CPR)/haem oxygenase (HO) system	40
1.7	Aims	41
1.8	Definition of terms	42
Chapter 2: Materials and methods		43
2.1	General approach used to study the metabolism of	

	AQ4N	44
2.2	Chemicals	45
2.2.1	Human tissue acquisition	46
2.2.2	Enzymes and transfected cell microsomes	48
2.3	Animal inducer treatments	49
2.3.1	Phenobarbitone	49
2.3.2	Clofibrate	49
2.3.3	Pregnenolone 16alpha-carbonitrile	49
2.3.4	Isoniazid	49
2.3.5	3-Methylcholanthrene	49
2.3.6	Inducer controls	50
2.3.7	Untreated controls	50
2.4	Preparation of tissue fractions	50
2.5	Protein quantitation	51
2.6	Reagent degassing	52
2.7	Metabolism of AQ4N and AQM in subcellular fractions	52
2.7.1	Effect of inhibitor addition on metabolism	53
2.7.2	Oxidative metabolism of AQ4	54
2.7.3	Kinetic analysis	55
2.8	SDS-PAGE	56
2.8.1	Haem oxygenase 1 (HO-1) activity	56

2.8.2	Metabolism of AQ4N using the CPR/ HO-1 system	57
2.8.3	BROD, cytochrome P450 reductase (CPR) and nitric oxide synthase (nNOS) activities	57
2.8.4	Metabolism of AQ4N using purified rat brain nitric oxide synthase (nNOS)	59
2.8.5	Metabolism of AQ4N in human lymphoblastoid cell microsomes expressing CYP 3A4, control, CYP 2B6 and cytochrome P450 reductase (CPR)	60
2.9	Deproteinisation, HPLC, metabolite detection and quantitation	60
2.9.1	Correlation analysis	62
2.9.2	Statistical analysis	63
2.9.3	Preliminary characterisation of the <i>in vivo</i> metabolism of AQ4N in tumour bearing mice	63
2.9.4	Drug and metabolite extraction	63
 Chapter 3: Metabolism of AQ4N and AQM in rat		
	subcellular fractions	65
3.1	Aims	66
3.2	Materials and methods	66
3.2.2	Animal pretreatment and tissue fractionation	66
3.2.3	Metabolism studies using rat subcellular fractions and the use of CYP specific inhibitors	66

3.2.4	Metabolism studies using the CPR/ HO system and rat nNOS	67
3.2.5	Chromatography and metabolite detection	67
3.2.6	Kinetic analysis and statistical significance	67
3.3	Results	68
3.3.1	Chromatography	68
3.3.2	Metabolism of AQ4N and AQM in rat hepatic tissue	68
3.3.3	Effect of animal pretreatment on the metabolism of AQ4N	80
3.3.4	Effect of animal pretreatment on the metabolism of AQM	80
3.3.5	Effect of inhibitors on the metabolism of AQ4N in rat microsomes	84
3.3.6	Effect of inhibitors on the metabolism of AQM in rat microsomes	84
3.3.7	Oxidative metabolism of AQ4 in rat hepatic tissue	87
3.3.8	Kinetics of AQ4N and AQM metabolism in untreated rat microsomes	87
3.3.9	SDS-PAGE characteristics and activities of purified CPR, HO- 1 and nNOS	93
3.4	Metabolism of AQ4N in experiments using nNOS and the CPR/ HO-1 system	94
3.5	Conclusions	96

Chapter 4: Metabolism of AQ4N and AQM in human

	subcellular fractions	98
4.1	Aims	99
4.2	Materials and methods	99
4.2.1	Protein determination	99
4.2.2	Metabolism of AQ4N and AQM in human subcellular fractions	100
4.2.3	Correlation analysis	100
4.2.4	Kinetic analysis	100
4.2.5	Metabolism of AQ4N in human gene transfected cell microsomes	101
4.2.6	HPLC and metabolite detection	101
4.3	Results	102
4.3.1	Metabolism of AQ4N and AQM in human hepatic tissue	102
4.3.2	Correlation between the metabolism of AQ4N and AQM in human liver microsomes	106
4.3.3	Effect of inhibitors on the metabolism of AQ4N in human liver microsomes	112
4.3.4	Kinetics of AQ4N metabolism in human liver microsomes	117
4.3.5	Oxidative metabolism of AQ4 in human liver microsomes	117
4.3.6	Metabolism of AQ4N in human lymphoblastoid cell microsomes	133

4.3.7	Metabolism of AQ4N in human tumour and paired healthy tissue	133
4.4	Conclusions	138
Chapter 5: Preliminary investigation into the <i>in vivo</i> metabolism of AQ4N in tumour and non tumour bearing mice		
		141
5.1	Aims	142
5.2	Materials and methods	142
5.2.1	Animal dosing procedure	142
5.2.3	Drug and metabolite extraction	143
5.2.4	Protein analysis	143
5.3	Results	144
5.3.1	Drug and metabolite recovery	144
5.3.2	Tumours	144
5.3.3	Plasma	146
5.3.4	Livers	148
5.3.5	Gall bladders	148
5.3.6	Muscle	148
5.4	Conclusions	152
Chapter 6: General discussion		153

6.1	General discussion	154
6.2	Future work	166
6.2.1	Concluding remarks	168
References		169
Publications		202

List of figures

- Figure 1a** Effect of increasing the concentration of an antiproliferative anticancer drug on slowly and rapidly proliferating tumours
- Figure 1** Model of Gompertzian growth
- Figure 2** pO₂ distributions in normal cervix mucosa and in cervix cancers at different clinical stages
- Figure 3** Structures of RSU1069 and RB6145
- Figure 4** Bioreduction of SR 4233
- Figure 5** Bioreductive activation of Mytomycin c (MMC)
- Figure 6** Structures of Mitoxantrone, Ametantrone and daunorubicin
- Figure 7** Reductive metabolism of the *N*-oxide based prodrug AQ4N
- Figure 8** Human NQO₁ gene promotor showing cis elements needed for induction and regulation
- Figure 9** Association of cytochrome P450 reductase (CPR) and cytochrome P450 in the endoplasmic reticulum (ER)
- Figure 10** Catalytic cycle of CYP
- Figure 11** Typical standard curves for AQ4 and AQM
- Figure 12** HPLC chromatograms for 100 μ M AQ4N, AQM , AQ4 and a mixture of all three
- Figure 13** Effect of temperature on the anaerobic metabolism of AQ4N
- Figure 14** Effect of pH on the anaerobic metabolism of AQ4N
- Figure 15** Effect of oxygen on the metabolism of AQ4N
- Figure 16** Effect of oxygen on the metabolism of AQM
- Figure 17** Effect of protein concentration on the anaerobic metabolism of AQ4N

- Figure 18** Effect of protein concentration on the anaerobic metabolism of AQM
- Figure 19** Effect of incubation time on the anaerobic metabolism of AQ4N
- Figure 20** Effect of incubation time on the anaerobic metabolism of AQM
- Figure 21** The effect of animal pretreatment on the anaerobic metabolism of AQ4N
- Figure 22** The effect of animal pretreatment on the anaerobic metabolism of AQM
- Figure 23** Typical HPLC chromatograms obtained after incubating 100 μ M AQ4N in NADPH supplemented rat hepatic microsomes
- Figure 24** Effect of CYP inhibitors on the anaerobic metabolism of AQ4N in rat hepatic microsomes
- Figure 25** Effect of CYP inhibitors on the anaerobic metabolism of AQ4N in rat hepatic microsomes
- Figure 26** Oxidative metabolism of AQ4 in untreated rat microsomes
- Figure 27** Effect of AQ4N concentration on the initial velocity of anaerobic metabolism
- Figure 28** Hanes- Woolf transformation plot of the kinetic data in figure 27
- Figure 29** Effect of AQM concentration on the initial velocity of AQ4 formation
- Figure 30** Hanes-Woolf transformation plot of the kinetic data in figure 29

- Figure 31** SDS-PAGE for HO-1 and CPR
- Figure 32** Anaerobic metabolism of 100 μM AQ4N in a panel of seventeen human liver microsome preparations
- Figure 33** Percentage anaerobic metabolism of 100 μM AQ4N in a panel of seventeen human liver microsome preparations
- Figure 34** Anaerobic metabolism of 100 μM AQM in a panel of seventeen human liver microsome preparations
- Figure 35** Correlation between benzoxyl *O*-deethylation (BROD) activity and the anaerobic metabolism of AQ4N
- Figure 36** Correlation between tamoxifen *n*-demethylation (TND) activity and the anaerobic metabolism of AQ4N
- Figure 37** Correlation between the anaerobic metabolism of AQM to AQ4 and various CYP activities
- Figure 38** Correlation between the anaerobic metabolism of AQM and the anaerobic metabolism of AQ4N
- Figure 39** Effect of CYP inhibitors on the anaerobic metabolism of AQ4N in microsomes from HLM 50
- Figure 40** Effect of CYP inhibitors on the anaerobic metabolism of AQ4N in microsomes from HLM 45
- Figure 41** Effect of CYP inhibitors on the anaerobic metabolism of AQ4N in microsomes from HLM 55
- Figure 42** Typical HPLC chromatograms for the anaerobic metabolism of 100 μM AQ4N in microsomes from HLM 55
- Figure 43** Effect of incubation time on the anaerobic metabolism of AQ4N in microsomes from HLM 50

- Figure 44** Effect of incubation time on the anaerobic metabolism of AQ4N in microsomes from HLM 50
- Figure 45** Effect of incubation time on the anaerobic metabolism of AQ4N in microsomes from HLM 55
- Figure 46** Effect of protein concentration on the anaerobic metabolism of 100 μM AQ4N in microsomes from HLM 50
- Figure 47** Effect of protein concentration on the anaerobic metabolism of 100 μM AQ4N in microsomes from HLM 45
- Figure 48** Effect of protein concentration on the anaerobic metabolism of 100 μM AQ4N in microsomes from HLM 55
- Figure 49** Effect of AQ4N concentration on the initial velocity of metabolite production in HLM 50
- Figure 50** Effect of AQ4N concentration on the initial velocity of metabolite production in HLM 45
- Figure 51** Effect of AQ4N concentration on the initial velocity of metabolite production in HLM 55
- Figure 52** Hanes-Woolf transform of the kinetic data shown in figure 49 for HLM 50
- Figure 53** Hanes- Woolf transform of the kinetic data shown in figure 50 for HLM 45
- Figure 54** Hanes-Woolf transform of the kinetic data shown in figure 51 for HLM 55
- Figure 55** Oxidative metabolism of AQ4 in microsomes from HLM 47
- Figure 56** Oxidative metabolism of AQ4 in microsomes from HLM 55
- Figure 57** Anaerobic metabolism of AQ4N in lymphoblastoid cell microsomes transfected with CYP gene inserts

- Figure 58** Anaerobic metabolism of 100 μ M AQ4N in microsomes from two patients having undergone surgery for primary renal cell carcinoma
- Figure 59** Anaerobic metabolism of 100 μ M AQ4N in microsomes from two patients having undergone surgery for primary adenocarcinoma of the colon
- Figure 60** Proposed mechanism of NADPH dependent cytochromeP450 mediated reduction of *N*-oxides

List of tables

Table 1	Clinically used anticancer agents
Table 2	Characteristics of human livers used
Table 3	Characteristics of human normal and neoplastic tissue used
Table 4	Markers used for CYP activity
Table 5	Control incubations of AQ4N and AQM in rat hepatic tissue
Table 6	Kinetic parameters for AQ4N and AQM imetabolism in rat microsomes
Table 7	Anaerobic metabolism of AQ4N by purified nNOS and the CPR/ HO-1 system
Table 8	Non significant Spearman rank correlations ($p>0.05$) between various CYP activities/ isoform content and the anaerobic metabolism of AQ4N in human microsomes
Table 9	Non significant Spearman rank correlations ($p>0.05$) between various CYP activities/ isoform content and the anaerobic metabolism of AQ4N in human microsomes
Table 10	Kinetic data for the anaerobic metabolism of AQ4N in three human livers
Table 11	AQ4N and its metabolites in HT 29 tumour xenografts excised from nude mice
Table 12	AQ4N and its metabolites in KHT tumour xenografts excised from C3H mice
Table 13	AQ4N and its metabolites in RIF-1 tumour xenografts excised from C3H mice

Table 14	AQ4N and its metabolites in SCCVII tumour xenografts excised from C3H mice
Table 15	AQ4N and its metabolites from plasma of mice (all groups) at various time points after dosing (ip) with 250 mg/kg of AQ4N
Table 16	AQ4N and its metabolites from livers of mice (all groups) at various time points after dosing (ip) with 250 mg/kg of AQ4N
Table 17	AQ4N and its metabolites from gall bladders of mice (all groups) at various time points after dosing (ip) with 250 mg/kg of AQ4N
Table 18	AQ4N and its metabolites from muscle of mice (all groups) at various time points after dosing (ip) with 250 mg/kg of AQ4N

Abbreviations

AQ4	1,4-Bis-{{2-(dimethylamino)ethyl}amino}-5,8-dihydroxyanthracene-9,10 dione
AQ4N	1,4-Bis-{{2-(dimethylamino- <i>N</i> -oxide)ethyl}amino}-5,8-dihydroxyanthracene-9,10 dione
AQM	1-{{2-(dimethylamino- <i>N</i> -oxide)ethyl}amino}-4-{{2-(dimethylamino)ethyl}amino}-5,8-dihydroxyanthracene-9,10-dione
3MC	3-methylcholanthrene
ANF	Alpha-naphthoflavone
AO	Aldehyde oxidase
AU	Absorbance units
BROD	Benzoxylresorufin <i>O</i> -dealkylase activity
CB 1954	5-(aziridin-1-yl)-2,4-dinitrobenzamide
CHA	Coumarin hydroxylase activity
CHO	Chinese hamster ovary
CL_{int}	Intrinsic clearance (hepatic)
CLO	Clofibrate
CPR	Cytochrome P450 reductase
CYP	Cytochrome P450
DACA	<i>N</i> -2-[(dimethylamino)ethyl]acridine-4-carboxamide
DIE	Diethylthiocarbamate
DNA	Deoxyribonucleic acid
DTD	DT diaphorase
ECOD	7-ethoxycoumarin <i>O</i> -deethylation
EDTA	sodium ethylenediamine tetraacetic acid

EO9	3-hydroxy-5-aziridiny-1-methyl-2-(1 <i>H</i> -indole-4,7-dione) prop-2-en-1-ol
ER	Endoplasmic reticulum
EROD	7-ethoxyresorufin <i>O</i> -deethylation
F	Female
FAD	Flavin adenine dinucleotide
FMN	Flavin mononucleotide
GSH	Glutathione
Gy	Gray
HCl	Hydrochloric acid
HIF	Hypoxia inducible factor
HIV	Human immunodeficiency virus
HLM	Human liver microsomes
HO	Haem oxygenase
HPLC	High performance liquid chromatography
ip	Intraperitoneal
ISO	Isoniazid
KCl	Potassium chloride
KDa	KiloDalton
KET	Ketoconazole
Kg	Kilogram
K_m	Apparent Michaelis constant
M	Male
MET	Metyrapone
mg	Milligramme
min	Minute

MMC	Mytomycin c
MS	Mass spectroscopy
NADH	Nicotinamide adenine dinucleotide, reduced form
NADPH	Nicotinamide adenine dinucleotide phosphate, reduced form
NC- NO	Nitracrine- <i>N</i> -oxide
NDEA	<i>N</i> -nitrosodiethylamine
NDMA	<i>N</i> -nitrosodimethylamine
NMR	Nuclear magnetic resonance spectroscopy
NOS	Nitric oxide synthase
NQO	Nicotinamide adenine dinucleotide phosphate dependent quinone oxidoreductase
OO	Olive oil
PB	Phenobarbitone
PBS	Phosphate buffered saline
PCN	Pregnenalone 16alpha-carbonitrile
pH	Minus log [H ⁺]
PNBP	4-(<i>p</i> -nitrobenzyl) pyridine
pO₂	Partial pressure of oxygen
RBC	Red blood cell
RNA	Ribonucleic acid
RSU1069	1-(2-nitro-1-imidazolyl)-3-(1-aziridino)-2 propanol
SDS	Sodium dodecyl sulphate
SR 4233	3-amino-1,2,4-benzotriazine-1,4-dioxide
SR 4317	3-amino-1,2,4-benzotriazine-1-oxide
SR 4330	3-amino-1,2,4-benzotriazine

TAO	Triacetyloleandomycin
TCDD	Tetrachlorodibenzo- <i>p</i> -dioxin
TND	Tamoxifen <i>N</i> - demethylase activity
Tris	Tris- hydroxymethylaminomethane
TWN	Tween 80
UT	Untreated
VEGF	Vascular endothelial growth factor
V_{max}	Apparent maximum velocity
XDH	Xanthine dehydrogenase
XO	Xanthine oxidase

Chapter 1

Chapter 1

Introduction

1.1 Cancer

In its broadest sense, cancer can be described as a group of diseases in which host cells become autonomous from normal growth control mechanisms (Holleb *et al* 1991). It has been estimated that 1 in 3 people will develop cancer during the course of their lives. In 1993, cancer claimed the lives of 161,770 people in the United Kingdom and, of these, lung cancer was the commonest male cancer, accounting for 30% of cancer mortality in men, and breast cancer was the most common female cancer, accounting for 19% of the cancer mortality in women (CRC Scientific yearbook 1996).

1.2 Conventional cancer treatments

Cancer treatments fall into three main categories, these are : Surgery, radiotherapy and chemotherapy.

Surgery is the oldest form of cancer treatment and is used in the diagnosis, staging and physical resection of malignant disease (reviewed by Eberlein and Wilson 1991). At present, more than 60% of patient with confirmed malignancy undergo some form of surgery (reviewed by Eberlein and Wilson 1991). Radiotherapy is a treatment regime which utilises ionising radiation, such as X- rays or gamma rays, to damage the nucleic acid of cancer cells. Lethal injury to DNA can occur by direct ionisation of the DNA molecule by a scattered electron or by an indirect mechanism whereby a photon interacts with a water molecule producing hydroxyl radicals. The short lived hydroxyl radicals

are able to interact with and damage cellular DNA (reviewed by Hendrickson and Withers 1991).

Modern chemotherapy originates from the 1940s when nitrogen mustards were developed during World War II as chemical warfare agents. Treatment of transplanted lymphosarcoma in mice with nitrogen mustards revealed that such tumours rapidly regressed (reviewed by Montgomery 1979). These early findings prompted the first clinical trial of these compounds conducted in a group of six patients with terminal neoplastic disease. In two of these individuals, a rapid dissolution of large tumour masses followed mustard administration (reviewed by Gilman and Philips 1946). Since then, numerous anticancer agents have been developed which work by direct or indirect action upon the nucleic acids of proliferating cells (reviewed by Cooper and Cooper 1991). Table 1 lists some clinically useful anticancer agents

Unfortunately, a growing tumour may consist of only a small fraction of proliferating cells at any one time, thus limiting the efficacy of these agents. In order to understand the full implications of this behaviour two aspects of tumour growth are further discussed.

1.2.1 Stem cell model of tumour growth and Gompertzian kinetics

Firstly, the stem cell model of tumour growth suggests that a hierarchy of cancer cells exist within any given tumour. The hierarchy consists of highly proliferative stem cells, with little or no specialised function and highly specialised (well differentiated) cells with little or no proliferative ability. A large subpopulation of the stem cells may be out of cell cycle in G_0 and can only enter cycle at G_1 upon a suitable physiological stimulus

(such as reduced cell number). Therefore, a tumour with a large number of cells in G_0 may be largely refractory to antiproliferative agents. Conversely, a tumour with a high proportion of cells in cell cycle may be more sensitive to the same treatment (reviewed by Cooper and Cooper 1991 and Dorr and Fritz, 1982). See Fig 1a.

Table 1) Clinically used anticancer agents (Adapted from Franks and Teich 1991)

Classification	Drug
Alkylating agents	Mechlorethamine Busulphan Chlorambucil Cyclophosphamide Melphalan Thiotepa
Antimetabolites	Methotrexate 6- mercaptopurine Thioguanine 5-fluorouracil Cytosine arabinoside 5-azacytidine
Plant alkaloids	Vinblastine Vincristine
Antibiotics	Mitomycin C Doxorubicin Daunorubicin Bleomycin
Nitrosoureas	Carmustine Lomustine Semustine Streptozotocin
Enzymes	L-asparaginase
Random synthetics	Cis- platinum diammine dichloride Dacarbazine Dibromomannitol Hexamethylmelamine Mitoxantrone Hydroxyurea

Secondly, the growth of many tumours can be fitted to a model of growth behaviour known as Gompertzian growth (Rygaard and Spang-

Thomsen 1997), see fig 1b. The model predicts that at the beginning of a tumours life span, well before clinical detection, it grows exponentially, having a large subpopulation of cells in cell cycle and fewer in G_0 . However, by the time the tumour becomes detectable the rate of growth has slowed and many of the cells that were in cycle have now moved back to G_0 (Tancock and Hill, 1987). This slowing down of growth (reduction in proliferative subpopulation) can be attributed to inhibitory cell- cell contacts, decreased nutrient supply, toxic metabolite build up and tumour hypoxia (Holleb et al, 1991). The result is that the potential target for antiproliferative agents is now smaller (Bassukas et al 1994)

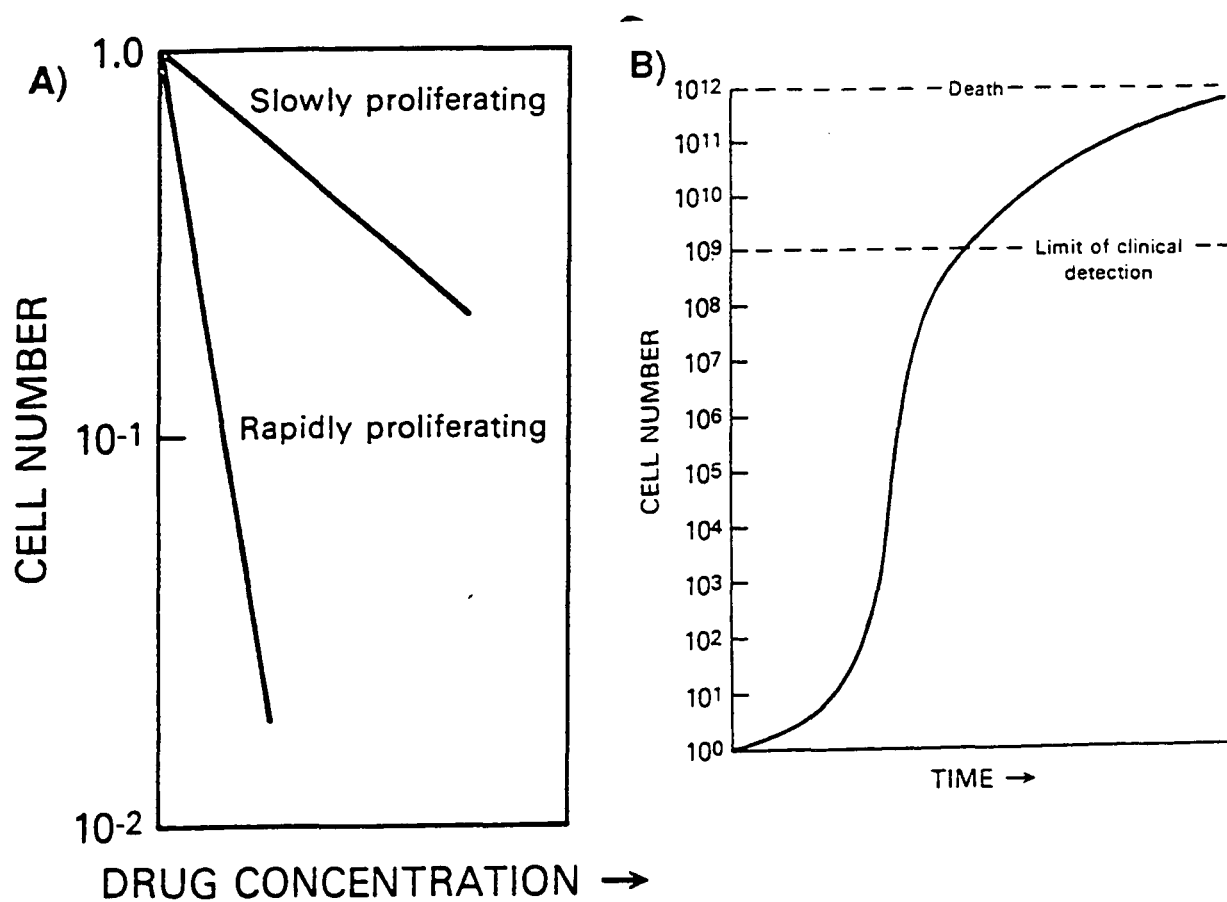


Fig 1. A) Effect of increasing the concentration of an antiproliferative anticancer drug on a slowly proliferating and a rapidly proliferating tumour. (Holleb 1991)
B) Model of Gompertzian growth (Holleb 1991)

1.3 Tumour Hypoxia

The existence of hypoxic cells within solid tumours was first suggested by Thomlinson and Gray in 1955 who analysed human bronchiogenic carcinoma specimens and found that tumour cords with a diameter $> 200\ \mu\text{m}$ contained areas of central necrosis. Moreover, tumour cords with diameters $> 160\ \mu\text{m}$ contained no necrotic areas. Based on their findings they calculated that oxygen could diffuse a distance of approximately $150\ \mu\text{m}$ in respiring tissue and concluded that viable tumour cells found on the edge of necrotic regions were probably severely hypoxic.

Direct evidence for hypoxic tumour cells came from the radiobiological experiments of Powers and Tolmach in 1964. Using mouse implanted lymphosarcomas, they found that cells from irradiated tumours produced survival curves that were biphasic with respect to cell sensitivity and resistance. However, when irradiated tumour cells were obtained from mice exposed to high oxygen concentrations the resultant cell survival curves showed a reduction in the resistant subpopulation of cells. This led them to conclude that the transplanted tumours were heterogeneous with respect to the degree of oxygenation.

Oxygen deficiency in tumour cells is thought to arise in one of two ways.. Firstly, as the tumour mass enlarges the rate of endothelial cell division (neovascularisation) is exceeded by the rate of tumour growth. This results in compromised microcirculation to a number of the malignant cells. Cells at a distance of between $120\text{--}150\ \mu\text{m}$ from an oxygenated blood vessel are believed to experience varying degrees of chronic hypoxia (Sartorelli 1986). Alternatively, the growth of the tumour itself may render cells transiently hypoxic (acute hypoxia) by intermittently

compressing a vascular network supplying a subpopulation of the neoplastic cells (Sutherland and Franko 1980).

Most solid tumours are believed to possess a hypoxic subpopulation of cells making up between 5 and 30 % of the total tumour mass (Sartorelli 1986). Indeed a large number of reports have appeared in the literature to document the extent of hypoxia within tumours of both human and animal origin. The work of Wendling *et al* (1984) compared red blood cells (RBC's) from the microvessels of a large number of normal and neoplastic rectal tissue and found the medians of oxyhaemoglobin saturation curves from RBC's decreased from 80% saturation, in normal tissue, to 49% in malignant. The median partial pressure of oxygen (pO_2) in a range of clinically resected cervical cancers has been found to be significantly lower than corresponding healthy tissue, see Fig 2 (Kolstad *et al* 1968, Bergsjö and Evans 1971, reviewed by Vaupel *et al* 1989).

1.3.1 Hypoxic cells and radio/chemoresistance

The failure of certain tumours to respond to radiotherapy (radioresistance) is believed to be a consequence of hypoxic cells (Hall 1975). In well oxygenated tissue, the effects of ionising radiation can lead to the production of superoxide radicals ($O_2^{\bullet-}$). These superoxide radicals can be "fixed" to form more stable peroxy radicals (RO_2^{\bullet}) which in turn are free to mediate cellular damage by interacting with cell membranes, DNA and other macromolecules (Halliwell and Gutteridge 1989). In oxygen deficient cells, peroxy radical formation is minimised and, as a result, hypoxic cells escape damage (Hellman 1993).

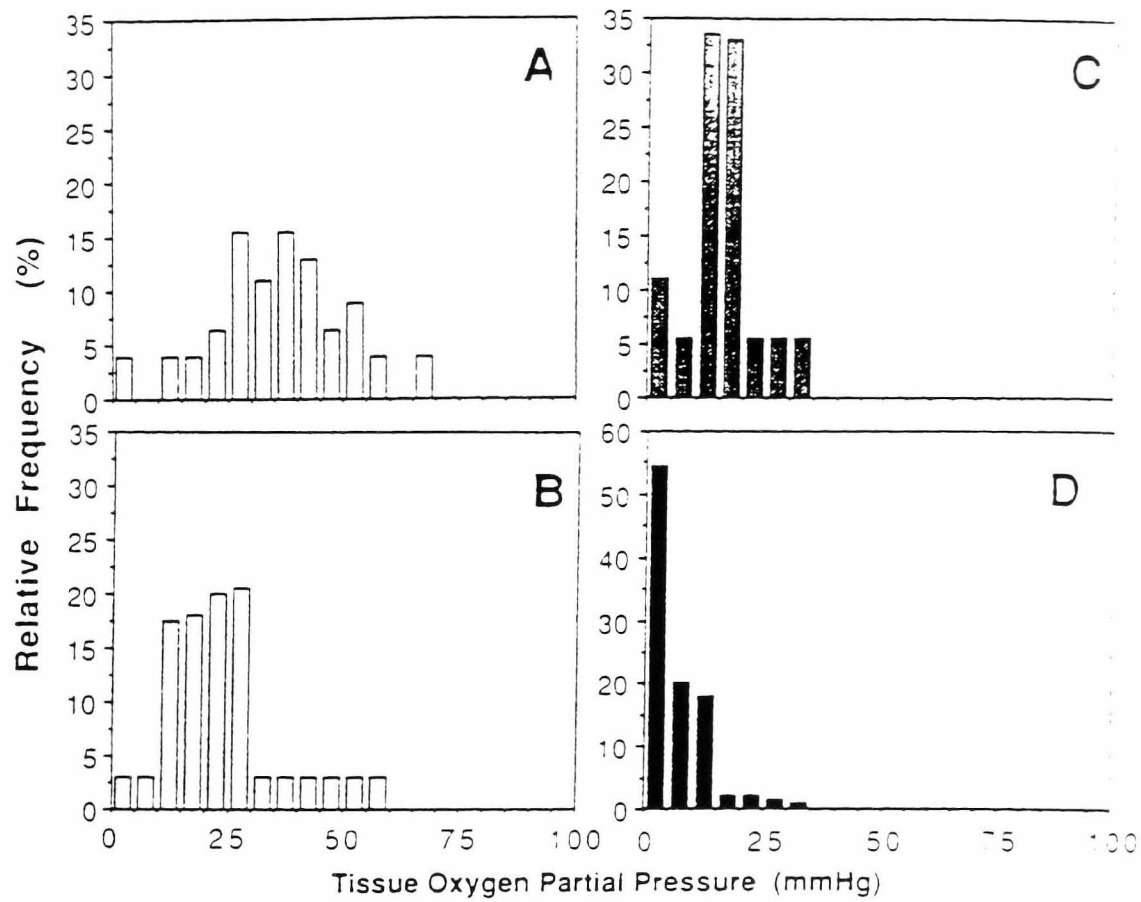


Fig 2. pO_2 distributions in normal cervix mucosa and in cervix cancers at different clinical stages.

A) pO_2 distributions in normal cervix mucosa. **B)** Stage 0 carcinoma, **C)** stage 1 carcinoma and **D)** stage 2 carcinoma. From Vaupel *et al* 1989

In addition to radioresistance, hypoxic cancer cells may become chemoresistant. The increased distance between a chronically hypoxic cell (compared to a normoxic cell) and a oxygenated blood vessel may exceed the distance a therapeutic agent can diffuse. In this respect, the hypoxic subpopulation are able to evade the action of the drug (Sartorelli *et al* 1995). In 1974, Bedford and Mitchell carried out some elegant experiments on the effect of hypoxia on chinese hamster ovary (CHO) cells and demonstrated that the percentage of cells in S phase decreased with the duration of hypoxic exposure and that the same cells spent a disproportionate time in G₁ and G₀ (out of cycle). Similar results were obtained from the laboratories of Born *et al* (1979) and Koch *et al* (1973). Collectively, these observations suggested that the sluggish nature of the cell cycle under hypoxia may create a situation in which an anticancer drug, if able to reach its cellular target, may be ineffective as the cell is at an inappropriate stage of cycle.

Additionally, elevated reduced glutathione (GSH) content may confer resistance upon hypoxic cells to anticancer drugs. Using a subclone of the A2780 human ovarian carcinoma cell line, a 50 fold elevation of GSH has been shown to cause a 1000 fold increase in resistance to cisplatin (Godwin *et al* 1992). Furthermore, exposure of HT 29 adenocarcinoma cells to hypoxic conditions has been reported to elevate intracellular GSH (O'Dwyer *et al* 1994).

Hypoxia mediated induction of gene expression may provide yet another mechanism whereby oxygen deficient cancer cells can become chemoresistance. For example, the upregulation of DT diaphorase (DTD) in adenocarcinoma cells exposed to hypoxia has been reported (O'Dwyer *et al* 1994). In this respect the elevated amount of DTD may be

able to detoxify a wide variety of anticancer drugs by virtue of a two electron reduction process (Reviewed by Ross *et al* 1993 and Joseph *et al* 1994).

1.3.2 Hypoxia inducible factor 1 (HIF- 1)

Tumour cells are able to adapt to hypoxia by the activation of a heterodimeric protein known as hypoxia inducible factor- 1 (HIF- 1). This transcription factor, composed of an alpha and beta subunit, HIF- 1 alpha and HIF- 1 beta respectively, is constitutively expressed under conditions of both normoxia and hypoxia (Huang *et al* 1996). However, the stability of HIF- 1 alpha protein is increased during hypoxia (Huang *et al* 1996) facilitating the dimerisation of both subunits, and subsequent binding of functional HIF- 1, to a number of promotor/enhancer sequences upstream of genes important for adaptation to low oxygen tensions (reviewed by Jiang *et al* 1997). Amongst the genes transcriptionally activated by HIF- 1 are the vascular endothelial growth factor glycoproteins (VEGF) (Forsythe *et al* 1996). VEGF proteins bind to the flt- 1 and flk- 1 receptors on endothelial cells (Seetharam *et al* 1995, Rockwell *et al* 1995 and reviewed by Cheng *et al* 1996) and in so doing initiate a signal transduction system which leads to cell proliferation and neovascularisation.

1.4 Tumour hypoxia as a target for bioreductive drugs

In 1936 it was shown that microbial cultures grown anaerobically had lower half wave redox potentials, and hence a greater capacity for reduction, than microbial cultures grown aerobically (Hewitt 1936, reviewed by Kennedy *et al* 1980). These early findings led Lin and co workers to speculate that hypoxic cells remote from the vascular supply of a tumour mass might, in an analogous way to anaerobic microbes,

have a greater capacity for reductive reactions compared to well oxygenated cells. The same workers then went on to synthesis the first bioreductive agents which were a series of benzo- and naphthoquinones (Lin *et al* 1972). These compounds were found to be potent inhibitors of both DNA and RNA synthesis in adenocarcinoma 755 cells and prolonged the life span of such tumour bearing mice (Lin *et al* 1972). Since the early seventies the concept of bioreductive drug activation has been viewed as a potential treatment regime whereby hypoxic tumour cells can be selectively destroyed. Ideally, the bioreductive agent, referred to as a prodrug (Workman 1992) should possess certain properties which are outlined below (reviewed by Friery 1997):-

- 1) It should not be toxic to normal oxygenated tissue.
- 2) It should be converted irreversibly to a stable oxygen insensitive cytotoxin under conditions of hypoxia.
- 3) The cytotoxic metabolite should maintain activity upon reoxygenation of tumour cells or upon diffusion away from the primary hypoxic region.
- 4) The cytotoxic metabolite should remain within the tumour tissue and not diffuse into normal surrounding tissue.
- 5) It should exert cytotoxic activity against acute and chronic hypoxic cells.

The following paragraphs review four classes of bioreductive agents namely: nitroheterocyclics, heterocyclic *N*-oxides, quinones and the

newly developed anthraquinone di *N*-oxides. Enzymes involved in bioreductive activation are discussed in section 1.2.2.

1.4.1 Nitroheterocyclics

RSU 1069 and its prodrug RB 6145 are both examples of this class of compound (Adams *et al* 1994), see Figure 3. Both agents have been shown to be preferentially toxic to hypoxic cells although the precise details of the bioactivation process remain, at present, unclear (Workman and Stratford 1993). Furthermore, both agents potentiate the effect of radiotherapy when used in the KHT rodent tumour model (Bremner 1993). RB 6145 is reported to be better tolerated in mice and less emetic in dogs than RSU 1069. In addition, both compounds are able to enhance the effect of photodynamic therapy (PDT) on the growth delay of RIF-1 murine sarcomas (Bremner 1993).

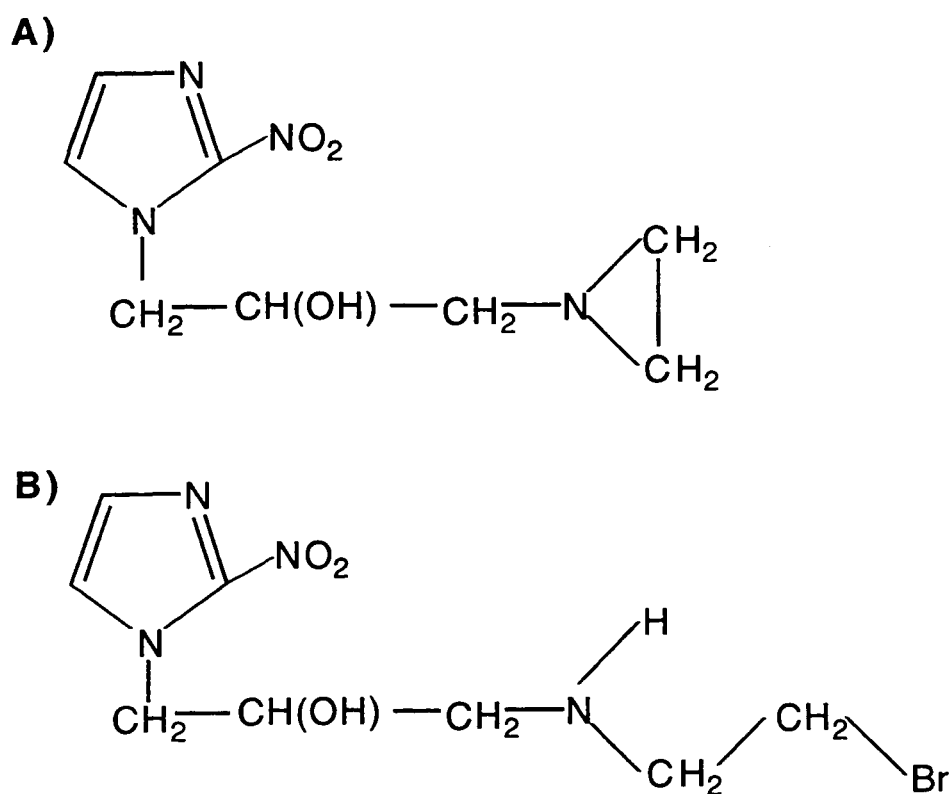


Fig 3. Structures of **A)** RSU 1069 and **B)** RB 6145

1.4.2 Heterocyclic *N*-oxides

Tirapazamine (SR 4233), the lead compound available in this class, has been shown to potentiate the anti tumour activity of radiotherapy (reviewed by Siim *et al* 1997) and enhance the sensitivity of transplantable murine neoplasms to various antineoplastic agents including: carboplatin, cyclophosphamide, doxorubicin, etoposide and taxol (Dorie and Brown 1997). In addition, SR 4233 has been shown to have a marked effect on the growth delay of the T50/80 and RIF-1 neoplasms (Mc Keown *et al* 1996 and Brown and Lemmon 1990). Presently, tirapazamine is undergoing a phase II clinical trial in combination with radiotherapy and a phase III trial in combination with the anticancer drug cisplatin (reviewed by Siim *et al* 1997).

SR 4223 is extensively metabolised under hypoxic conditions (Baker *et al* 1988) and is 75 to 200 times and 15 to 50 times more toxic to hypoxic rodent and human cell lines respectively, compared to normoxic controls (Zeman *et al* 1986). Mechanistically, the drug undergoes a one electron reduction to form a reactive nitroxyl radical. In air, the radical can be back oxidised to SR 4233 with the subsequent generation of a superoxide radical. In the absence of air, the one electron reduced radical mediates a hydrogen abstraction from a cellular macromolecule such as DNA, to form the two electron reduced molecule SR 4317. The hydrogen abstraction causes single and double strand breaks within DNA and this, in turn, leads to cell damage (Elwell *et al* 1997). SR 4317 can be further metabolised via a two electron reduction to form the stable product SR 4330 (Naylor 1994 and Costa *et al* 1989). The mechanism of SR 4233 bioactivation is depicted in Figure 4.

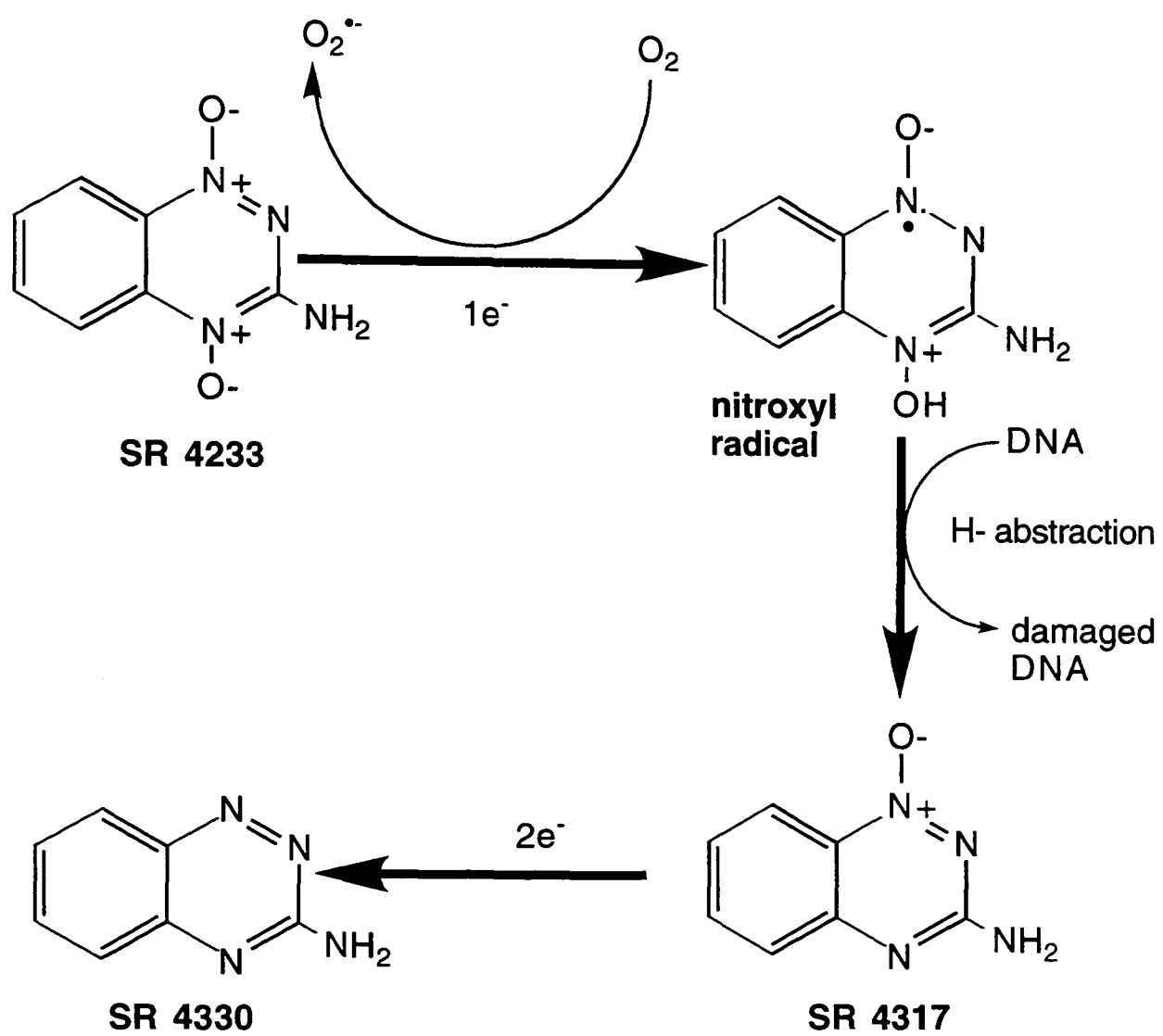


Fig 4. Bioreduction of SR 4233 (adapted from Costa *et al* 1989)

1.4.3 Quinones

Mitomycin C (MMC) and porfiromycin are both antineoplastic antibiotics isolated from *Streptomyces caespitosus* (Sartorelli 1986). The drugs are preferentially more toxic to murine EMT6 tumour and V79 chinese hamster lung fibroblasts under hypoxic conditions but MMC appears to be equitoxic to chinese hamster ovary (CHO) cells in the presence and absence of oxygen (Keyes *et al* 1984). MMC has been shown to improve the effect of radiotherapy in patients with cancers of the head and neck (reviewed by Sartorelli *et al* 1995).

MMC may be considered as the prototype bioreductive alkylating agent and both MMC and porfiromycin are bioactivated *via* a one or two electron reduction which generates intermediates capable of producing interstrand cross links between complementary DNA strands (Iyer and Szybalski 1964), see Figure 5. These cross links are considered to be the major cause of anti tumour activity (Iyer *et al* 1964, reviewed by Lin *et al* 1972). Toxicity of both drugs under aerobic conditions occurs from redox cycling, where the presence of molecular oxygen facilitates the re-oxidation of the semiquinone radical to the parent compound with the liberation of a superoxide radical. In the presence of ferrous ions the superoxide radical can be converted to hydroxyl radicals which are able to damage DNA, protein and cell membranes (Kappus 1986).

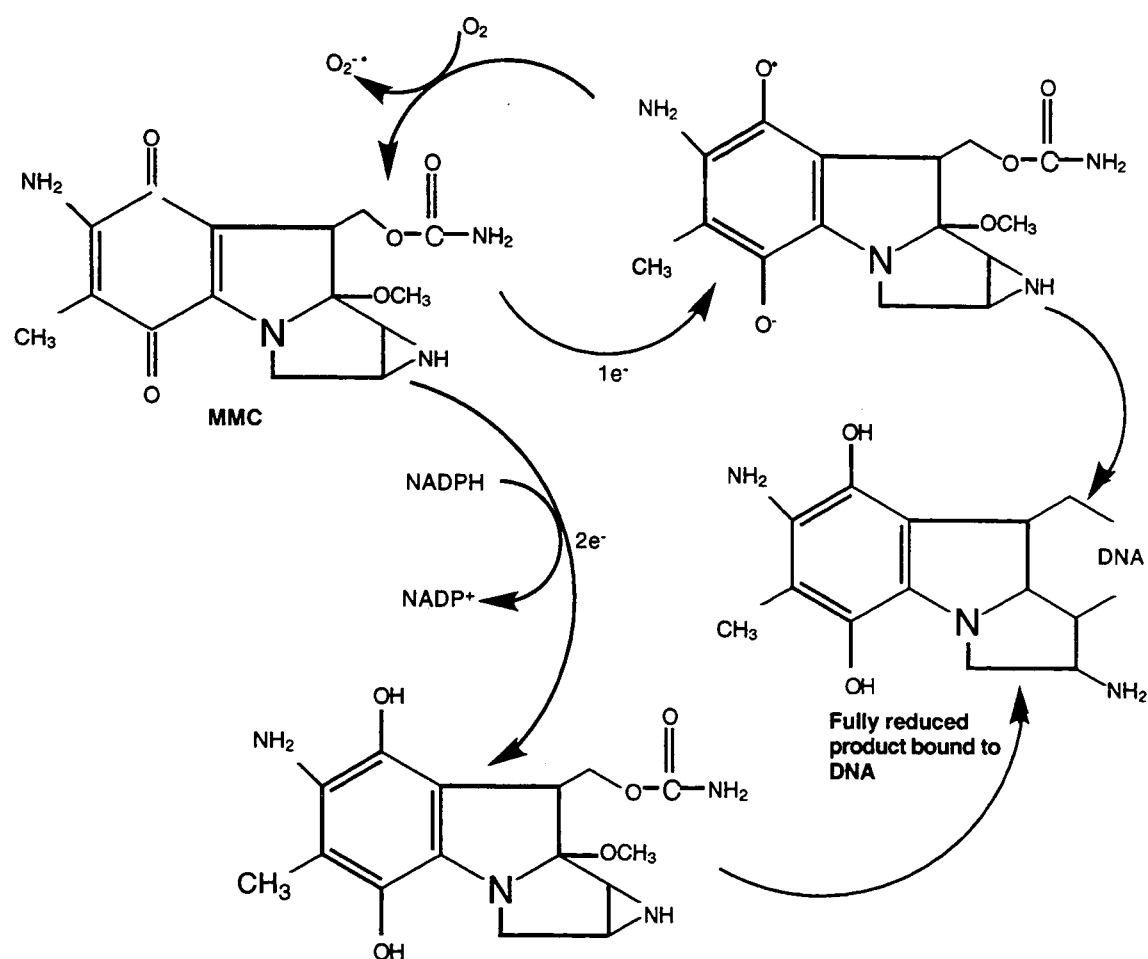


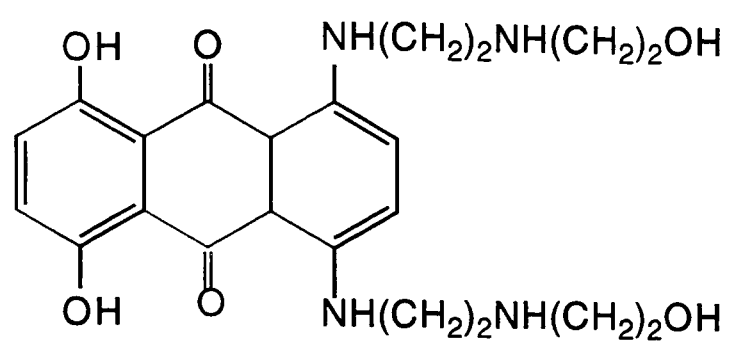
Fig 5. Bioreductive activation of Mytomycin C (MMC). Adapted from Sartorelli 1986

1.4.4 The development of AQ4N (1,4-bis-[[2-(dimethylamino-*N*-oxide)ethyl]amino]-5,8-dihydroxyanthracene-9,10-dione), a novel anthraquinone di-*N*-oxide based prodrug and structural analogue of mitoxantrone.

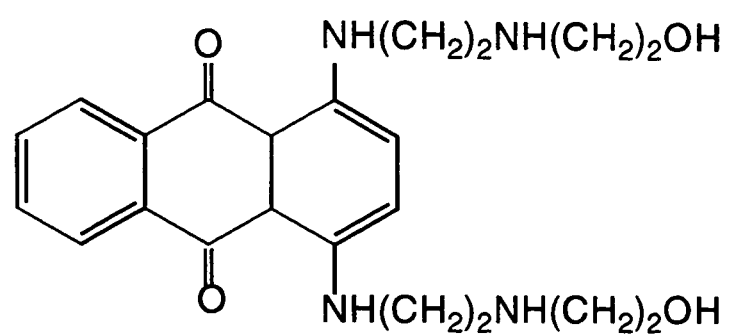
The antitumour effects of the 1,4- bis substituted anthraquinones have been well documented and are reviewed by Wiseman and Spencer (1997), and Dunn and Goa (1996). Included in this class of compounds are mitoxantrone (NSC 301739) and the related analogue ametantrone, (Figure 6). Both compounds possess a planar electron deficient anthraquinone chromophore and are thought to exert toxicity by intercalation of the chromophore between electron rich DNA bases (Johnson *et al* 1979 and Patterson 1993). The 1,4 bis substituted alkylamino side chains are cationic and enhance the strength of the drug/DNA complex by non-covalently interacting with the deoxyribose phosphate backbone of DNA (Denny and Wakelin 1990). The 5,8-dihydroxy substituents of mitoxantrone aid tighter binding of the drug to DNA and this is thought to explain the ten fold increase in toxicity of mitoxantrone, compared to analogues, to a range of transplantable murine neoplasms (Johnson *et al* 1979).

Mitoxantrone has been shown to inhibit DNA and RNA dependent polymerases in a variety of cultured cell lines (Traganos *et al* 1980 and Foye *et al* 1982), topoisomerases in human breast cancer cells (Crespi *et al* 1986) and elicit DNA single and double stranded breaks in murine 1210 leukaemia cells (Cohen *et al* 1980), an observation consistent with the general inhibition of DNA synthesis.

A)



B)



C)

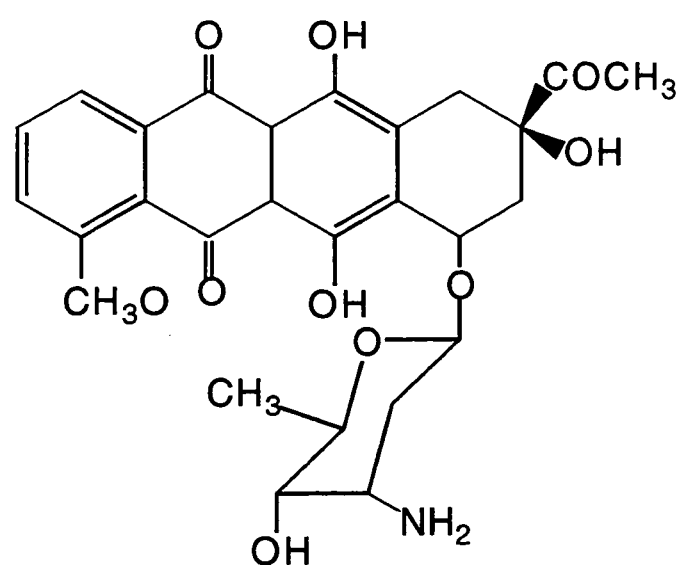


Fig 6. Structure of **A)** mitoxantrone **B)** ametantrone and **C)** daunorubicin.

Although a number of anthraquinones, such as doxorubicin, have been shown to undergo one electron reduction and subsequent redox cycling there is no convincing evidence to suggest that either mitoxantrone or ametantrone are subjected to the same fate (reviewed by Patterson 1993). Neither compound, compared to doxorubicin, generates detectable free radicals in MCF-7 cells (Fisher and Patterson 1990). Conversely, evidence of oxidative activation has been published (Reska *et al* 1989). The apparent lack of redox cycling observed in cells treated with mitoxantrone has, in part, prompted the development of a series of tertiary amine-*N*-oxide analogues of this compound which can be considered as bioreductive prodrugs. The rationale behind this idea is that the *N*-oxide functionality masks the cationic charge of the amine group. Under anaerobic conditions these compounds undergo reductive activation to yield a cytotoxic tertiary amine.

The lead compound in this series is AQ4N, a prodrug scheduled to enter clinical trial in 1998. AQ4N has been shown to be inactive aerobically in V79 cells *in vitro* as the partial negative charge on the *N*-oxide group is repulsive to the partial charge on the phosphate groups of DNA (Patterson *et al* 1994). This property makes the prodrug a poor DNA binding agent, consistent with the inability of AQ4N to elevate the melting temperature of calf thymus DNA (Patterson 1993). Under hypoxic conditions, and in the presence of NADPH supplemented liver microsomes, AQ4N undergoes a two electron reduction to yield the mono-*N*-oxide AQM, followed by a second two electron reduction to produce the cytotoxic tertiary amine AQ4 (Fig 7), which, unlike its *N*-oxide, is retained in cell nuclei (Smith *et al* 1997), binds to DNA, has similar cytotoxic activity *in vitro* to mitoxantrone and is a potent inhibitor of V79 topoisomerase II (Patterson *et al* 1992). The prodrug nature of

AQ4N has been investigated in a variety of murine models. Using B6D2F mice bearing the T50/80 mammary carcinoma the antitumour effect of AQ4N was potentiated *in vivo* by combination with hypobaric hypoxia (McKeown *et al* 1995). The same workers reported reduced systemic toxicity when using AQ4N compared to the other bio-reductive drugs RSU 1069 and tirapazamine.

AQ4N and other bio-reductives have also been investigated in clamped RIF-1, KHT and SCCVII neoplasms. Using this approach, Cole and coworkers (1995) were able to maximise the hypoxic subpopulation of cell within the tumour (*via* the clamp) and so study the effect of each bio-reductive used singly or in combination with radiation. They discovered that AQ4N alone (250 mg/kg) had a significant effect on the growth delay of RIF-1 and SCCVII tumours. Furthermore, following a dose of 25 Gy radiation the growth delay of these tumours was greatly enhanced in the presence of AQ4N (Cole *et al* 1995).

The antineoplastic effects of three *N*-oxide prodrugs namely: nitracine *N*-oxide (NC-NO), AQ4N and *N*-2-[(dimethylamino)ethyl] acridine-4-carboxamide DACA (NSC 601316) have been evaluated with respect to their ability to kill cells from a number of rodent and human cell lines and to retard the growth of the MDAH-MCA-4 mammary carcinoma. All three compounds were found to be cytotoxic to the cell lines under conditions of hypoxia. However, AQ4N was found to be superior to the other compounds in retarding the growth of the mammary tumour with or without a single dose (20Gy) of radiation prior to the drug treatment (Wilson *et al* 1996)

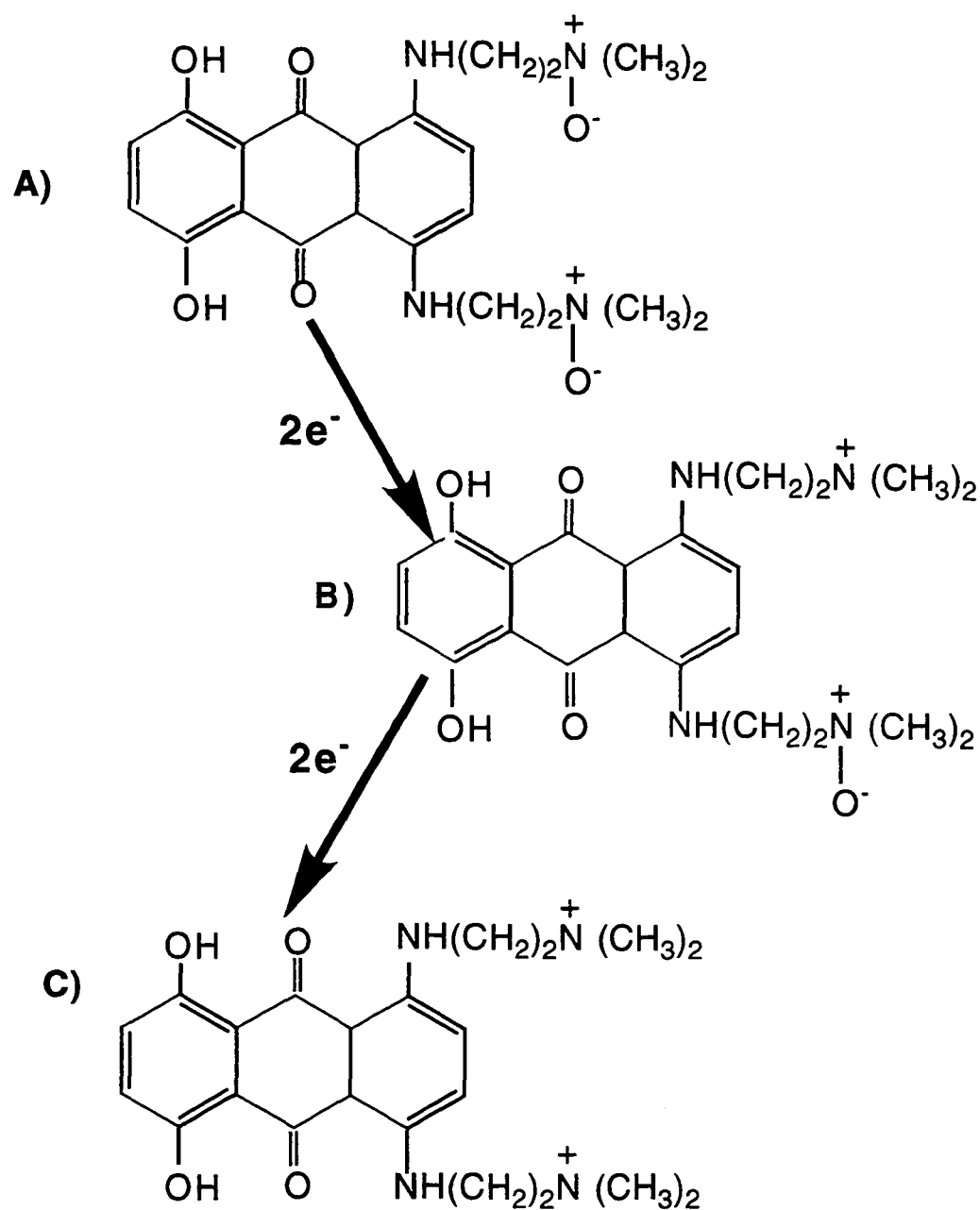


Fig 7. Reductive metabolism of the N-oxide based prodrug AQ4N.

AQ4N (**A**), undergoes a two electron reduction to produce the mono *N*-oxide intermediate AQM (**B**). A second two electron reduction produces the tertiary amine AQ4 (**C**)

1.5 Enzymology of bioreductive drug activation.

The effectiveness of hypoxia directed bioreductive therapy will be enhanced by identifying tumours that express high levels of appropriate reductase enzymes (Workman and Walton 1990). The following discussion reviews enzyme systems known to mediate the reductive metabolism of a number of pre-clinical and clinically relevant bioreductives. Furthermore, a number of enzyme systems that may have potential as bioreductases are also reviewed.

1.5.1 Aldehyde oxidase (AO)

Aldehyde oxidase (AO) is a molybdenum containing flavoprotein known to be located in the cytosolic compartment of mammalian cells (Wolpert *et al* 1973). The enzyme is able to catalyse the oxidation of a range of aldehydic and *N*-heterocyclic substrates (reviewed by Wolpert *et al* 1973). Furthermore, AO has been reported to catalyse the two electron reduction of SR 4233 to SR 4317 under anaerobic conditions (Walton and Workman 1990).

1.5.2 NADH: Cytochrome b₅ reductase.

NADH cytochrome b₅ is an enzyme which catalyses the NAD⁺ dependent reduction of cytochrome b₅ from the ferric state (+3) to the ferrous state (+2). The enzyme, isolated from rabbit erythrocytes, has been shown to metabolise mytomycin C to metabolites which are capable of alkylating 4-(*p*-nitrobenzyl) pyridine (PNBP) (Hodnick and Sartorelli 1993). The metabolism was found to have a pH optimum of 6.0, conform to Michaelis-Menten kinetics and was inhibited by dicoumarol in a concentration dependent manner. In addition, the alkylation of PNBP was shown to occur 1.5 times greater under hypoxic conditions (Hodnick and Sartorelli 1993).

NADH: cytochrome b₅ reductase has been immunochemically detected in a number of clinically resected human brain tumours (Rampling *et al* 1993). The same workers found that these tumours have significant regions of hypoxia and concluded that human brain tumours may be ideal candidates for bioreductive therapy.

1.5.3 Xanthine dehydrogenase/ Xanthine oxidase (XDH/ XO)

Xanthine dehydrogenase (XDH), a cytosolic molybdenum containing hydroxylase, is found in the cytosol and catalyses the rate limiting step in purine catabolism. Specifically, the enzyme hydroxylates hypoxanthine to xanthine followed by hydroxylation of xanthine to uric acid.(Pritsos and Gustafson 1994). The reaction is NADH dependent unlike the identical reaction catalysed by xanthine oxidase (XO) which is oxygen dependent and liberates two molecules of superoxide radicals (Pritsos and Gustafson 1994). Purified xanthine oxidase (XO) has also been shown to catalyse SR 4233 to both the two (SR4317) and the four (SR4330) electron reduced metabolites under hypoxic conditions (Walton and Workman 1990).

XDH has been shown to catalyse mytomicin C *via* a two electron reduction forming the stable metabolite 2,7-diaminomitosenone (Gustafson and Pritsos 1992). The metabolism again occurs more readily under hypoxia and the effect of mytomicin C concentration on velocity of reaction produces rectangular hyperbolic plots consistent with Michaelis-Menten kinetics (Gustafson and Pritsos 1993). The optimum pH for the reaction is found to be 6 and metabolism at pH 7.4 causes a doubling in K_m (halving of enzyme affinity) and a halving of V_{max} (Gustafson and Pritsos 1993).

A number of reports have documented a decreased level of XDH in a number of tumours from a variety of species. For example, decreased XDH protein has been described in two rat neoplasms, namely hepatoma 3924A (fast growing) and hepatoma 20 (slow growing) where levels of the protein were 2% and 33% of values observed in normal livers respectively (Ikegami *et al* 1986). Decreased XDH has also been reported in mouse colon (Weber *et al* 1978) and human kidney tumours (Weber *et al* 1977).

1.5.4 NAD(P)H: Quinone Oxidoreductase (DT diaphorase or NQO)

NQO activity was first reported in 1958 by Ernster and Navazio. Since then, four isozymes have been identified and are the products of separate gene loci designated *D1A 1* to *D1A 4* (Edwards *et al* 1980). The protein product of *D1A 4* has also been well studied and is referred to as NQO₁ (Riley and Workman 1992a). NQO₁ exists as a dimeric flavoprotein with a molecular mass of around 55 KDa. Activity is predominantly located in the cytosolic fraction (>90%) where it links the oxidation of NADH or NADPH, with equal preference, to the obligate two electron reduction of quinones and their derivatives (Riley and Workman 1992 a). In this respect NQO activity has a cytoprotective function limiting the formation of semiquinones and oxygen free radicals and so reducing oxidative stress (Ross *et al* 1993 and Riley and Workman 1992 a). The protective function of NQO has been demonstrated in cDNA transfection studies of COS-1 cells, where cells transfected with cDNA for NQO₁ prevent the binding of damaging semiquinones to DNA by eliminating their formation (Joseph *et al* 1994).

NQO's have also been implicated in the bioactivation of a variety of antitumour agents including mytomyacin C (Workman and Walton 1990). However, the role of these enzymes in the metabolism of MMC remains controversial (Workman and Walton 1990 and Workman *et al* 1989). The controversy centres around the effectiveness of dicoumarol as a specific inhibitor of NQO in experiments using subcellular fractions. Interestingly though, studies using purified rat and human NQO's have clearly shown that the enzyme is capable of bioactivating mytomyacin C, mytomyacin A, streptonigrin, CB 1954 and diaziquone (Beall *et al* 1994). The metabolism of MMC by NQO's was shown to induce cross linking of pBR322 DNA (Beall *et al* 1994). Although antitumour quinones EO9 and EO4 are both substrates for purified rat and human NQO's (Phillips 1996), only EO4 could produce cross linking of pKK233- 2 DNA following incubation with human or rat NQO. EO9, on the other hand, could only induce cross linking of DNA following incubation with the rat enzyme (Phillips 1996)

The metabolism of SR 4233 (figure 4) has also been shown to be mediated by NQO₁ purified from Walker 256 rat tumour cells (Riley and Workman 1992 b). The main products of this metabolism are the two (SR 4317) and four (SR 4330) electron reduced metabolites. As neither of these two metabolites are cytotoxic under conditions of hypoxia or normoxia, cells expressing high levels of NQO's may well be protected against this agent (Riley and Workman 1992 b).

Human NQO₁ is an inducible enzyme and its regulation is governed by a promoter sequence which contains a number of *cis* controlling elements (Figure 8 A). The induction of the enzyme by environmental and endogenous compounds has been reviewed by Joseph and co-workers

(Joseph *et al* 1994). The same laboratory has formulated a hypothetical model for the induction of NQO₁ (Figure 8 B).

NQO activity has been reported in brain tumours (Rampling *et al* 1993), and colorectal tumours (De Waziers *et al* 1991), is increased in colon tumours (Schor and Cornelisse 1983) and highly elevated (20-50 fold) in hepatoblastomas and hepatocarcinomas (Cresteil and Jaiswal 1993). The elevated expression of NQO's detected in these human tumours opens up exciting possibilities for the future development of novel bioreductives that can be specifically activated by NQO₁ enzymes.

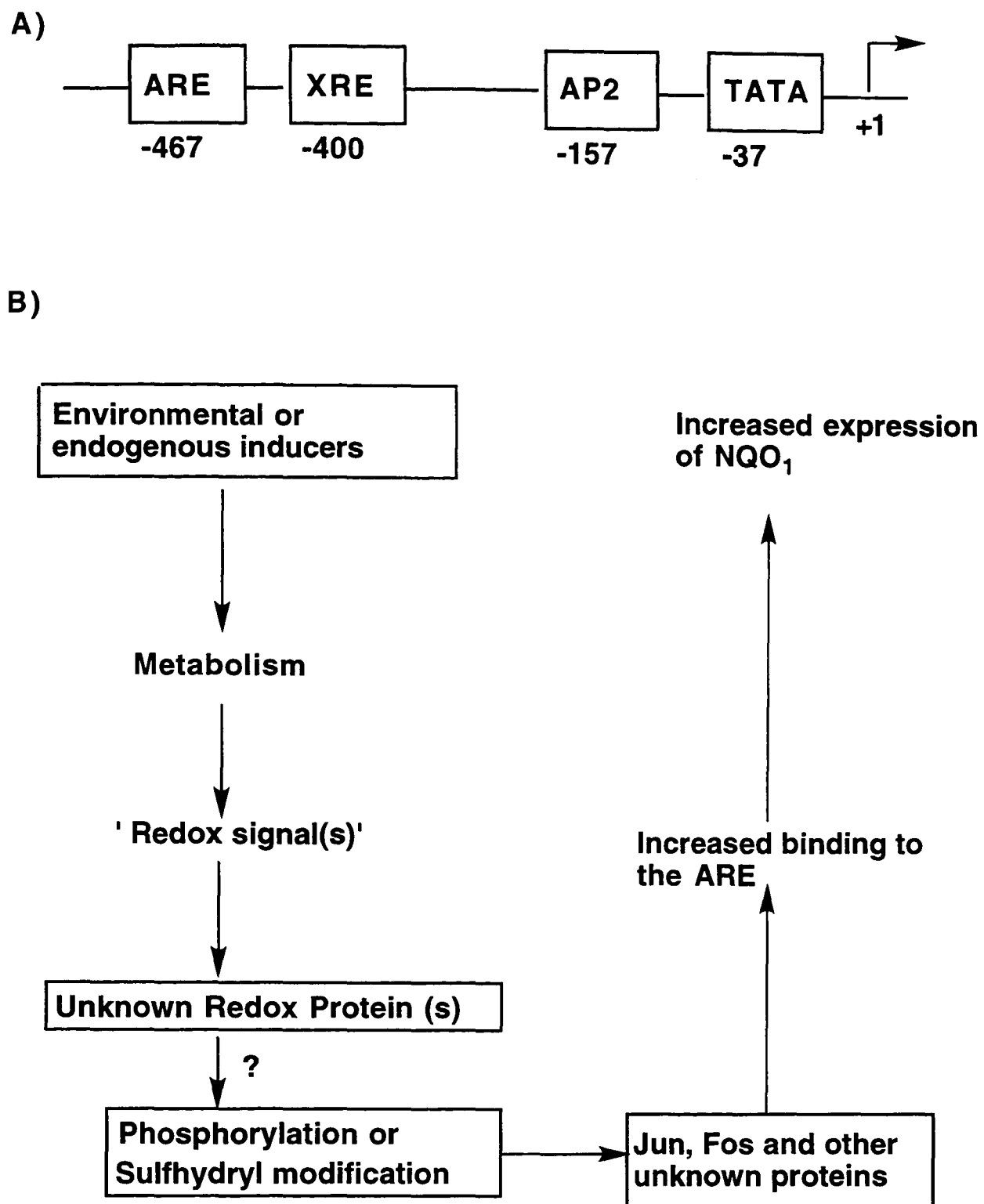


Fig 8. A) Human NQO1 gene promotor showing *cis* - elements needed for induction and regulation. ARE=antioxidant response element, XRE= xenobiotic response element. Numbers are base pairs downstream of initiation codon (+1). **B)** Hypothetical model for the induction of NQO₁ by environmental or endogenous compounds. Both figures are adapted from Joseph *et al* 1994.

1.5.5 NADPH Cytochrome P450 reductase (CPR)

NADPH cytochrome P450 reductase (CPR) is a flavoprotein with a molecular mass of 78 KDa (Backes 1993) each molecule of the enzyme contains one molecule of FMN and FAD. The enzyme is an integral component of the mixed function oxidase system (MFOS) and is located in the endoplasmic reticulum (ER) where its intimately associated with cytochrome P450 and cytochrome b₅, (Figure 9). The close association between CPR and cytochrome P450 is crucial to catalysis as CPR catalyses the transfer of electrons from NADPH to cytochrome P450 (Backes 1993).

CPR is encoded by a single gene which is highly conserved across mammalian species (Porter *et al* 1990). In rats, CPR levels are transcriptionally regulated by thyroid hormone (Ram and Waxman 1992) hypophysectomy or treatment with the antithyroid drug methimazole which leads to a 75-80% decrease in hepatic and 30-50% decrease in extrahepatic activity respectively (Ram and Waxman 1992).

CPR is a versatile enzyme and, as well as cytochrome P450, catalyses the reduction of a number of other substrates including haem oxygenase (Schacter *et al* 1972), cytochrome b₅ (Enoch and Strittmatter 1979), fatty acid elongase (Keyes *et al* 1979) and cytochrome c (Backes 1993). The reduction of oxidised cytochrome c is often used in the laboratory to measure CPR activity. Furthermore, CPR can catalyse the oxidative catabolism of free haem to biliverdin (Yoshinaga *et al* 1982, Docherty *et al* 1982 and Guengerich 1978). The latter reaction may assume particular importance during periods of haem overload and subsequent haem oxygenase saturation (Guengerich 1978).

Under hypoxic conditions purified rat CPR has been shown to bioactivate SR 4233 to the mono-*N*-oxide SR 4317 (Walton *et al* 1992). Indeed a human CPR cDNA transfected into human breast cancer cells was able to express the 78 KDa protein and confer enhanced sensitivity to both SR 4233 and RSU 1069 under conditions of hypoxia (Patterson *et al* 1997). In liver microsomes, the metabolism of the same drug was found to be inhibited by an inhibitory antibody to CPR (Walton *et al* 1992). CPR has also been implicated in the bioactivation of mytomycin C (Workman and Walton 1990) and resistance to this compound in CHO cells has also been attributed to decreased levels of CPR (Walton *et al* 1989)

To date, only a modest number of laboratories have investigated the expression of CPR in neoplastic tissue. For example, the enzyme has been found in rat glioma cells (Geng and Strobel 1995), and in human breast adenocarcinoma (Patterson *et al* 1995) and is elevated in colon carcinoma relative to normal mucosa (Mekhail- Ishak *et al* 1989).

1.5.6 Cytochrome P450 (CYP)

Cytochrome P450 (CYP) is a collective term used to describe a gene superfamily of proteins involved in the oxidative, peroxidative and reductive metabolism of a wide range of structurally diverse xenobiotic and endogenous compounds (Gonzalez 1989 and Nelson *et al* 1993). CYP was first identified as a reduced hepatic pigment which bound carbon monoxide to give a characteristic absorption maxima at 450 nm (Klingenberg 1958 and Garfinkle 1958). The reduced pigment was later characterised as a haemoprotein and named cytochrome P450 by Omura and Sato (Omura and Sato 1964).

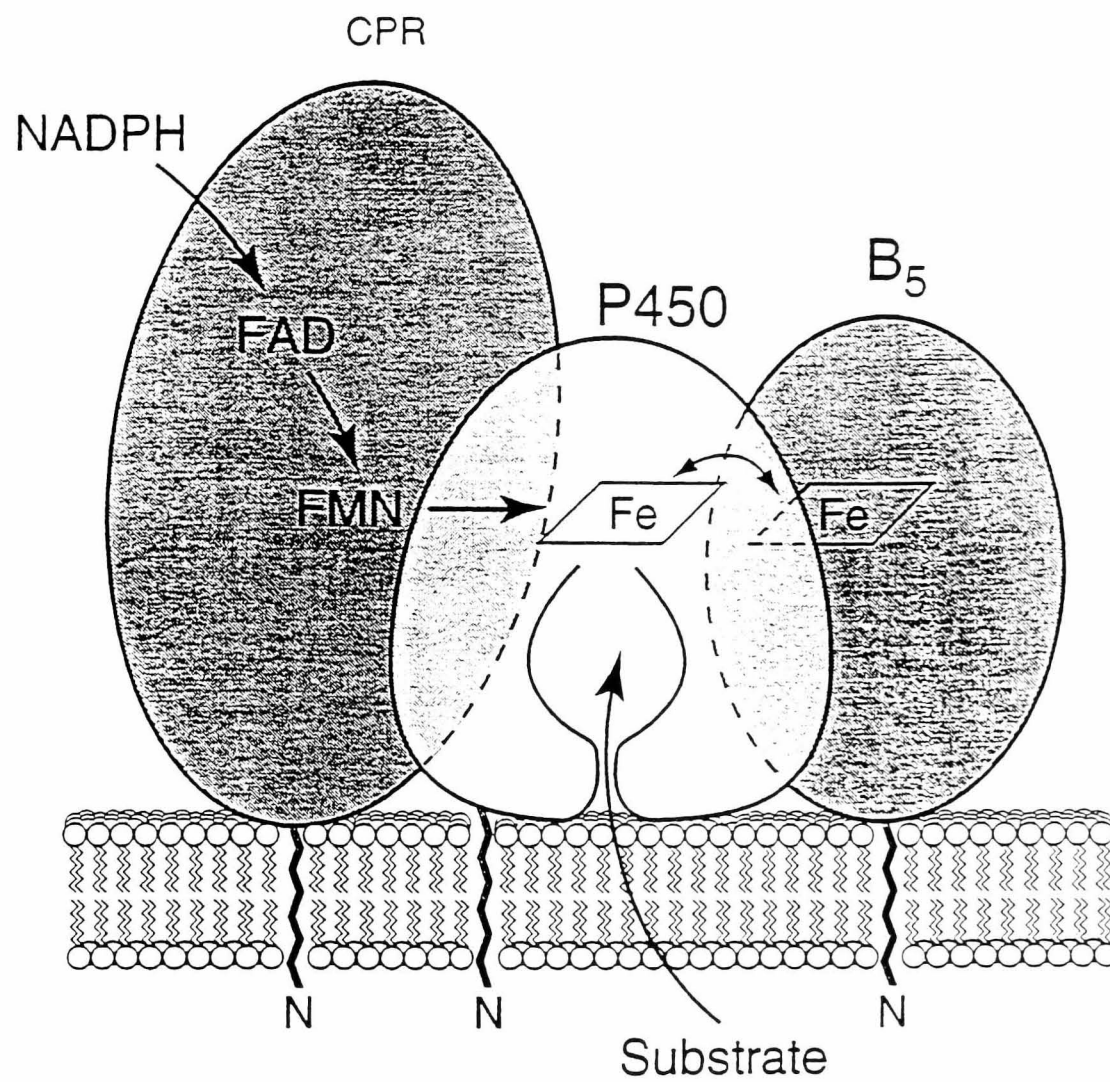


Fig 9 Association of Cytochrome P450 Reductase(CPR) and Cytochrome P450 in the endoplasmic reticulum (ER) (From Jefcoate 1995).

Since the identification of this spectrally apparent haemoprotein, numerous isoforms have been purified and characterised with respect to their catalytic specificity (Gonzalez 1989). However, until fairly recently, CYP research had been hampered by the lack of a systematic method for the naming of existing and newly discovered isoforms. To overcome this problem, a system of nomenclature has been introduced which categorises CYPs based on their primary amino acid sequence (reviewed by Nelson 1995). Specifically, any CYP with a sequence homology $\geq 40\%$ of another CYP is placed in the same family which are designated by roman numerals. Furthermore, any CYP with a sequence homology $\geq 55\%$ of another family member is placed in the same subfamily (represented by capital letters). Genes within a subfamily are identified by sequential numerals. For example, two genes in the CYP 1A subfamily are CYP 1A1 and CYP 1A2 respectively (Paine 1991).

As of 1994, 325 separate CYPs have been sequenced. The sequences belong to 50 families, 82 subfamilies and originate from 67 separate species (Nelson 1995). In mammals, families 1 to IV encode microsomal CYPs involved in xenobiotic metabolism whereas families XI, XVII, XIX and XXI code for CYPs involved in endogenous metabolism (Paine 1991 and Gonzalez 1989). Families 1 to IV will be briefly reviewed below. However, the mechanistic nature of CYP catalysis is discussed first with particular emphasis on CYP mediated reduction.

1.5.6.1 The Catalytic Cycle of CYP

The oxidative catalysis of a substrate molecule by CYP has been extensively discussed (reviewed by Murray and Reidy 1990 and Groves and Yuan- Zhang 1995). The essential steps in catalysis are believed to follow the sequence (1) Substrate (RH) binding. (2) Reduction of ferric Fe^{3+} to ferrous Fe^{2+} . (3) Binding of dioxygen to give a ferrous CYP-dioxygen complex. (4) Transfer of a second electron to the complex. (5) Protonation and breaking of the O- O bond with subsequent incorporation of the distal oxygen atom into a molecule of water and the formation of a reactive- oxo species. (6) Finally, transfer of the bound oxygen to the substrate and dissociation of the new molecule (ROH) away from the active site (Groves and Yuan- Zhang 1995). The catalytic cycle is shown in Figure 10.

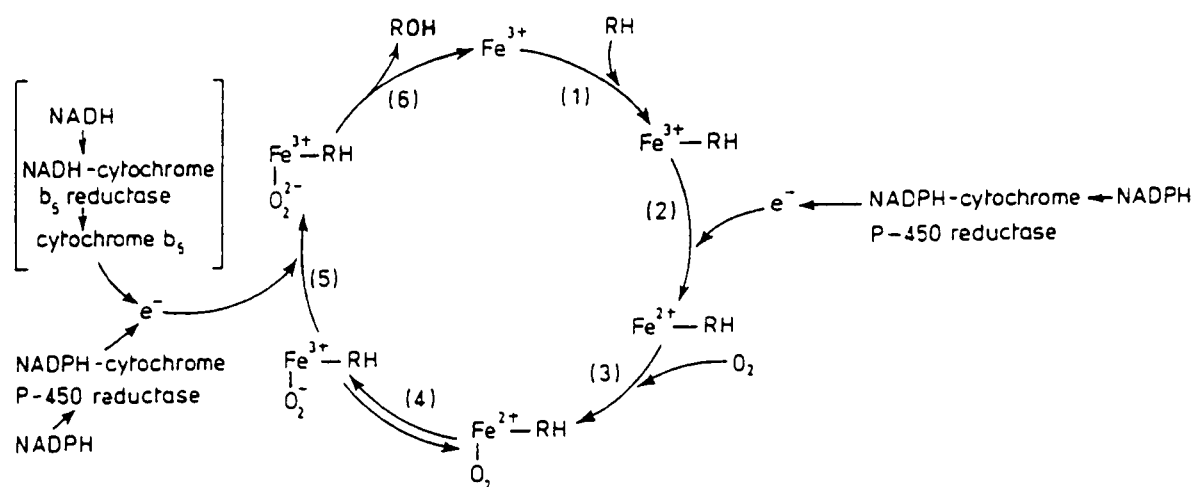


Fig 10. Catalytic cycle of CYP mediated metabolism
RH= substrate and ROH= the hydroxylated metabolite (From Gibson and Skett 1994)

Evidence for CYP mediated reduction under anaerobic conditions came from investigations using imipramine *N*-oxide, tiaramide *N*-oxide, and *N,N*-dimethylaniline *N*-oxide. All three of these compounds were found to be extensively reduced in liver, kidney, lung and intestinal microsomes by a process that occurred optimally at physiological pH and temperature, showed a preference for NADPH over NADH as reduced cofactor, and was inhibited by carbon monoxide and oxygen (Sugiura *et al* 1976). In addition, microsomes from phenobarbital treated rats metabolised indicine *N*-oxide with a higher V_{\max} than untreated animals, the K_m for both treated and control remained the same (Powis and Wincentzen 1980). Induction/ inhibition studies prompted Powis and Wincentzen to speculate on a novel CYP isoform that could reduce indicine *N*-oxide by utilising NADH as cofactor but would not contribute to oxidative metabolism (Powis and Wincentzen 1980). Furthermore, purified rabbit CYP's reconstituted with CPR have also been shown to reduce indicine *N*-oxide under conditions of hypoxia.

1.5.6.2 The CYP 1A subfamily

In rats, members of the CYP 1A subfamily are inducible by 3-methylcholanthrene (3 MC), beta-naphthoflavone (beta-NF), aroclor 1254 and tetrachlorodibenzo-p-dioxin (TCDD) (Funae and Imaoka 1995 and Paine 1991). CYP1A1 from both rat and man can catalyse 7-ethoxycoumarin and 7-ethoxyresorufin O-deethylations (ECOD and EROD) (Burke *et al* 1985). The same enzymes are able to mediate the hydroxylation of benzo[a]pyrene (Nebert and Gonzalez 1987). Rat and human CYP 1A1 are reported to share an amino acid sequence homology of 80% (reviewed by Soucek and Gut 1992). Human CYP 1A1 is highly inducible in extrahepatic tissue by cigarette smoke (Nedelcheva and

Gut 1994). and its induction in lung tissue has been linked to the onset of carcinogenesis in heavy smokers (Garcia- Closas *et al* 1997).

Human CYP 1A2 has 75% sequence homology to the rat orthologue and 68% homology with human 1A1 (Spazenegger and Jaeger 1995). CYP 1A2 from rat or man is responsible for the catalysis of a number of carcinogens to various products (Quattrochi *et al* 1994) aswell as metabolising a range of drugs in clinical use(Nedelcheva and Gut 1994).

1.5.6.3 The CYP 1B subfamily

The CYP 1B subfamily have only recently been described (Sutter *et al* 1994) and to date, only one dioxin inducible member, CYP 1B1, is known to exist (Sutter *et al* 1994). CYP 1B1 will be discussed later with reference to its expression in cancer tissue.

1.5.6.4 The CYP 2B subfamily

The rat CYP 2B subfamily consists of three separate genes namely 2B1, 2B2 and 2B3 (Paine 1991). CYP 2B1/2B2 are both inducible by phenobarbital whereas 2B3 is refractory to phenobarbital treatment (Paine 1991). Rat CYP 2B has been linked to the reductive activation of tirapazamine (Walton *et al* 1992).

To date, the only 2B enzyme known to be expressed in human liver is CYP 2B6 (Mimura *et al* 1993). As well as nicotine metabolism, CYP 2B6 is thought to metabolise the oxidative activation of the anticancer drug cyclophosphamide (reviewed by Gonzalez 1993). Furthermore, human CYP 2B6 overexpressed in lymphoblastoid cell lines has been shown to bioactivate tirapazamine under hypoxic conditions (Lewis *et al* 1995).

1.5.6.5 The CYP 2C subfamily

Five CYP 2C isoforms are presently known to exist in the rat, namely: CYP 2C6, 2C7, 2C11, 2C12 and 2C13 (Gonzalez 1989). CYP 2C11 and 2C12 are male and female specific respectively and their expression is controlled in part by testosterone (Paine 1991 and Gonzalez 1989). CYP 2C13 is also a male specific isoform, its expression varies considerably between individual animals and increases during the onset of sexual maturation (Mc Clellan- Green 1989). The rat 2C subfamily members have been implicated in the hypoxia dependent activation of tirapazamine (Walton *et al* 1992).

There appears to be at least six different human CYP 2C isoforms (reviewed by Guengerich 1995). The isoforms known are CYP 2C8, 2C9, 2C10, 2C17, 2C18 and 2C19 (reviewed by Guengerich 1995 and Nedelcheva and Gut 1994). Human 2C enzymes are involved in a large number of drug biotransformations including the 6 alpha hydroxylation of the anticancer drug taxol (Cresteil *et al* 1994), hydroxylation of (S)-mephenytoin (Relling *et al* 1990) and the 7-hydroxylation of the anticoagulant (S)-warfarin (reviewed by Spatzenegger and Jaegar 1995). CYP 2C9 is the most abundant 2C form in human liver and has a high catalytic activity towards tolbutamide (reviewed by Guengerich 1995). All human CYP 2C enzymes have a sequence homology which is 80% identical to each other (Romkes 1991).

1.5.6.6 The CYP 2D subfamily

CYP 2D1 and 2D2 have been isolated from untreated male rats (Gonzalez 1987). These two isoforms share a sequence identity of around 73% and appear to be differentially regulated (reviewed by Funae and Imaoka 1995). Humans express CYP 2D6 and the enzyme

has been the focus of much research as it is responsible for the debrisoquine/ sparteine polymorphism. Approximately 7% of American and European Caucasians possess two mutant alleles for CYP 2D6 and, as such, are unable to metabolise debrisoquine, spartein and around twenty other drugs (reviewed by Spatzenegger and Jaeger 1995). The expression of functional CYP 2D6 has also been linked to an increased risk of tobacco activated lung cancer (Crespi *et al* 1991)

1.5.6.7 The CYP 2E subfamily

The ethanol inducible CYP 2E enzyme has been identified in rats, rabbits and man (reviewed by Nedelcheva and Gut 1994) and all three of these proteins share an amino acid sequence homology of around 80% (Gonzalez 1989). CYP 2E is able to mediate the catalysis of ethanol, acetone and halogenated hydrocarbons (reviewed by Nedelcheva and Gut 1994). Moreover, the enzyme has been linked to the activation of a number of xenobiotics to damaging electrophilic metabolites that may be responsible for the initiation of carcinogenesis (Yang *et al* 1990 and reviewed by Nedelcheva and Gut 1994). For example, the activation of *N*-nitrosodimethylamine (NDMA) and *N*-nitrosodiethylamine (NDEA) via the process of alpha carbon oxygenation have both been reported to occur in human cell lines expressing a CYP 2E1 gene (Crespi *et al* 1990). Furthermore, the activation of NDMA has been found to correlate significantly with the expression of CYP 2E in a panel of sixteen different human liver microsome preparations (Yoo *et al* 1988). Under anaerobic conditions CYP 2E, like CYPs 2B/2C and 3A, has also been reported to bioactivate the anticancer prodrug SR4233 to a nitroxyl radical which is capable of DNA damage (Khan and O' Brien 1995). The bioactivation of SR4233 has been discussed in section 1.4.2 and is depicted in Figure 4.

1.5.6.8 The CYP 3A subfamily

In rats two CYP 3A proteins exist, namely CYP 3A1 and CYP 3A2 (Paine 1991). Both forms are induced in the liver by phenobarbitone but the level of induction is less than that seen for CYP2B enzymes (Paine 1991). Interestingly, rat CYP 3A1 is also induced by PCN whereas 3A2 is refractory to the same treatment (Paine 1991). Rat CYP 3A enzymes demonstrate catalytic activity towards testosterone 6-beta-hydroxylation (Halvorson *et al* 1990), ethylmorphine and erythromycin demethylation (reviewed by Paine 1991) and nifedipine oxidation (Guengerich *et al* 1986). Furthermore, PCN induced rat liver microsomes bioactivate SR4233 to the mono-*N*-oxide SR 4317 under anaerobic conditions, a finding consistent with the involvement of CYP 3A (Walton *et al* 1992).

In humans the CYP 3A subfamily currently comprises four separate enzymes, namely CYP 3A4, 3A3, 3A5 and 3A7 (reviewed by Li *et al* 1995). Human CYP 3A enzymes are constitutively expressed in the liver where their expression makes up approximately 30% of total hepatic CYP. CYP 3A5 is expressed in about 20% of adult livers. For review see Li *et al* (1995).

The CYP 3A subfamily are a remarkable group of enzymes as they have been implicated in the metabolism of over 50% of drugs administered to man (Wacher *et al* 1995). Interestingly, the CYP 3A mediated catalysis of amitriptyline and aflatoxin B₁ have both recently been reported to conform to sigmoid kinetics (Schmider *et al* 1995 and Gallagher *et al* 1996) implying that CYP 3A enzymes can undergo steric activation in a manner more commonly observed in multimeric proteins (Dickins and Bayliss 1996).

1.5.6.9 The CYP 4A subfamily

A number of structurally diverse xenobiotics including the industrial plasticiser di-2-(ethylhexyl) phthalate, chlorinated phenoxy acid herbicides and the hypolipidaemic drug clofibrate induce a rat hepatic CYP termed CYP 4A1 (reviewed by Paine 1991) and (Sundseth and Waxman 1992). CYP 4A1 catalyses the terminal (omega) carbon atom hydroxylation of medium and long chain fatty acids and has been linked to the induction of peroxisome proliferation (reviewed by Sundseth and Waxman 1992). The amino acid sequence homology of CYP 4A1 to that of the other CYP proteins is less than 35% (Gonzalez 1989) suggesting CYP 4A1 diverged early on in the process of CYP evolution (Paine 1991).

1.5.7 CYP expression in cancer

The expression of CYPs in neoplastic tissue has important clinical consequences if these enzymes are to be exploited as potential therapeutic targets for novel and existing bioreductives. The last few years has witnessed an emerging trend within the scientific literature documenting the presence of various CYP isoforms in a increasing number of cancers both of human and animal origin. In particular, CYP 1A and CYP 3A have both been detected in human tumours of the colon (McKay *et al* 1993), breast (Murray *et al* 1993 ^a), oesophagus, liver (reviewed by Wacher *et al* 1995) and various soft tissue sarcomas (Murray *et al* 1993 ^b). CYP 3A has been also detected in human lung tumours (Kivisto *et al* 1995) and renal cell carcinomas (G Murray personal communication). Indeed a link between CYP 3A and P-glycoprotein expression in cancer cells has been described by Wacher *et al* (1995). Moreover, the expression of CYP 2A, 2B, 2C and 3A have all

been reported to be induced in human breast and colon xenografts (Smith *et al* 1993).

The recently sequenced CYP 1B1 enzyme has been reported to be highly expressed in a number of human cancers (Murray *et al* 1997) and its expression within these cancers seems to exceed the expression observed in paired normal tissue (Murray *et al* 1997).

1.6 Enzyme systems with potential to activate bioreductive agents.

Both nitric oxide synthase (NOS), and the cytochrome P450 reductase (CPR)/haem oxygenase (HO) system may have the potential to reductively activate prodrugs under conditions of hypoxia. These two enzyme systems are briefly outlined below.

1.6.1 Nitric Oxide Synthase (NOS)

Several forms of nitric oxide synthase (NOS) are known to exist (Knowles and Moncada 1994) which catalyse the formation of nitric oxide (NO) from L-arginine (Bredt and Snyder 1989). NO is involved in a number of important physiological processes serving both as a neurotransmitter and vasodilator (reviewed by Wang *et al* 1993). Consequently, inhibition of NOS leads to vasoconstriction and increased hypoxia (Reviewed by Butler *et al* 1997). The increased hypoxia caused by NOS inhibition has prompted Butler and coworker to exploit this phenomenon for the activation of bioreductive prodrugs. Indeed, nitro-L-arginine mediated inhibition of NOS enhances the bioreductive toxicity of RB 6145 in KHT and SCCVII murine tumours (Butler *et al* 1997).

However, apart from NOS inhibition, NOS may be able to act as a reductase of bioreductive agents itself. The author bases this postulate

on the following points. (i) The enzymes are haem based proteins similar to members of the CYP family (White and Marletta 1992). (ii) the enzymes contain a CPR like domain with binding sites for NADPH, FAD and FMN and can be envisaged as a self contained CPR/ CYP chimeric protein (reviewed by Schmidt *et al* 1993).and (iii), elevated NOS expression has been detected in a number of human tumours, compared to normal tissue (Thomsen *et al* 1994).

1.6.2 The Cytochrome P450 reductase (CPR)/ haem oxygenase (HO) system

Microsomal haem oxygenases (HOs) are monomeric enzymes which (in conjunction with CPR) utilise NADPH and oxygen to oxidise haem to biliverdin with the subsequent liberation of carbon monoxide (Abraham *et al* 1988). Biliverdin is broken down further to bilirubin by the action of cytosolic biliverdin reductase (Ewing *et al* 1993). Two HO enzymes are known to exist (HO-1 and HO-2) and both are the products of two separate genes (Cruse and Maines 1988). Hypoxic conditions, and a variety of other environmental stresses, leads to the up regulation of HO-1 mRNA and, in turn, elevated HO-1 protein (Murphy *et al* 1991, Applegate *et al* 1991 and reviewed by Choi and Alam 1996). Under these conditions, the CPR/ HO system might act as a make shift haemoprotein with a reduced potential to oxidise haem (due to a poverty of molecular oxygen) but , instead, passing electrons onto another electron acceptor molecule such as the nitrogen atom of an N-oxide based prodrug. If this scenario did occur, then HO proteins would be ideal targets for prodrug therapy as they are highly expressed in a variety of neoplastic tissue including Hodgkin's disease (reviewed by Schacter 1988), squamous carcinomas (Murphy *et al* 1993) and renal cell carcinomas (Goodman *et al* 1997).

1.7 Aims

From the preceding discussion it is clear that bioreductive activation of anti cancer prodrugs is a process dependent on the presence of appropriate 'activating' enzymes. The identity of enzymes known to mediate the reductive activation of a number of model bioreductives, such as the mitomycins and the heterocyclic-*N*-oxide tirapazamine, have been widely published in the scientific literature (reviewed by Workman and Stratford 1993). AQ4N, on the other hand, is a novel anthraquinone di-*N*-oxide prodrug due to enter clinical trial in 1998. To date, detailed investigations into the enzymatic conversion of AQ4N to its active metabolites have not been published. There is, however, evidence that rodent cytochrome P450s (CYP) can reductively activate a number of model *N*-oxides (reviewed by Bickel 1969, Sugiura *et al* 1977 and Powis and Wincentzen 1980). With this in mind the aims of the present work were:

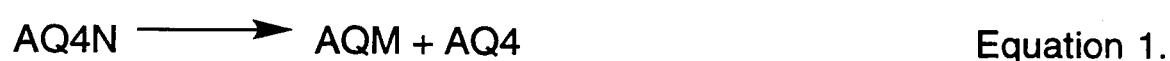
1) To investigate the metabolism of AQ4N and its mono-*N*-oxide AQM in rat subcellular fractions, a rich source of enzymes, and determine whether rat cytochrome P450 enzymes (CYP) were able to metabolise both compounds. Furthermore, preliminary experiments were performed to investigate the ability of a recombinant nitric oxide synthase (NOS) and the cytochrome P450/haem oxygenase (CPR/ HO) enzyme complex to bioreduce AQ4N.

2) To extend the findings of the above to establish whether human CYP enzymes were capable of AQ4N and AQM metabolism. Furthermore, experiments were performed to determine whether renal and colonic human tumours were able to support the metabolism of AQ4N.

3) To conduct a preliminary investigation into the *in vivo* metabolism of AQ4N in mice bearing a number of different tumours with a view to (i) Identifying metabolites of AQ4N in tumour material and so confirm AQ4N metabolism is not restricted to the *in vitro* setting and (ii) establish whether the quantity of AQ4 detected in the tumours correlates with their *in vivo* sensitivity to AQ4N treatment as determined by Cole and co workers (1995).

1.8 Definition of terms

Throughout the course of this thesis the terms 'metabolism of AQ4N' have been used to represent the process shown in Figure 7 and summarised in equation 1.



Where AQ4N = The anathraquinone di-*N*-oxide prodrug

AQM = The two electron reduced mono-*N*-oxide of AQ4N

and AQ4 = The fully reduced cytotoxic tertiary amine.

The terms 'total metabolism' or 'total substrate turnover' have been used and refer to the sum of metabolites (AQM +AQ4) produced following incubation of AQ4N with various subcellular fractions.

Furthermore, where AQM has been used as substrate, the terms 'metabolism of AQM', 'AQM to AQ4' and/ or 'AQ4 from AQM' refer to the process shown in equation 2.



Chapter 2

Chapter 2

Materials and methods

2.1 General Approach used to study the metabolism of AQ4N

The approach followed in identifying the major bioreductive enzymes of AQ4N and AQM was broadly based on enzyme directed methodology as described by Workman and Walton (Workman and Walton 1990). Firstly, metabolic studies were conducted in rat subcellular fractions under various conditions of pH, temperature and various oxygen tensions. The results of these experiments would indicate the nature and extent of metabolism and help identify the optimum conditions under which AQ4N and AQM metabolism occurred. Furthermore, preliminary *in vitro* metabolism studies were conducted on the ability of some purified CYP related enzyme systems to metabolise AQ4N, namely nitric oxide synthase (NOS) and the cytochrome P450 reductase/haem oxygenase system (CPR/ HO).

Secondly, to establish the involvement of CYP's in the metabolism of AQ4N and AQM a selection of microsomes prepared from rats pretreated with known CYP inducers were incubated with both substrates under optimum metabolising conditions. To clarify the findings of these experiments incubations were repeated using the general CYP inhibitors, carbon monoxide and ketoconazole and chemical, isoform specific, inhibitors. The kinetics parameters of AQ4N metabolism in rat microsomes, V_{\max} and K_m , were established by firstly carrying out pre-kinetic experiments. These experiments were designed to determine at what point metabolite production deviated from linearity and hence establish a range over which metabolism is first order with respect to time and protein concentration. These experiments were conducted at

optimum pH, temperature and using saturating substrate and cofactor solutions.

AQ4N and AQM metabolism was investigated in 17 human liver microsome preparations which had been phenotyped with respect to their CYP expressions / activities. Correlation analysis was then used to determine which CYP's were responsible for the metabolism of both substrates. The kinetic data, V_{\max} , K_m and intrinsic clearance CL_{int} for three individual livers was determined using a similar protocol to that used for the rat. The CYP involvement in metabolism of AQ4N was then confirmed by the use of isoform specific inhibitors and the use of microsomes prepared from human lymphoblastoid cell lines transfected with a vector insert carrying a cDNA specific for a single CYP. Basic metabolism experiments were then carried out in a variety of human normal and paired neoplastic tissue, along with experiments using carbon monoxide as a general CYP inhibitor to ascertain the involvement of CYP in any metabolism observed.

Finally, the *in vivo* metabolism of AQ4N was investigated in tumour and non tumour bearing rodents. AQ4N was given i.p. to the animals and, following animal sacrifice, tissues were removed and assayed for the presence of AQ4N and its metabolites.

2.2 Chemicals

Chemicals used were obtained from the following sources: All standard laboratory reagents were purchased as the highest commercially available grade and obtained from BDH Ltd, Poole, UK. 1,4-Bis-{{2-(dimethylamino-*N*-oxide)ethyl}amino}-5,8-dihydroxy-anthracene-9,10-dione (AQ4N), 1,-{{2-(dimethylamino-*N*-oxide)ethyl}amino}-4-{{2-[

dimethylamino]ethyl]amino}-5,8-dihydroxyanthracene-9,10-dione (AQM) and 1,4-Bis-{{2-(dimethylamino)ethyl]amino}-5,8-dihydroxy-anthracene-9,10 dione (AQ4) were synthesised in house by Mr K. Ruparelia and shown to be pure and authentic by HPLC, MS, NMR and elemental analysis. Benzoxyresorufin and Diethylthiocarbamate (DIE) were both obtained from Aldrich, Ltd, Dorset, UK. Clofibrate (CLO), haemin, isoniazid (ISO), ketoconazole (KET), 3-methylcholanthrene (3MC), metyrapone (MET), reduced nicotinamide adenine dinucleotide (NADH), olive oil (OO), phenobarbitone (PB), pregnenolone-16alpha-carbonitrile (PCN), Triacetyloleandomycin (TAO), and Tween 80 (TWE), were all obtained from Sigma Ltd, St Louis, USA. Nicotinamide adenine dinucleotide phosphate (NADPH) was obtained as the tetra sodium salt from Park Scientific Ltd. Ethylenediamine tetra acetic acid (EDTA) was obtained from BDH Ltd, Poole, UK. Bromophenol blue, Dithiothreitol, glycine, sodium dodecyl sulphate (SDS), TEMED, and TRIS (hydroxymethylaminomethane) were all obtained from Biorad Laboratories, CA, USA

2.2.1 Human tissue acquisition.

Human livers were kindly provided by Professor M Danny Burke. Permission having previously been obtained from the Joint Ethics Committee of Aberdeen University and Aberdeen Royal Hospital NHS Trust. Livers, from either road accident victims or organ donor patients were removed within 30 min of circulatory arrest, placed in ice cold isotonic saline and cut into 2 x 2 x 4 cm pieces before being stored at - 80 °C. All samples had previously been screened for hepatitis B and HIV infection and found to be negative for both. Kidney and colon samples from patients having undergone surgical resection for a number of neoplasms, along with samples of normal tissue resected from the same

patients, were provided from Dr G I Murray, Department of Pathology, Aberdeen University, UK. The clinical data associated with the human liver microsome preparations and the human tumours are shown in tables 2 and 3 respectively. Gloves were used when handling human tissue and at the end of experiments all work surfaces and other equipment were washed in Viron disinfectant. (Antec Ltd, Sudbury, UK).

Table 2 Characteristics of human livers used .

† Smoking is classed as either nil, minor (≤ 5 cigarettes per day) or major (≤ 6 cigarettes per day). * Alcohol consumption is classed as either nil, minor (social or occasional drinker) or major (regular or heavy drinker)

Sample	Age	Sex	Drug history(Smoking [†] /Alcohol*)
HLM 26	55	F	Moderate alcohol/ Nil smoker.
HLM 29	63	F	Minor alcohol/ No information.
HLM 32	66	F	Moderate alcohol/ Heavy smoker.
HLM 33	47	F	Moderate alcohol/ No information.
HLM 34	41	F	Moderate alcohol/ Heavy Smoker.
HLM 35	No information		No information.
HLM 36	39	F	Minor alcohol/ Heavy smoker.
HLM 38	53	F	Nil alcohol/ Nil smoker.
HLM 44	44	F	Moderate alcohol/ Heavy smoker.
HLM 45	21	M	Major alcohol/ Medium smoker.
HLM 47	22	F	Moderate alcohol/ Heavy smoker.
HLM 48	31	M	No information/ No information.
HLM 50	37	M	Major alcohol/ Heavy smoker.
HLM 52	48	M	Major alcohol/ Heavy smoker.
HLM 53	38	M	Major alcohol/ Heavy smoker.
HLM 54	58	M	Major alcohol/ Heavy smoker.
HLM 55	60	M	Moderate alcohol/ Ex smoker.

Table 3 Characteristics of human normal and neoplastic tissue used.

Sample and ID	Age/ Sex	Type of Tumour
Kidney/ HKT 5	62/ M	Clear cell carcinoma
Kidney/ HNK 5	"	Paired normal tissue from HKT 5
Kidney/ HKT 6	65/ F	Clear cell carcinoma
Kidney/ HNK 6	"	Paired normal tissue from HKT 6
Colon/ HCT 4	66/ F	Adenocarcinoma
Colon/ HNC 4	"	Paired normal tissue from HCT 4
Colon/ HCT 5	52/ F	Adenocarcinoma
Colon/ HNC 5	"	Paired normal tissue from HCT 5

2.2.2 Enzymes and transfected cell microsomes

Lymphoblastoid cell microsomes (10 mg/ mL) expressing CYP 3A4, CYP 2B6, control and CPR were obtained from Gentest Inc. (Woburn, MA, USA). The individual microsome preparations were prepared by cDNA mediated gene transfection into recipient b- lymphoblastoid cells (AHH-1 TK \pm cell lines) as described by Crespi *et al* (1993). Microsomes were provided with the following marker activities of CYP as documented in the manufacturers literature: CYP 2B6 (360 pmole/min/mg of 7-ethoxy- 4-trifluoromethylcoumarin deethylation) and CYP 3A4 (2020 pmole/min/mg of testosterone 6 beta-hydroxylation). The activities of transfected microsomes bearing the cytochrome P450 reductase and CYP 3A inserts are described in section 2.9.2. Haem oxygenase protein (HO- 1) was the gift of Professor Ortiz de Montellano (The University of California, San Francisco, USA). The enzyme provided was a truncated form of the human HO-1 protein. In essence, a DNA sequence without the bases coding the terminal 23 amino acids was constructed in the pBAce vector and expressed in *E. coli*. The purification and activity of this protein has been described in detail by Wilks and Ortiz de Montellano (Wilks and Ortiz de Montellano 1993). Recombinant rat brain nitric oxide synthase (nNOS) was provided by Dr V Riveros- Moreno (Wellcome Research Laboratories, Beckenham, UK). The enzyme was expressed in the baculovirus system (Charles *et al* 1993), and purified by the method described by Riveros- Moreno *et al* (1995). Rat cytochrome P450 reductase (CPR) was provided by Professor C R Wolf (Molecular Pharmacology Unit, Ninewells Hospital and Medical School, Dundee, UK). Molecular mass markers (range: 14- 70 KDa) were obtained as pre made mixtures from The Sigma chemical Company, St Louis, MO, USA.

2.3 Animal inducer treatments

Male Sprague Dawley (200-250 g) rats were housed in standard laboratory cages and allowed free access to food and water before the following treatments were started.

2.3.1 Phenobarbitone (PB) an inducer of CYP 2B (Guengerich *et al* 1982): Rats were given a 0.1% (w / v) solution of sodium phenobarbitone (BDH) in drinking water for 6 days followed by a day of rest with normal drinking water before being killed.

2.3.2 Clofibrate (CLO) an inducer of CYP 4A (Sundseth and Waxman 1992): clofibrate (Sigma) was administered (i.p.) at a concentration of 200 mg / kg of body weight dissolved in 0.5 mL of 2.5% tween 80 once a day for 4 days prior to 1 day of rest before being killed. CYP 4A inducer

2.3.3 Pregnenolone 16alpha-carbonitrile (PCN) an inducer of CYP 3A: (reviewed by Murray and Reidy 1990): Rats were given a 5% (w/v) solution of PCN (Sigma), approximately 50 mg dissolved in 0.5 mL of 2.5% tween 80 (Sigma) once a day for 4 days prior to 1 day of rest prior to being killed.

2.3.4 Isoniazid (ISO) an inducer of CYP 2E (Ryan *et al* 1985): Rats were given 0.1% isonicotinic acid hydrazide (Sigma) (w /v) dissolved in drinking water *ad libitum* for 10 days, followed by a day of normal drinking water, before being killed.

2.3.5 3-Methylcholanthrene (3 MC) an inducer of CYP 1A (Ryan *et al* 1979): Rats were given 2 mL of 1% (w/v) 3 MC (approximately 80 mg / kg

body weight) dissolved in olive oil (Sigma) by i p injection and killed 72 hours later.

2.3.6 Inducer controls. Rats were treated in an identical manner to treated animals but given the injection vehicle minus the inducing agent. Specifically, controls for PCN and CLO treated rats were given 0.5 mL of 2.5% tween 80 (TWN) once a day for 4 days prior to 1 day of rest before being killed. Controls for MC treated rats were given 2 mL of olive oil (OO) by i.p injection and killed 72 hours later.

2.3.7 Untreated controls (UT): Controls for PB and ISO treated rats. Rats were given free access to food and water *ad libitum* before being killed

The above rat induction treatments were conducted at The Department of Biomedical Sciences, University of Aberdeen, Aberdeen UK. The induction methods are described by Weaver *et al* 1995.

2.4 Preparation of tissue fractions.

Human tissue was removed from the - 80° freezer, thawed on ice and rinsed in a solution of ice cold 1.15% KCl in 0.01M Tris buffer pH7.6. For animal studies, male Spague Dawley rats weighing 200-250g were obtained from Charles River Ltd, Margate, Kent UK. After appropriate inducer treatment, as outlined above, animals were killed by cervical dislocation and the livers rinsed in the ice cold rinse solution mentioned above. Livers from either human or rat were blotted dry, placed in a solution of ice cold 0.1M Tris buffer pH 7.4 and cut into small pieces by immersing scissors into the suspension of buffered liver. The following procedures were then carried out on ice and all centrifuge tubes/ homogenising equipment were precooled before use.

All ice cold buffered tissue was homogenised using an Ultra Turax automated homogeniser at low speed (Type 18/2, Janke and Kundel, Germany), in order to prevent enzyme denaturation. Homogenised samples were then placed in ice cold 13.5 mL plastic centrifuge tubes (Nalgene Ltd , Rochester, New York USA) and weighed using a pan balance (Mettler Ltd Switzerland). All samples were then placed in a refrigerated preparative centrifuge (Beckmann Ltd, UK) and centrifuged at 12500 g (13500 rpm) in a 50 Ti rotor for 20 minutes at 4°C.

The sample supernatants obtained from this initial spin were then poured into fresh ice cold centrifuge tubes, re weighed and centrifuged at 100 000 g (40 000 rpm) for 60 minutes at 4°C. The crude microsomal fractions obtained were then resuspended in ice cold 0.1M Tris buffer / 1mM EDTA containing 15% glycerol v/v pH 7.4 placed in clean, ice cold centrifuge tubes and centrifuged (washed) at 100 000 g for a further 60 minutes at 4°C. The supernatants obtained from this second 100 000 g spin were carefully decanted into 1.5mL eppendorf tubes and stored at -80°C. The washed microsomal pellets were re suspended in an ice cold solution of 0.01M Tris buffer / 1mM EDTA containing 15% glycerol v/v pH 7.4, aliquoted into 1.5 mL eppendorf tubes and stored at - 80°C prior to use.

2.5. Protein quantitation.

Total tissue protein was determined by the use of a modified Bradford assay (Bradford 1976) using a Biorad kit. Briefly, a standard curve of bovine serum albumin (BSA) was prepared in 0.1M sodium / potassium phosphate buffer pH 7.6 to cover a concentration range of 0 to 1 mg / mL BSA. The absorbance of the standard curve was then measured at 595 nm using a Perkin Elmer lambda 16 spectrophotometer. Following this

the absorbance and protein concentration of unknown samples was determined by reference to a standard curve.

2.6. Reagent degassing and hypoxic conditions

Anaerobic metabolism was performed in a steel glove box fitted with a transparent perspex top (Gallenkamp Ltd). All reagents including: incubation buffer (0.1 *M* sodium/potassium phosphate buffer, pH 7.6), and 1 *mM* stock solutions of AQ4N and AQM were adjusted to the desired %O₂ by bubbling each solution with oxygen free nitrogen or air (BDH Ltd). All equipment needed for a metabolism experiment were then transferred to the glove box. The glove box and contents were then sealed by the use of an arm length pair of rubber gloves (BDH Ltd). Finally the interior of the glove box was made hypoxic by allowing oxygen-free nitrogen to pass into the chamber at a flow rate of 1-2 L per min. The %O₂ was monitored throughout the course of an experiment by the use of a model 781 oxygen meter (Strathkelvin Instruments Ltd) fitted with an E5 oxygen electrode (Uniprobe Instruments Ltd). The oxygen meter was calibrated as described in the manufacturers instructions

2.7. Metabolism of AQ4N and AQM in subcellular fractions.

Aliquots of rat or human microsomes or cytosol were removed from the -80°C freezer and allowed to thaw at 37°C in a temperature block (Grant Instruments Ltd). Upon thawing samples were stored on ice and transferred to the steel glove box in preparation for a metabolism experiment. In a typical metabolism experiment, degassed 0.1 *M* sodium / potassium phosphate buffer (pH 7.6) was pre-warmed with a solution of NADPH (4*mM*) for a period of 5 min in a Grant temperature block at 37°C. Microsomal protein (100- 400 µg) was then added to the incubate and allowed to warm for another 5 minutes. Finally, 100 µ*M* AQ4N or 100 µ*M*

AQM was added to the incubation mixture, to initiate reaction, giving a final incubation volume of 250 μ L. Tubes were then mixed by three inversions and rapidly replaced in the temperature block to allow metabolism. In anaerobic experiments the oxygen content of all reagents and the interior of the glove box never exceeded a value of 0.5%. This was achieved as described in section 2.6. For single time point metabolism, the reaction mixture was quenched by the addition of an equal volume of ice cold 50% acetonitrile / 50% (v/v) water adjusted to pH 2.0 using several drops of a 10 M solution of HCl followed by placing in ice. Using an appropriate modification of the above procedure, the effect of protein concentration, cofactor addition, pH, temperature, time, substrate concentration, and %O₂ on metabolism were determined. Metabolic incubations were carried out in triplicate and expressed as mean metabolite formed / mg protein / minute \pm SE unless otherwise stated. Metabolism of AQ4N was investigated also in human normal and neoplastic kidney and colon. These incubations were conducted in an identical manner to that outlined above but 800 μ g of protein were used with an appropriate adjustment of incubation buffer to maintain the incubation volume at 250 μ L. Control reactions for each tissue type investigated included incubates minus NADPH, incubates plus air, incubates minus microsomes or cytosol and incubates plus heat denatured microsomes.

2.7.1 Effect of inhibitor addition on metabolism

Inhibition studies were conducted using a modified method of the basic metabolism studies. In brief, ketoconazole (KET) at a final concentration of 100 μ M, used as a general CYP inhibitor (Ervine *et al* 1995, Sequeira and Strobel 1996 and Dushkin *et al* 1995), and alpha-naphthoflavone (ANF) at a final concentration of 10 μ M used as an inhibitor of CYP's 1A1,

1A2, 2C8 and 2C9 (Chang *et al* 1994) were both dissolved in ethanol and evaporated to dryness at 37°C. Triacetyloleandomycin (TAO; final concentration 50 μ M) an inhibitor of CYP's 3A3, 3A4 and 3A5 (Chang *et al* 1994) and metyrapone (MET; final concentration of 10 μ M and 1 μ M) an inhibitor of CYP 2B1 (Adeagbo 1997) were both dissolved in DMSO. Diethyldithiocarbamate (DIE) used at a final concentration of 30 μ M as an inhibitor of CYP's 2A6 and 2E1 (Onos *et al* 1996) was dissolved in water. All metabolic incubations followed the method described earlier apart from experiments using TAO, and MET where a pre incubation time of 10 minutes was allowed for mechanism based inactivation of CYP's before adding substrate. Control incubations were treated in an identical manner but using DMSO in place of inhibitor. Carbon monoxide (CO) was bubbled into prewarmed anaerobic incubates at an approximate rate of one bubble per second for a period of two minutes prior to substrate addition.

2.7.2 Oxidative metabolism of AQ4.

The oxidative metabolism of AQ4 was investigated in rat and human subcellular fractions using the following method. For rat experiments, 200 μ g of microsomal protein and cytosol were added to air saturated 0.1M sodium/potassium phosphate buffer (pH 7.6) containing 4mM NADPH and 50 μ L DMSO and prewarmed for 10 minutes at 37°C in an incubation chamber (Stuart Scientific Ltd). Reaction was initiated by the addition of AQ4 to give a final concentration of 100 μ M in a total reaction volume of 1 mL. The effect of ketoconazole on metabolism was determined in separate incubations by replacing the 50 μ L DMSO with an equivalent volume of 2 mM ketoconazole to give an inhibitor concentration of 100 μ M. All incubations were carried out in open glass vials and reactions were terminated after 60 min by the addition of 1 mL

of 50% acetonitrile/ 50% water. For human hepatic studies, the above procedure was followed but 400 µg of microsomes and/or cytosol were used. Oxidative metabolism of AQ4 was investigated in liver preparations ID 47 and ID 55. All results were expressed as the mean of two incubations. Control reactions consisted of aerobic incubates minus NADPH, aerobic incubates depleted of microsomes and aerobic incubates plus heat denatured microsomes. Furthermore, the metabolism of AQ4 was investigated under conditions of hypoxia as described in section 2.6. All control incubations were carried out in duplicate for both rat and human subcellular fractions.

2.7.3 Kinetic analysis

The kinetic data from at least six substrate concentrations (10-200 µM) versus initial reaction velocity were simultaneously fitted to the Michaelis - Menten and Hill equations, equations 3 and 4 below. Hanes- Woolf transforms ($[S]/v$ versus $[S]$) were used to (1) confirm the calculated values for K_m and V_{max} and (2) expose any deviation from Michaelis-Menten behaviour. All operations were performed on a Macintosh IIfx computer running Ultrafit (2.0) kinetic software (Biosoft, Cambridge, UK).

$$v = V_{max} [S] / K_m + [S] \quad \text{Equation 3}$$

Where v = initial reaction velocity, V_{max} = maximum reaction velocity, K_m = the Michaelis constant (concentration at which reaction velocity is half maximal) and S = substrate concentration.

$$v = V_{\max} [S]^n / K_m + [S]^n$$

Equation 4.

where n = the Hill coefficient (equivalent to the number of substrate binding sites).

2.8. SDS PAGE

Protein samples diluted to a concentration of 0.25 mg/ mL from a stock solution of sample buffer comprising of: 1 mL 0.5 M TRIS- HCl (pH 6.8), glycerol (10% v/ v), SDS (2% w/ v), dithiothreitol (1.5% w/ v) and bromophenol blue (0.05% w/ v) in a total volume of 8 mL, were boiled for 5 min along with a sample of preprepared molecular mass markers (Sigma Ltd). Protein samples (3 μ g of HO-1 and 4 μ g CPR) as well as 4 μ L of molecular mass markers were then carefully loaded on to two separate stacking gels (10% acrylamide) supported by two different separating gels comprising of: 12% acrylamide for HO-1 and 7.5% acrylamide for CPR. Both gels were placed upright in a mini protean II unit (Biorad Ltd), and covered with 300 mL of running buffer comprising of: TRIS (3 g/ L) and glycine (14.4 g/ L). The complete gel assembly was then connected to a Biorad power box and both gels were run at 200 V for 45 min at room temperature. Protein bands were subsequently identified by the use of a Biorad Silverstain plus kit.

2.8.1 Haem Oxygenase 1 (HO- 1) activity

HO- 1 activity was measured by the linear increase in absorption (bilirubin formation) at 468 nm in an assay containing 0.1M sodium/potassium phosphate buffer (pH 7.6) pre incubated for 5 min at 37°C with 12.5 μ g HO-1, 80 μ g CPR, 30 μ M haemin and 100 μ L rat

cytosol (source of biliverdin reductase). The reaction was initiated by the addition of NADPH to a final concentration of 100 μ M. The total reaction volume was 1 mL.

2.8.2 Metabolism of AQ4N using the CPR / HO-1 system*

Incubations consisted of 0.1 M sodium/potassium phosphate buffer (pH 7.6) preincubated under hypoxic conditions at 37°C for 5 min with 1.5 μ g of CPR (equivalent activity to 0.003 μ mol cytochrome c reduction/min), 7.5 μ g of HO-1 (equivalent activity to 0.7 nmol/min bilirubin formation) 40 μ M haemin and NADPH (to give a final concentration of 200 μ M). Reaction was initiated by the addition of AQ4N to give a final concentration of 100 μ M in a total reaction volume of 100 μ L. Control incubations consisted of the above mixture minus the HO-1 protein. Additional controls consisted of the mixture minus HO-1 run separately in the absence of a) NADPH b) haemin and c) CPR. Aerobic metabolism was also investigated in both mixtures (with and without HO-1 protein) using air saturated 0.1 M sodium/potassium phosphate buffer in open eppendorf tubes. Reactions were terminated after 120 min of incubation by the addition of 100 μ L of 50% acetonitrile/ 50% water. Samples were processed and metabolites detected and quantified by the method described in section 2.9.

*The incubations using the CPR/ HO system were performed by Miss P. Tein, Department of Pharmaceutical Sciences, De Montfort University, Leicester.

2.8.3 BROD, Cytochrome P450 reductase (CPR) and nitric oxide synthase (nNOS) activities.

The benzoxyl O-deethylation (BROD) reaction was performed under yellow light, by a method modified from Burke *et al* 1985, using a Perkin Elmer 3000 fluorescence spectrophotometer. Each assay consisted of:

transfected cell microsomes (20 μ L of 10 mg/mL) pre incubated in 0.1 *M* sodium/potassium phosphate buffer (pH 7.6) at 37°C for 10 min with NADPH (250 μ M in final incubation volume) and 5 μ L DMSO. Reaction was initiated by the addition of 5 μ L of benzoxyl resorufin to give a final concentration of 0.05 mM and the total reaction volume was 1mL. The linear formation of the fluorescent metabolite was monitored at excitation and emission wavelengths of 530 nm and 585 nm respectively. Quantitation was achieved by addition of 0.025 nmol of authentic resorufin to the reaction cuvette. The effect of the CYP 3A inhibitor TAO was determined by replacing the DMSO in the pre incubation step with 5 μ L of TAO giving a final inhibitor concentration of 50 μ M.

The activity of cytochrome P450 reductase (CPR) in human lymphoblastoid cell microsomes was measured with a Perkin Elmer spectrophotometer using a modification of the method provided in the manufacturers literature. Specifically, an NADPH generating system consisting of: NADP⁺ (1.3 mM) , glucose-6-phosphate (3.3 mM) glucose-6-phosphate dehydrogenase (0.4 U/ mL), magnesium chloride (3.3 mM) and 0.95 mg/mL oxidised horse heart cytochrome C were all preincubated in 0.1 *M* sodium phosphate buffer (pH 7.6) at 37°C for 5 min. The reaction was initiated by the addition of 25 μ L of transfected microsomes (giving a final a final concentration of 0.25 mg/mL) to the sample cuvette and 25 μ L of 0.1 *M* sodium / potassium phosphate buffer (pH 7.6) was simultaneously added to the reference cuvette, giving a final volume of 1mL in both cuvettes. The linear increase in cytochrome C reduction was monitored at 550 nm and CPR activity was calculated using a millimolar extinction coefficient of 19.6 $\text{mM}^{-1} \text{cm}^{-1}$.(Gibson and Skett 1994). Semi purified CPR activity was measured as described above using 1.5 μ g of semi purified enzyme (2 μ L) in place of transfected

microsomes. The reaction was initiated by the addition of NADPH to a final concentration of 100 μM in place of the NADPH generating system. nNOS activity was measured by cytochrome c reduction (reviewed by Schmidt *et al* 1993) using 3 μg of the enzyme (3 μL) pre warmed in 0.1 M sodium/ potassium phosphate buffer (pH 7.6) and 5 mg/ mL cytochrome c. The reaction was started by the addition of NADPH to a final concentration of 100 μM in a total incubation volume of 1 mL. The reduction of cytochrome c was measured and calculated in an identical manner to that described above.

2.8 4 Metabolism of AQ4N using purified rat brain nitric oxide synthase (nNOS).

Incubations consisted 5 μL of nNOS and NADPH (200 μM final concentration preincubated under hypoxic conditions in 0.1 M sodium/potassium phosphate buffer (pH 7.6) at 37°C for a period of 5 min before the addition of AQ4N to a final concentration of 500 μM . The total reaction volume was 200 μL and metabolism was terminated after a period of 120 min by the addition of ice cold 200 μL of 50% acetonitrile/ 50% water. Control incubations were performed in the absence of NADPH and nNOS. Aerobic metabolism was also investigated using identical conditions to the anaerobic incubations but using air saturated buffer in open eppendorf tubes. Metabolites were detected and quantified by the method described in section 2.9.

2.8.5 Metabolism of AQ4N in human lymphoblastoid cell microsomes expressing CYP 3A4, control, CYP 2B6, and cytochrome P450 reductase (CPR)

Metabolism of AQ4N in the transfected microsomes was carried out in a similar fashion to the metabolism experiments described in section 2.6. In brief, incubations consisted of 40 μL of 10 mg/mL microsomes pre incubated for 5 min at 37°C in 0.1M sodium phosphate buffer (pH 7.6) containing 20 μL of NADPH (4 mM of final incubation volume). Reductive metabolism was initiated by the addition of AQ4N to a final concentration of 100 μM in a total reaction volume of 250 μL . Reactions were terminated by the addition of an equal volume of ice cold 50% acetonitrile / 50% water adjusted to pH 2.0 using several drops of a 10 M solution of HCl followed by placing on ice.

2.9. Deproteinisation, HPLC, metabolite detection and quantitation

After the termination of metabolism samples were deproteinised by centrifugation at 6 000 rpm for 5 min using a Jouan benchtop centrifuge. Sample supernatants were then removed for HPLC analysis. AQ4N and the two metabolites AQM and AQ4 were resolved isocratically using a 3.9 x 2.0 cm sentry guard cartridge mounted in a Waters steel sentry guard cartridge holder immediately followed by a Novopak (4 μm) 3.9 x 15 cm C8 analytical column. Samples were delivered *via* a Waters 510 pump and 712 wisp in a mobile phase consisting of 80% 0.5 M ammonium formate / 20% acetonitrile (pH 4.2) at a constant flow rate of 1 mL/min. The injection syringe was automatically purged in methanol between each sample injection to prevent sample carry over. At 635 nm, the lambda max for all three compounds, AQ4N, AQM and AQ4 have approximate retention times of 10.5, 7.6 and 5.5 minutes respectively.

The authenticity of each peak was confirmed by continually monitoring the visible spectrum from 500 nm to 700 nm using a Waters 994 photodiode array detector for the duration of each chromatographic run. In experiments using purified CPR/ haem oxygenase-1, AQ4N and its metabolites were detected in an identical manner to the above procedure using a modified mobile phase which consisted of: 5mM 1-heptanesulphonic acid, triethanolamine (2%), formic acid (0.7%) and acetonitrile (30%). Using these conditions AQ4N and AQ4 were shown to have retention times of 6.6 and 3.8 min respectively*. Quantitation was achieved by automated AUC determination using an NEC powermate 486 / 66i computer running millennium 2.10 chromatographic software and subsequent extrapolation to a standard curve. Standard curves were constructed in triplicate using authentic compounds synthesised in our laboratory prepared in incubation buffer containing an appropriate amount of tissue protein followed by dilution in 50% acetonitrile / 50% water. Standards were deproteinised and injected into the HPLC system in an identical manner to test samples. The recovery of AQ4 and AQM after deproteinisation was checked against standard curves prepared in a similar manner but minus tissue protein. Within run and between day coefficients of variation (CVs) were checked by comparing the AUC for independently processed, but identical concentrations of AQ4 and AQM. The stability of buffered AQ4, AQM and AQ4N was checked by preparing and storing stock concentrations of each compound at 4°C followed by HPLC analysis to detect any significant breakdown of compound as a function of time.

* Detection of metabolites from the experiment using the CPR / HO-1 system was conducted by Miss P. Tien.

2.9 1 Correlation analysis

Non-parametric Spearman rank Correlation analysis between the metabolism of both substrates (AQ4N and AQM) and various CYP activities were based on the markers listed in table 4. Data for each CYP activity were collected by several members of the CYP research group, headed by Professor M D Burke at Aberdeen University and Spearman coefficients (r_s) were generated by the use of an Macintosh Ilci computer running Statview II software. Significance was determined as described in section 2.9.2.

Table 4. Markers used for CYP activity

CYP	CYP marker	Reference (activityonly)
CYP 3A	Benzoxylresorufin <i>O</i> -deethylation	Burke <i>et al</i> 1994
CYP 3A	Tamoxifen <i>N</i> -demethylation	Crewe <i>et al</i> 1997
CYP 2C	Tolbutamide hydroxylation	Nedelcheva and Gut1994
CYP 2C	Anti- CYP 2C antibody	
CYP 1A	Anti- CYP 1A antibody	
CYP 2A	Coumarin 7-Hydroxylation	Yun <i>et al</i> 1991
CYP 2D	Dextromethorphan <i>O</i> -demethylation	Dayer <i>et al</i> 1988

Anti- CYP 1A and 2C antibodies were used to detect CYPs 1A and 2C apoprotein by western blotting. Blots were conducted by members of the CYP research group at Aberdeen Univesity. Benzoxylresorufin *O*-deethylase activity was conducted by Mr E.Wanogho by a modified method to that decribed by Burke *et al* 1985. Tolbutamide hydroxylation and Tamoxifen *N*- demethylation were conducted by Dr R Weaver and Mary Maley respectively using appropriate modifications of the methods decribed by Miners *et al* 1988 and Jacolot *et al*1991. Coumarin 7-hydroxylase activity was conducted by Duncan Webster by a modification of the method described by Miles *et al* (Miles et al 1990).

2.9.2 Statistical analysis

Significance was determined by the use of an Macintosh Ilci computer running Statview II software. Data were subjected to a paired two tailed Student's t- test. The null hypothesis was rejected at $p < 0.05$

2.9.3 Preliminary characterisation of *in vivo* metabolism of AQ4N in tumour bearing mice.

C3H female and male nude mice were used to determine the *in vivo* metabolism of AQ4N in a variety of rodent and human tumour xenografts. Mice (C3H females, 15 per group, bearing RIF- 1 fibrosarcomas, KHT fibrosarcomas, and SCCV11 carcinomas) along with 15 nude males bearing HT29 human tumour xenografts and a non tumour bearing control group (15 C3H females) were all kept in standard laboratory cages and allowed free access to food and water. When tumours reached an approximate diameter of 7 mm each mouse was given an intraperitoneal dose of AQ4N (250 mg/kg, 0.5 mL/ 25 g mouse body wt in PBS). At 15 minutes, 1 hr, 24 hr and 48 hr three mice from each tumour group, including the non tumour control group, were sacrificed and samples of plasma, tumour, liver, hind leg muscle and gall bladder were snap frozen in liquid nitrogen. The tissues were then taken for the analysis of AQ4N and its metabolites.

2.9.4 Drug and metabolite extraction

Tissue samples were removed from liquid nitrogen and allowed to thaw. Each sample of tumour, liver, gall bladder and muscle were then homogenised, by the method described in section 2.4, in a small enough volume of 0.1 M sodium/potassium phosphate buffer (pH 7.6) to produce an approximate 50% (w/v) homogenate. Aliquots of plasma were used without any buffer addition or homogenisation. An equal volume of water

saturated butanol was then added to the homogenate followed by shaking. Each sample was then vacuum dried at 45 °C by the use of a Vac- drier (PLS Ltd). The blue residue was then re suspended in 50 µL of a solution comprising: 0.5 *M* ammonium formate/ acetonitrile (70:30 v/v), pH 4.2. AQ4N and metabolites were then detected as described in section 2.9. Drug and metabolite recovery were checked by spiking appropriate tissue homogenates with a known concentration of authentic compound and comparing it to an identical concentration made up in 0.1 *M* sodium / potassium phosphate buffer (pH 7.6).

Chapter 3

Chapter 3

Metabolism of AQ4N and AQM in rat subcellular fractions and by purified enzymes

3.1 Aims

To investigate the metabolism of AQ4N and AQM in rat subcellular fractions and to establish whether prodrug AQ4N and its mono-N-oxide AQM are both substrates for hepatic CYP. A second aim was to perform preliminary investigations into the ability of some CYP related enzymes to mediate AQ4N bioactivation.

3.2 Materials and methods

The general approach used in identifying and characterising the enzymes involved in the metabolism of both compounds has been outlined in chapter 2, section 2.1. All reagents were obtained from the sources detailed in section 2.2.

3.2.2 Animal pre treatment and tissue fractionation

Male Sprague-Dawley rats (Charles River, Margate, UK), were subjected to CYP induction experiments as outlined in section 2.3. Microsomes and cytosol were prepared as described in section 2.4 and protein was quantified as described in section 2.5.

3.2.3 Metabolism studies using rat subcellular fractions and the use of CYP specific inhibitors

Assay conditions with regard to the anaerobic conditions of buffers, substrates and the interior of the steel glove box used for metabolism were as described in section 2.6. In addition, O₂ tension was kept at a level which never exceeded 0.5% that of atmospheric O₂ levels for the

duration of each experiment unless otherwise stated. The metabolism of AQ4N and AQ4 by rat microsomes and cytosol was based on the method outlined in section 2.7. CYP specific inhibitors were preincubated with microsomes and either AQ4N or AQM again as described in section 2.7.1 and oxidative metabolism of AQ4 was investigated as described in section 2.7.2.

3.2.4 Metabolism studies using the CPR/ HO system and rat nNOS

Purified nNOS, HO and partially purified CPR were obtained from the sources cited in section 2.2.2 and activity of these enzymes was determined as described in section 2.8.1 and 2.8.3. The anaerobic metabolism of AQ4N by each of these enzyme preparations has been described in sections 2.8.2 and 2.8.4.

3.2.5 Chromatography and metabolite detection

The HPLC method used for detection of AQ4N and its two metabolites AQM and AQ4 is described in section 2.9. Analytical variables were determined by the procedures described in the same section.

3.2.6 Kinetic analysis and statistical significance

Untransformed kinetic data were subjected to the observer independent analysis outlined in section 2.7.3. Statistical significance was established as previously described in section 2.9.2. Probability values of <0.05 were considered statistically significant.

3.3 Results

3.3 1 Chromatography

Typical standard curves for AQM and AQ4 along with HPLC chromatograms are shown in figures 11 and 12 respectively. Standard curves were constructed in triplicate and prepared by spiking drug free tissue samples (of appropriate protein concentration) with varying amounts of authentic metabolites. Drug recovery, after protein precipitation was consistently $\geq 85\%$ compared to metabolite standards made up in the absence of tissue. Within-run and between-run coefficients of variation (CVs) never exceeded a value of 11% for either AQM or AQ4 over a concentration range of 0- 25 nmole. Furthermore, due to automated syringe washing in methanol at the end of each injection, compound carry over was undetectable.

3.3 2 Metabolism of AQ4N and AQM in rat hepatic tissue

In rat hepatic tissue the metabolism of AQ4N yielded two chromatographically distinct metabolites identified, by reference to authentic compounds, as AQM and AQ4. In experiments using AQM as the substrate a single metabolite, AQ4, was detected. AQ4N was metabolised at physiological temperature and pH (Figs 13 and 14 respectively) and the metabolism of both compounds was inhibited by air (Figs 15 and 16) and carbon monoxide. Furthermore, the anaerobic metabolism of both compounds showed a marked preference for NADPH over NADH as reduced cofactor. Table 5 shows the results of control incubations for both compounds in rat hepatic tissue. The anaerobic metabolism of AQ4N was shown to be linear with respect to protein (0 to 300 μg per incubate) whereas the generation of AQ4 from AQM was linear over a protein range of 0 to 200 μg per incubate (Figs 17

and 18 respectively). Metabolism of both compounds was found to be linear over a time period of 0 to 40 min (Figs 19 and 20).

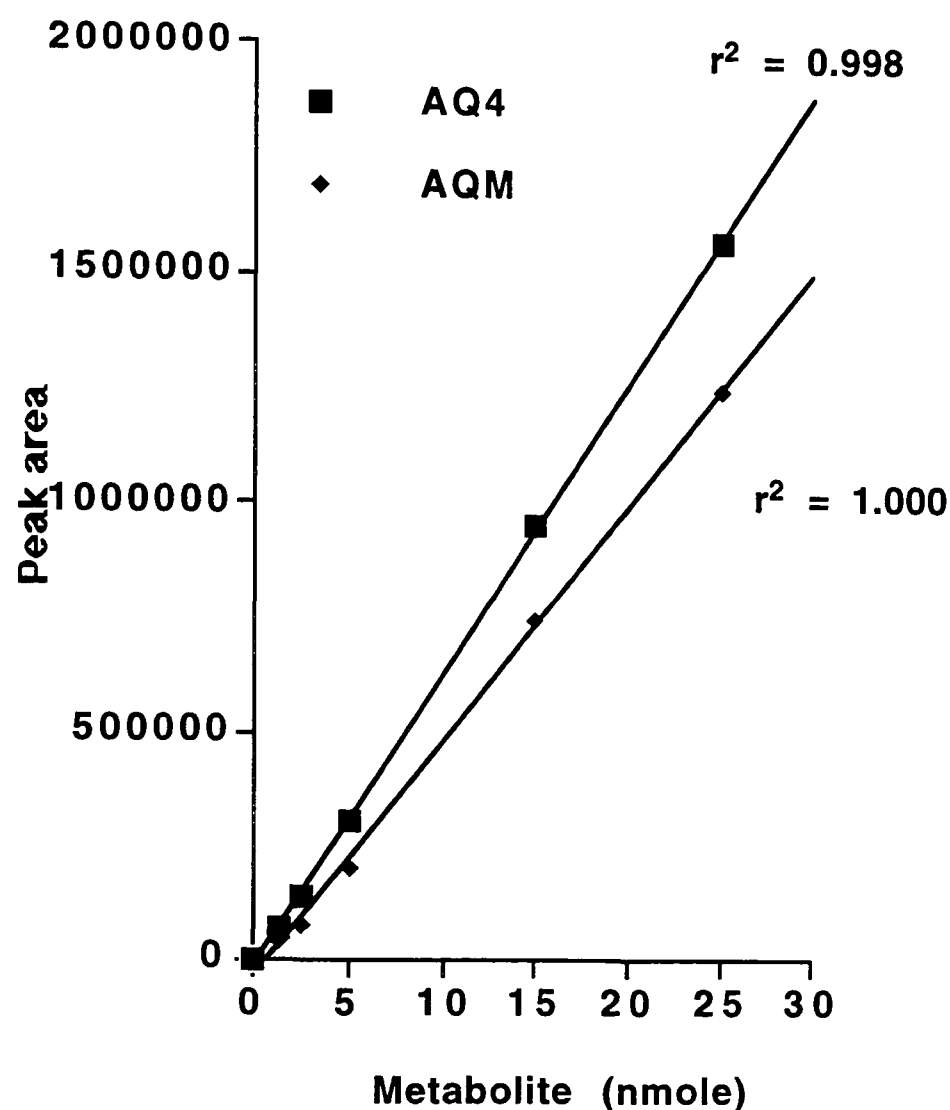


Fig 11. Typical Standard curves for AQ4 and AQM. Each data point represents the mean of three independent determinations. Measurements were taken using 400 μ g of rat microsomes spiked with authentic AQ4 or AQM. Linear regression coefficients are displayed next to their appropriate curve. See materials and methods.

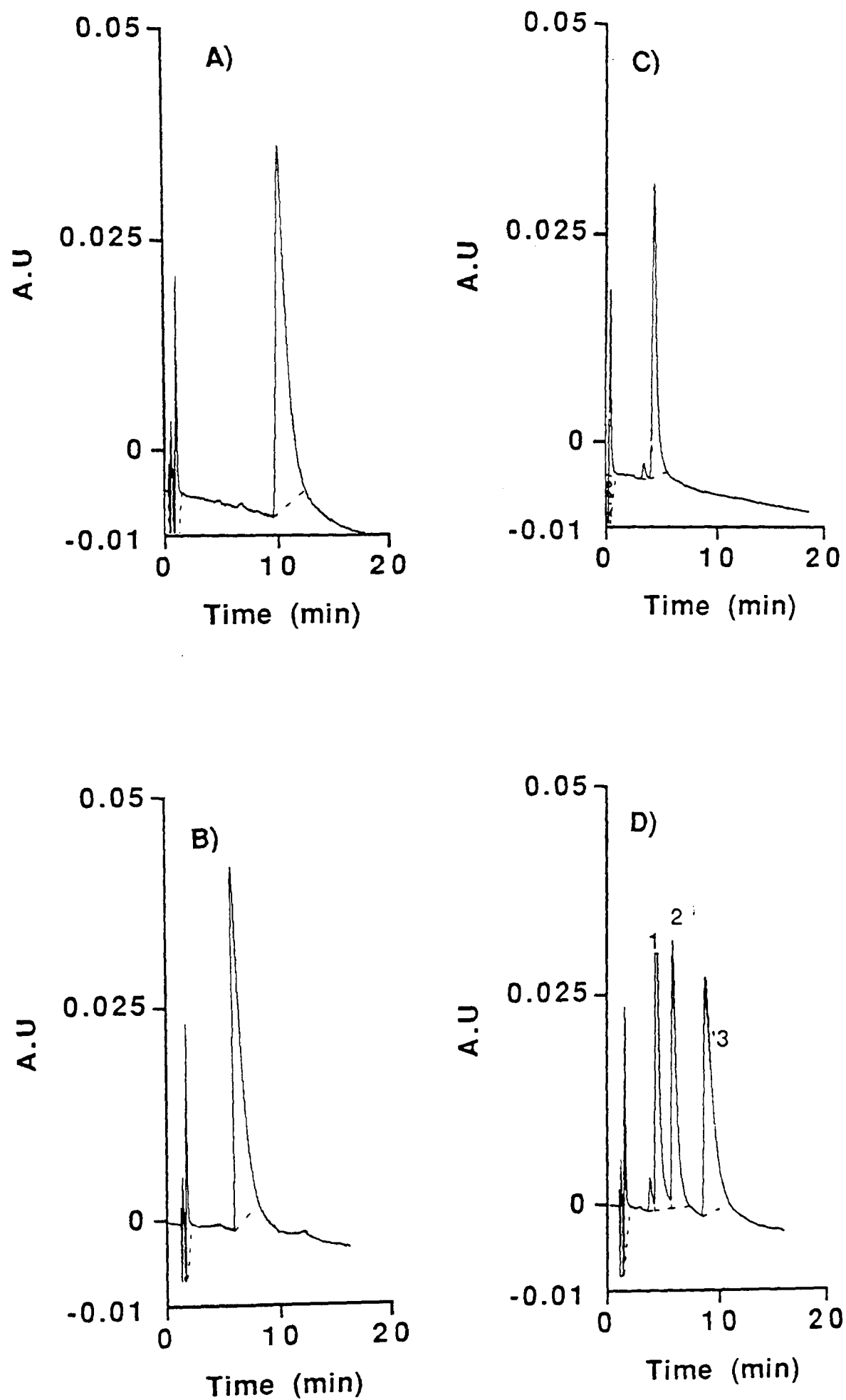


Fig 12 HPLC chromatograms for 100 μ M of **A)** AQ4N, **B)** AQM **C)** AQ4 and **D)** a mixture of all three.

Individual peaks are: **1)** AQ4, **2)** AQM and **3)** AQ4N. See section 2.9 for HPLC conditions and detection.

Table 5. Control incubations of AQ4N and AQM in rat hepatic tissue

Conditions	Metabolism of AQ4N (nmol/incubate)		Metabolism of AQM (nmol/incubate)
	AQM	AQ4	AQ4
Full system + N ₂	5.20 ± 0.90	1.75 ± 0.45	7.0 ± 0.80
Full system + Air	N D	N D	0.50 ± 0.2
Full system - NADPH	N D	N D	N D
Full system + NADH*	0.65 ± 0.20	N D	0.81 ± 0.2
Full system + CO	N D	N D	N D
Full system + cytosol	N D	N D	0.71 ± 0.2
Full system + boiled**	N D	N D	N D
Full system - microsomes	N D	N D	N D

Results are expressed as the mean metabolite formed ± SE for 60 min incubation. N D= not detected. Full system were incubates containing 200 µg of protein and 100 µM of either substrate (AQ4N or AQM) under anaerobic conditions in 0.1 M sodium/ potassium phosphate buffer (pH 7.6), with NADPH (4mM final concentration). Total reaction volume was 250 µL.*= 4mM NADH, **= microsomes boiled for 5 min before incubation.

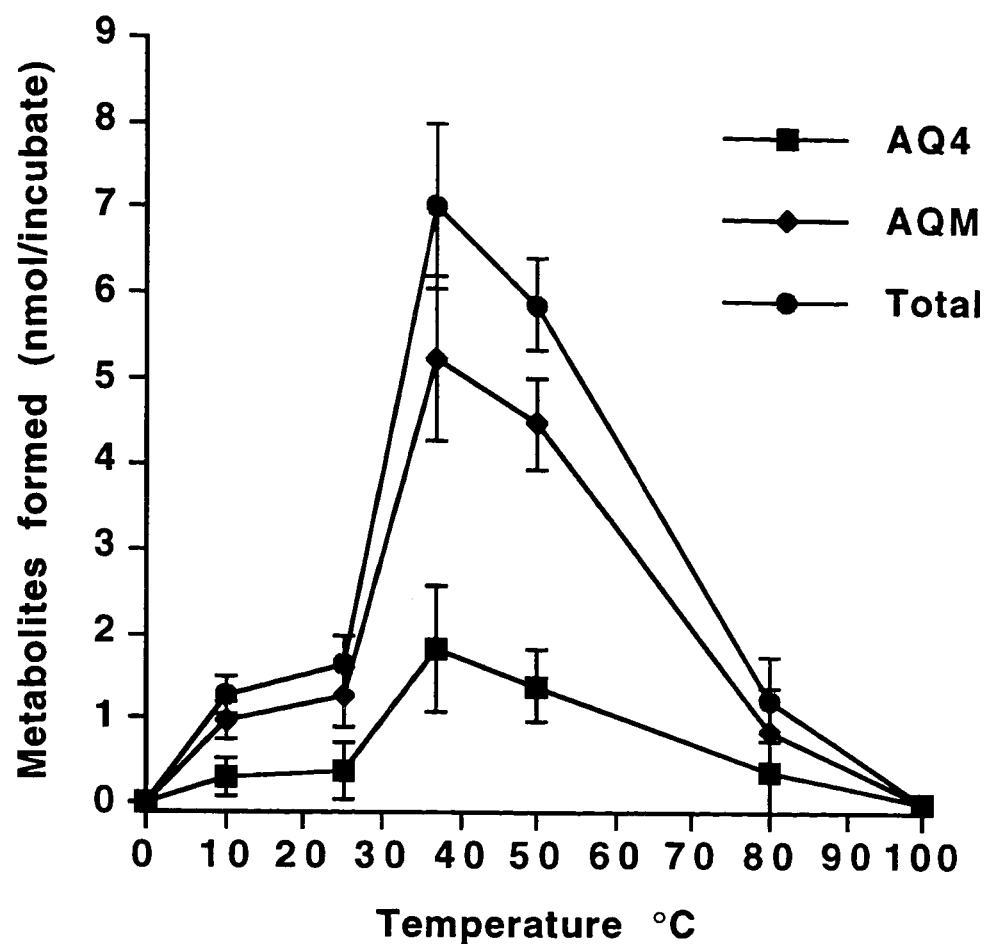


Fig 13. Effect of temperature on the metabolism of AQ4N.

Results are expressed as mean metabolite formed \pm SE. for three independent incubations. Each incubate contained 200 μ g of protein and 100 μ M AQ4N. Data obtained at 100°C are metabolites formed after a period of 5 minutes of boiling microsomes prior to incubation. Data were obtained after 60 min incubation. See section 2.7 for methods.

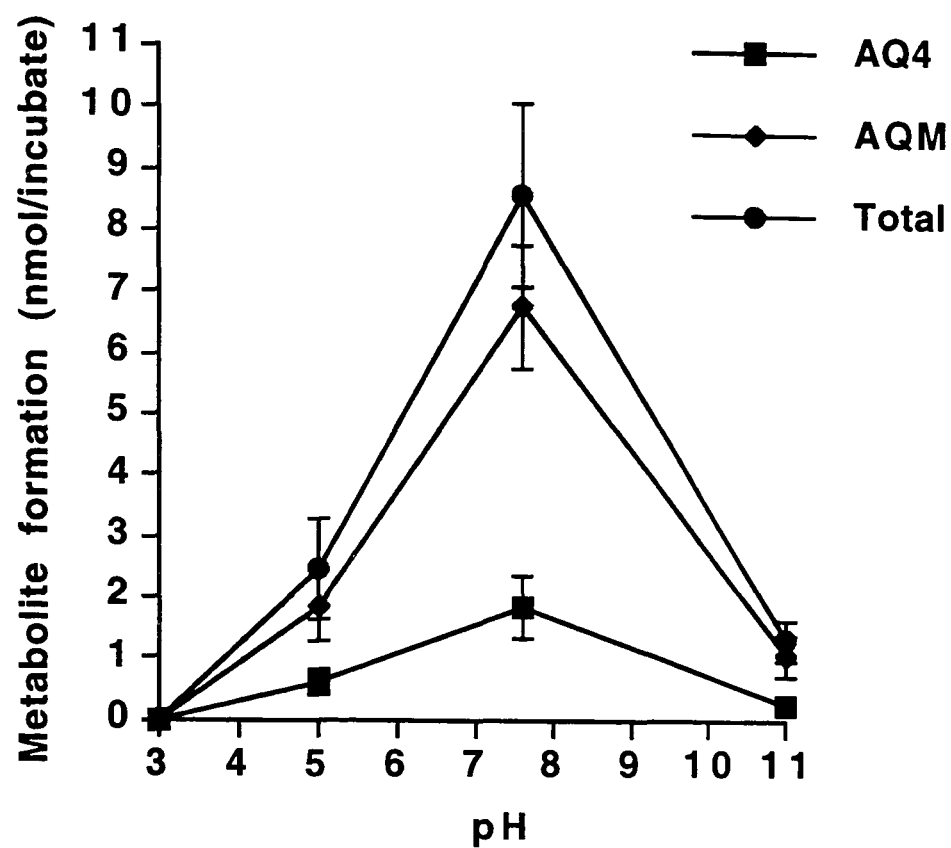


Fig 14. Effect of pH on the anaerobic metabolism of AQ4N.

Results are expressed as mean metabolite formed \pm SE for three independent incubations. Each incubate contained 200 μ g of protein and 100 μ M AQM. Data were obtained after 60 min of incubation. See section 2.7 for experimental conditions.

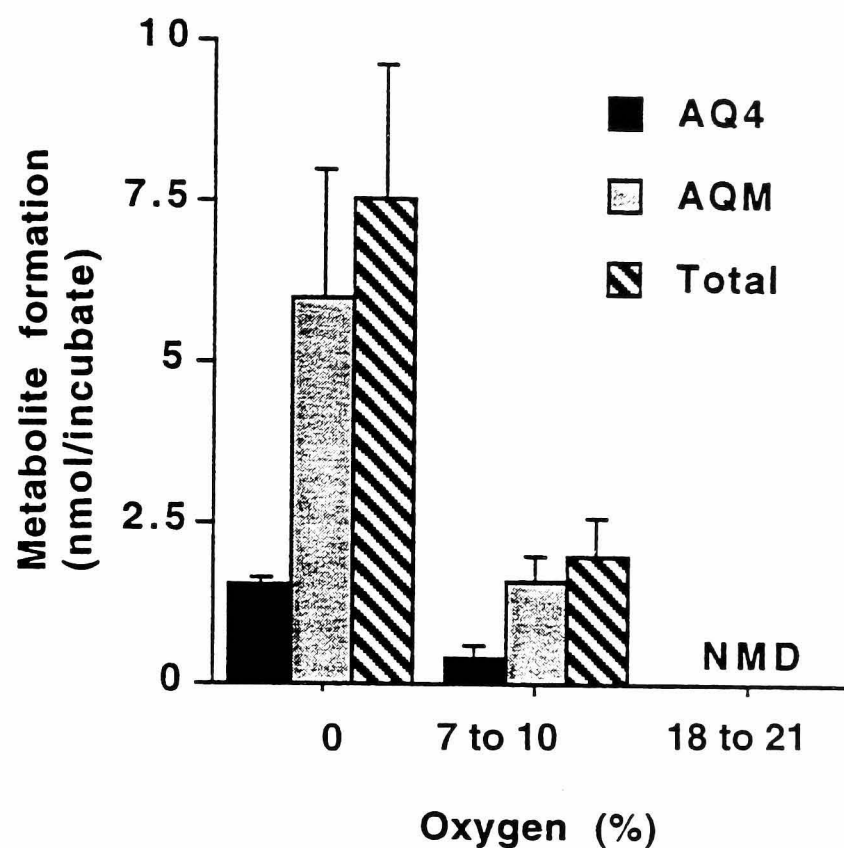


Fig 15. Effect of oxygen on the metabolism of AQ4N.

Data were collected after 60 min incubation. Oxygen concentration (y axis) was measured at the start of an experiment (upper value) and at the end of the experiment (lower value). Each incubate contained 200 μ g of protein and 100 μ M AQ4N. Values are the mean \pm SE for three determinations. See sections 2.6 and 2.7 for experimental conditions. NMD= No metabolites detected.

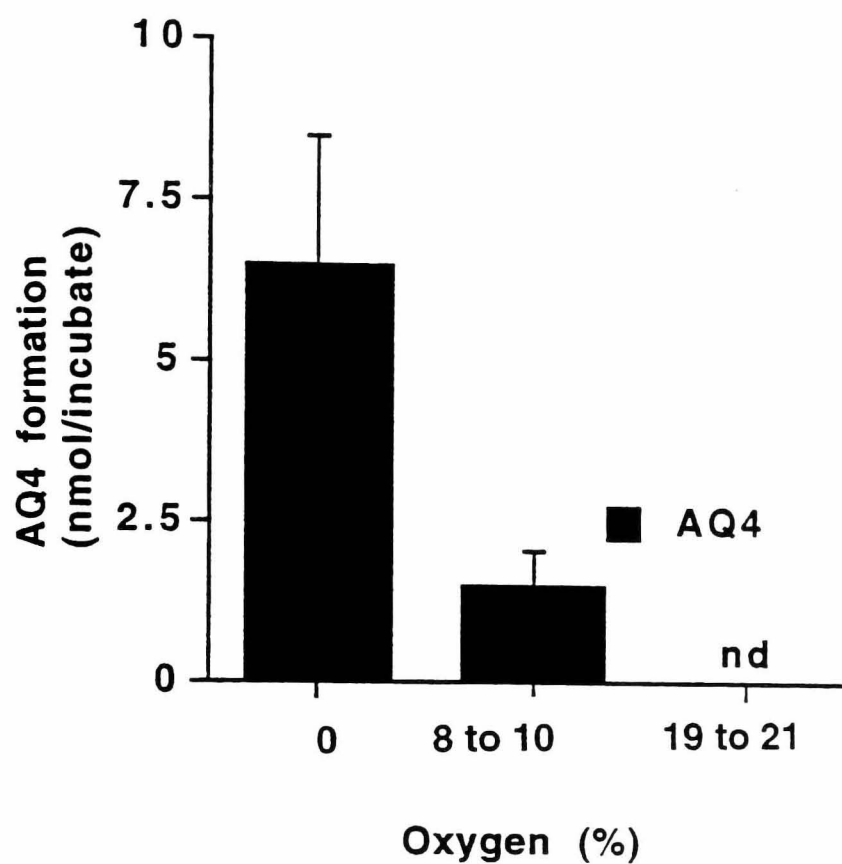


Fig 16. Effect of oxygen on the metabolism of AQ4N

Data were collected after 60 min incubation. Oxygen concentration (y axis) was measured at the start of an experiment (upper value) and at the end of the experiment (lower value). Each incubate contained 200 μ g of protein and 100 μ M AQM. Values are mean \pm SE for three determinations. See sections 2.6 and 2.7 for experimental conditions. nd= not detected.

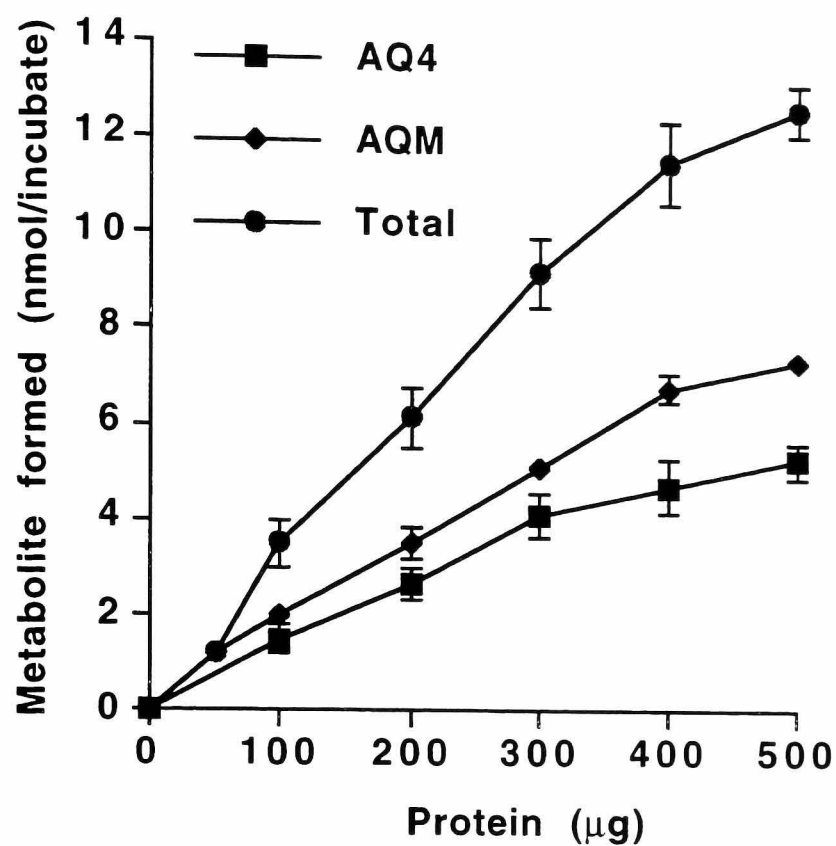


Fig 17. Effect of protein concentration on the anaerobic metabolism of AQ4N.

Results are expressed as the mean metabolite formed \pm SE for three independent incubations. Incubates contained 100 μ M AQ4N and data were obtained after 60 min of incubation. See section 2.7 for experimental conditions.

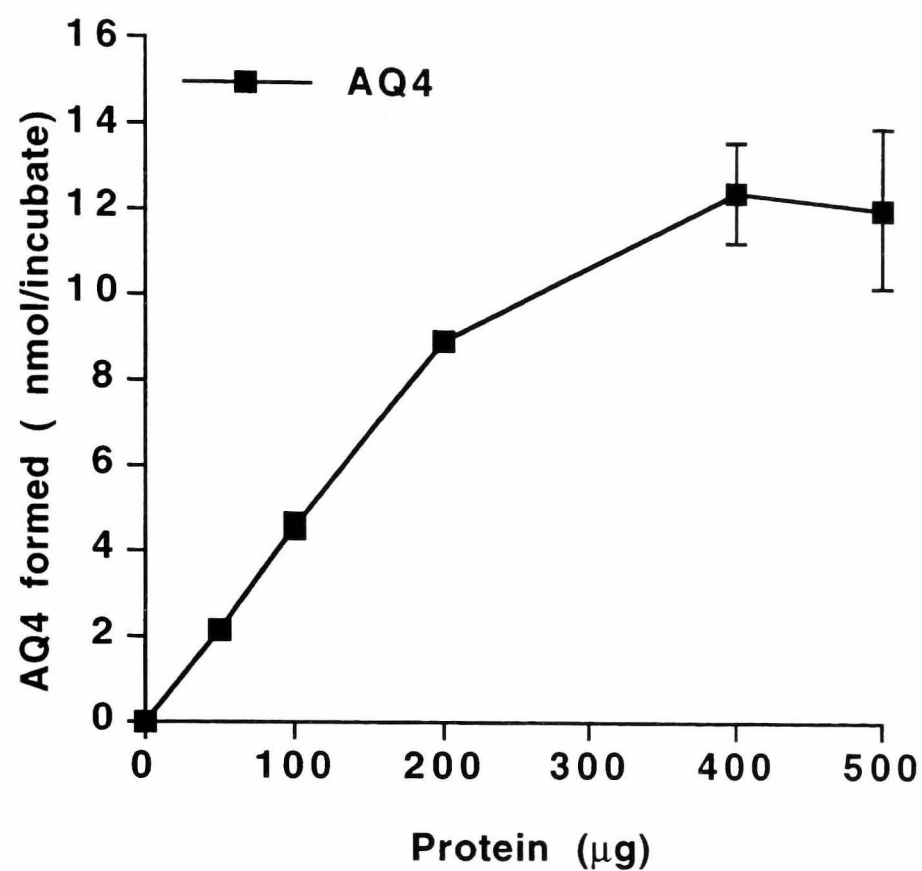


Fig 18. Effect of protein concentration on the anaerobic metabolism of AQM.

Results are expressed as mean formation of AQ4 \pm SE for three independent incubations. Incubates contained 100 μ M AQM and results were obtained after 60 min of incubation. See section 2.7 for experimental conditions.

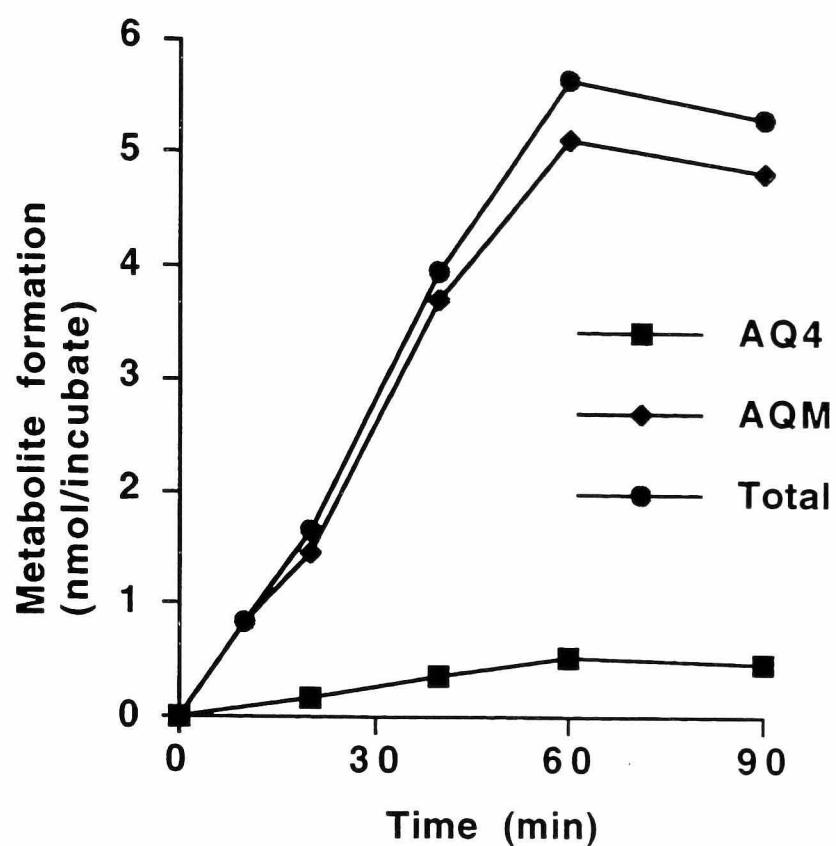


Fig 19. Effect of incubation time on the anaerobic metabolism of AQ4N.

Results are expressed as the mean of duplicate incubations. Each incubate contained 200 μg of protein and 100 μM AQ4N. Results were obtained after 60 min of incubation See section 2.7 for experimental conditions.

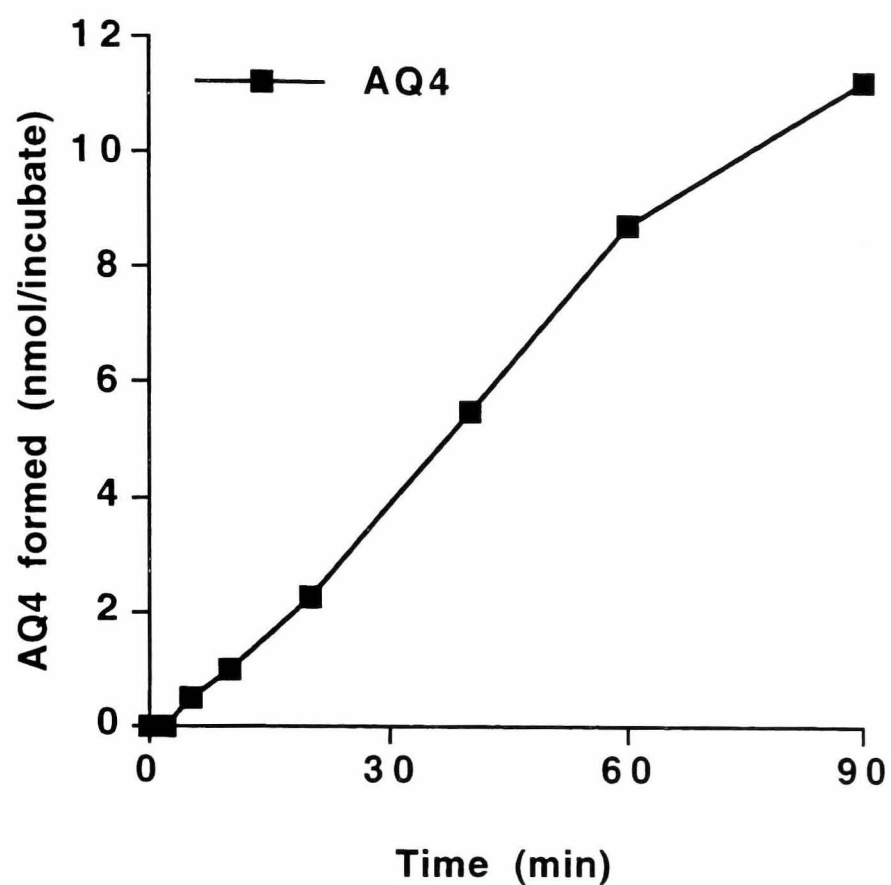


Fig 20. Effect of incubation time on the anaerobic metabolism of AQM.

Results are expressed as mean AQ4 formed for duplicate incubations. Each incubate contained 200 μg of protein and 100 μM AQM. Data were obtained after 60 min incubation. See section 2.7 for experimental conditions.

3.3.3 Effect of animal pretreatment on the metabolism of AQ4N.

The anaerobic production of AQ4 and AQM from AQ4N was increased ($p < 0.05$) in microsomes from isoniazid (ISO) treated animals compared to untreated controls (Fig 21). Phenobarbitone (PB) pretreatment also caused an increase ($p < 0.05$) in AQ4 generation but AQM formation did not significantly exceed control levels (Fig 21). The production of AQ4 from AQ4N under anaerobic conditions was reduced ($p < 0.05$) in rats pretreated with pregnenolone-16 α -carbonitrile (PCN) when compared to tween 80 controls (Fig 21). However, the formation of AQM was essentially unaffected. The generation of both metabolites by microsomes from 3-methylcholanthrene (3MC) pretreated animals was significantly reduced ($p < 0.01$) compared to olive oil controls (Fig 21). Clofibrate pretreatment had no significant effect on the metabolism of AQ4N compared to control incubates (Fig 21). Typical chromatograms obtained for the anaerobic metabolism of AQ4N in various untreated and control microsomes are shown in figure 23.

3.3.4 Effect of animal pretreatment on the metabolism of AQM

In metabolism studies using AQM as substrate a similar trend of differential metabolism was obtained to that of AQ4N. ISO and PB induced microsomes caused an increase in AQ4 production which was highly significant ($p < 0.001$) compared to control values (Fig 22). Conversely 3MC and PCN induced microsomes both reduced the formation of AQ4 ($p < 0.002$ and $P < 0.01$ respectively) compared to control values. The production of AQ4 in CLO induced microsomes was not significantly different to tween 80 control values (Fig 22).

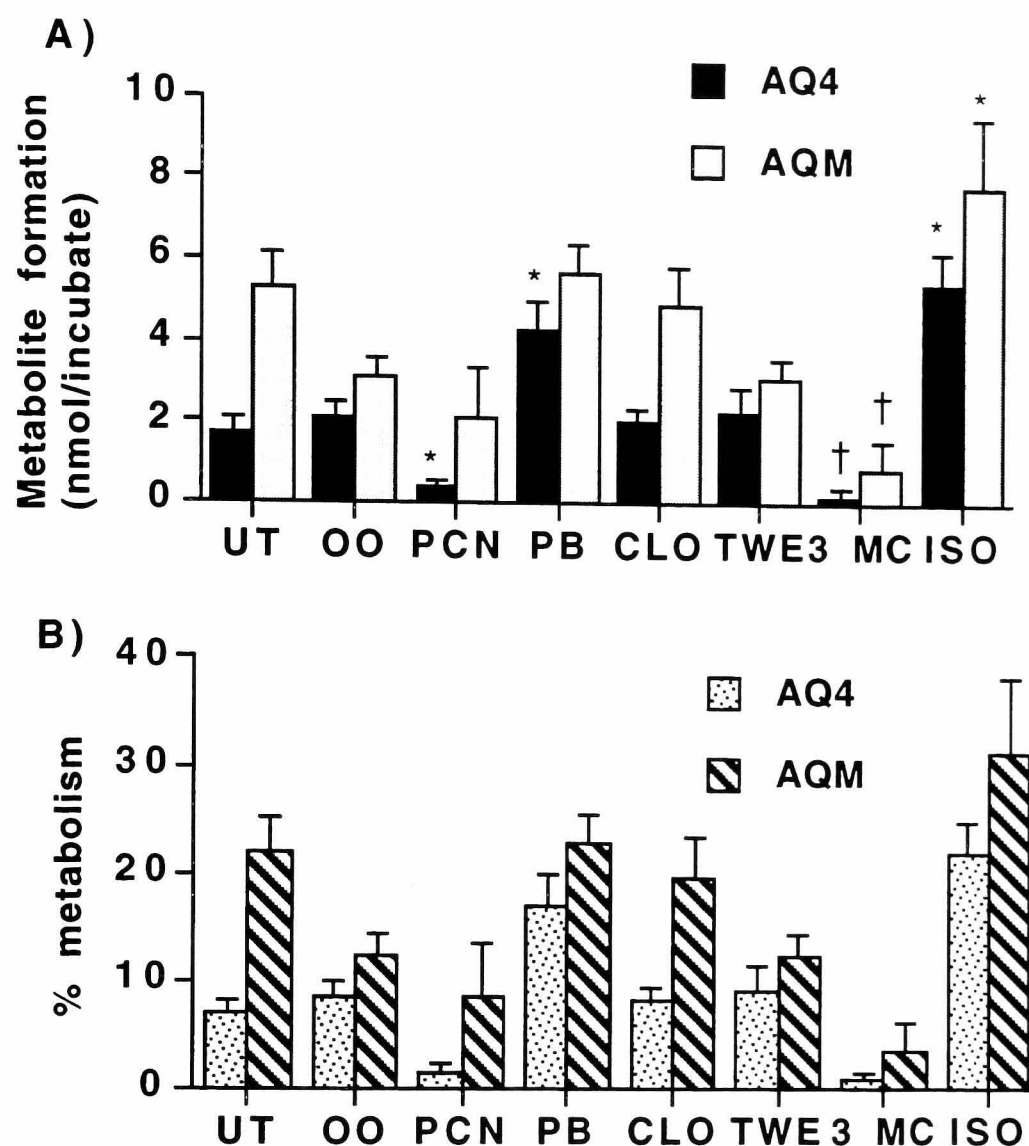


Fig 21. Effect of animal pretreatment on the anaerobic metabolism of AQ4N.

Microsomes (200µg of protein/incubate) from untreated rats (UT) and rats pretreated with inducers of CYP were incubated with 100 µM of AQ4N for 60 min as described in section 2.7. Results are expressed as **A)** the mean \pm SE for three determinations. Inducers are: pregnenolone-16- alpha carbonitrile (PCN), phenobarbitone (PB), clofibrate (CLO), 3- methylcholanthrene (3 MC) and isoniazid (ISN). Tween 80 (TWE) was the control vehicle for PCN and CLO. Olive oil (OO) was the control vehicle for 3 MC. *= $p < 0.05$, †= $p < 0.01$. **B)** Same data expressed as percentage of metabolism (levels of significance are shown in **A)** only).

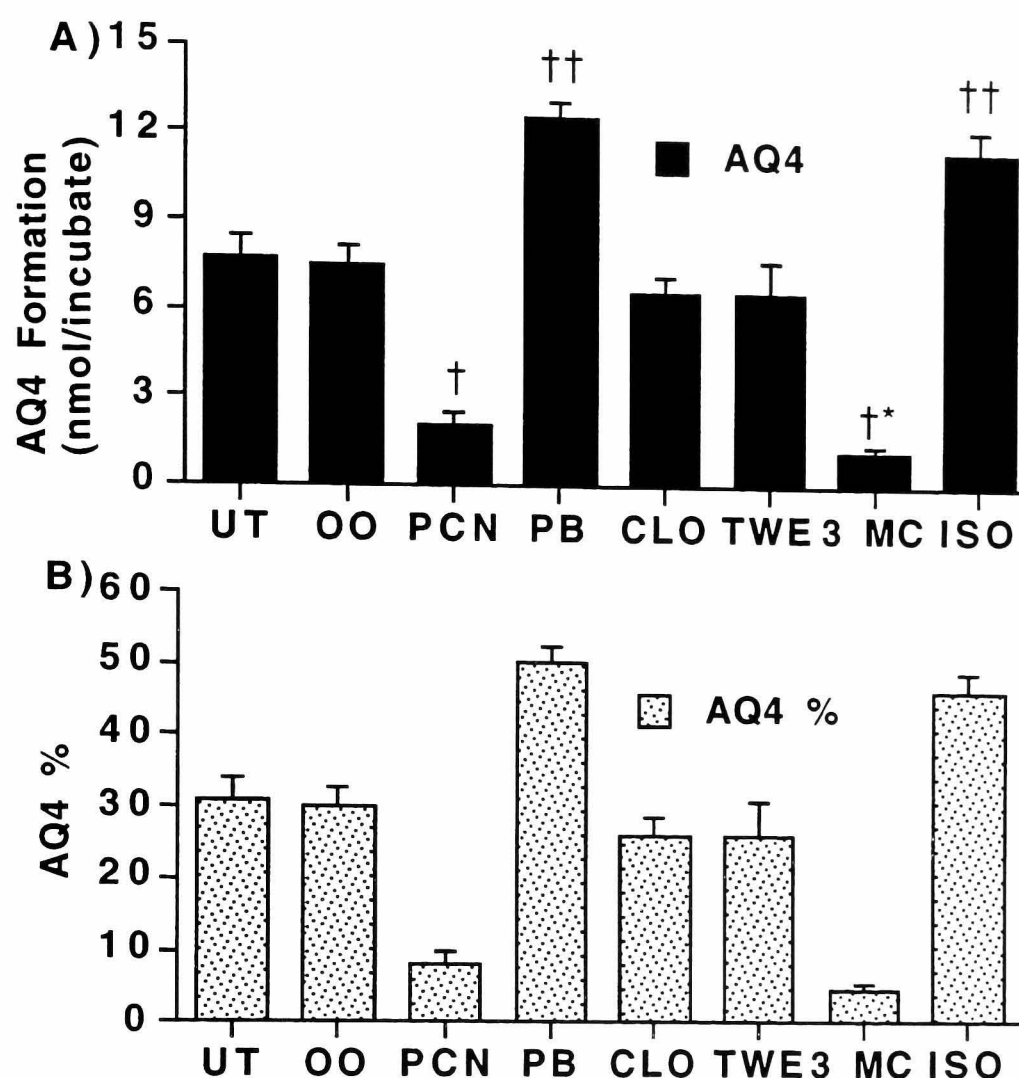


Fig 22. The effect of animal pretreatment on the anaerobic metabolism of AQM.

Microsomes (200 μ g of protein/incubate) from untreated rats (UT) and rats treated with CYP inducers were incubated with 100 μ M of AQM for 60 min as described in section 2.7. Results are expressed as **A)** the mean \pm SE for three determinations. Inducers are: pregnenolone- 16- α carbonitrile (PCN), clofibrate (CLO), 3-methylcholanthrene (3MC) and isoniazid (ISN). Tween 80 (TWE) was the control vehicle for PCN and CLO. Olive oil (OO) was the control vehicle for 3MC. †= p <0.01, ††= p <0.001 and †*= p <0.002 **B)** is the same data expressed as percentage of metabolism (levels of significance are shown in **A)** only.

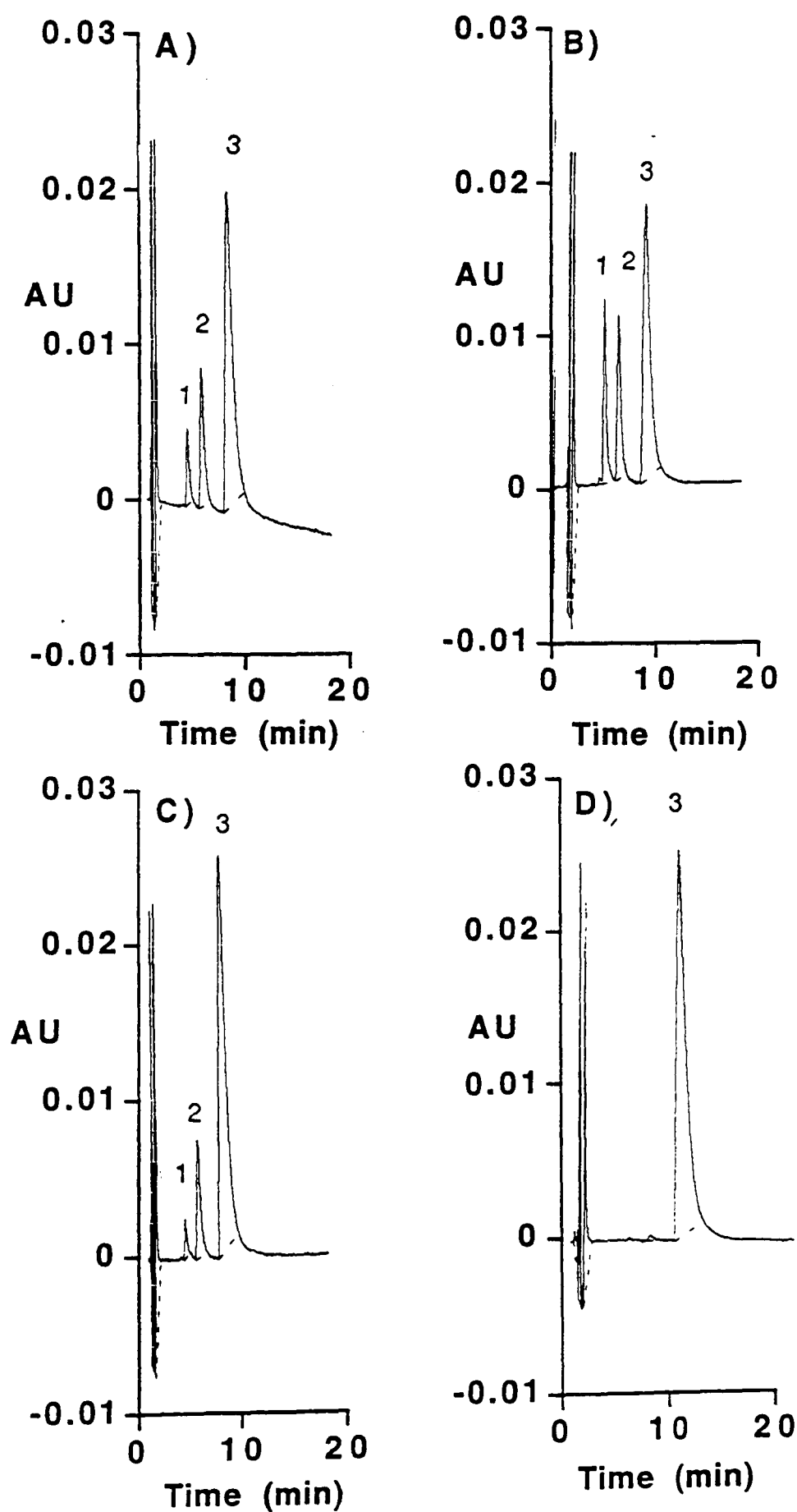


Fig 23. Typical HPLC chromatograms obtained after incubating 100 μ M AQ4N in NADPH supplemented rat microsomes for 60 min. Incubations were carried out under anaerobic conditions as described in section 2.7. Chromatograms are from A) untreated (UT) animals, B) Isoniazid (ISO) induced animals, C) 3-methylcholanthrene (3 MC) induced animals and D) UT animals after carbon monoxide purge. Peaks are: 1) AQ4, 2) AQM and 3) AQ4N

3.3.5 Effect of inhibitors on the metabolism of AQ4N in rat microsomes

Ketoconazole (100 μM) completely inhibited the formation of AQ4 by untreated rat microsomes and the formation of AQM was reduced to 15 % of control levels. 30 μM diethyldithiocarbamate (DIE) completely inhibited AQ4 formation in ISO induced microsomes and reduced AQM production to 57 % of control values. Metirapone (MET) inhibition of PB induced microsomes was concentration dependent, having essentially no effect at 1 μM , but reducing AQ4 and AQM production to 21 and 59% respectively of control values at 10 μM (Fig 24). Carbon monoxide and air completely abolished the metabolism of AQ4N in untreated rat microsomes (Table 5).

3.3.6 Effect of inhibitors on the metabolism of AQM in rat microsomes

KET (100 μM) reduced the formation of AQ4 to 10% of control values in untreated microsomes. ISN induced microsomes produced 32% of AQ4 compared to control values in microsomes preincubated with 30 μM DIE. MET was effective at 10 μM in inhibiting the formation of AQ4 to 20% of control values in PB induced microsomes (Fig 25). Carbon monoxide inhibited completely the anaerobic metabolism of AQM and air saturated incubates caused a reduction in AQ4 generation to 6.4% of anaerobic incubations (Table 5).

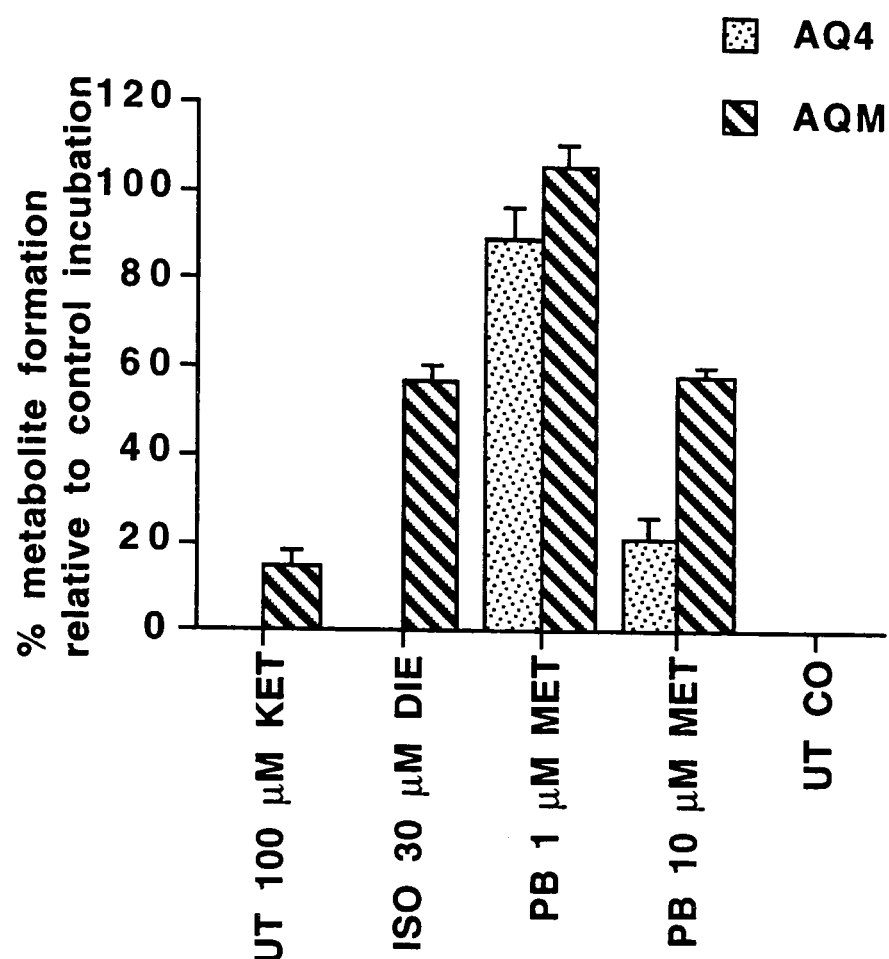


Fig 24. Effect of CYP inhibitors on the anaerobic metabolism of AQ4N in rat hepatic microsomes.

Results are expressed as percentage metabolite formation \pm % SE for three determinations relative to control incubations carried out in the absence of inhibitor. Each incubation contained 200 μ g of protein and 100 μ M AQ4N. Animal pretreatments were: untreated (UT), isoniazid (ISN) and phenobarbitone (PB). Inhibitors were: ketoconazole (KET), diethyldithiocarbamate (DIE), metyrapone (MET) and carbon monoxide (CO). See section 2.7.1 for experimental conditions.

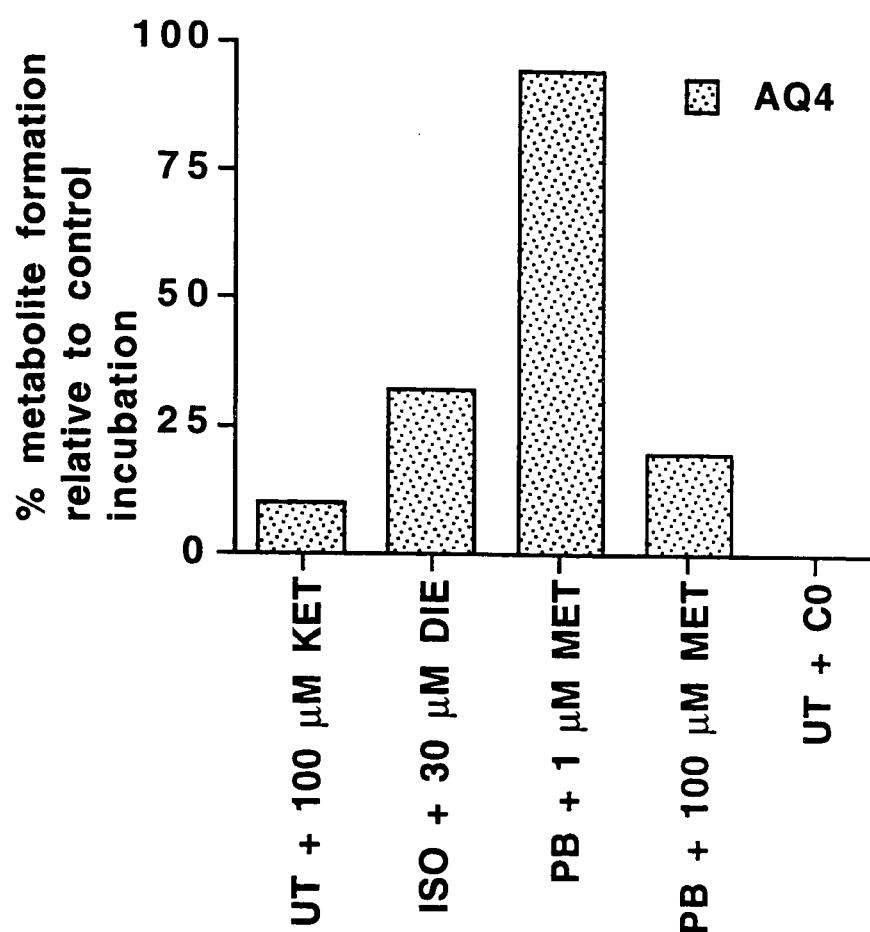


Fig 25. Effect of CYP inhibitors on the anaerobic metabolism of AQ4 in rat hepatic microsomes.

Results are expressed as percentage metabolite formation for replicate determinations relative to control incubations carried out in the absence of inhibitor. Each incubation contained 200 μ g of protein and 100 μ M AQ4N. Animal pretreatments were: untreated (UT), isoniazid (ISO) and phenobarbitone (PB). Inhibitors were: ketoconazole (KET), diethyldithiocarbamate (DIE), metyrapone (MET) and carbon monoxide (CO). See section 2.7.1 for experimental conditions.

3.3.7 Oxidative metabolism of AQ4 in rat hepatic tissue

The investigation into the oxidative metabolism of AQ4 produced results which are shown in figure 26. Only 8% of AQ4 was oxidised to a metabolite with identical spectral and chromatographic properties to AQM. The process was 64% inhibited in incubates containing 100 μ M KET and completely inhibited in incubates gassed with carbon monoxide. Furthermore, anaerobic conditions abolished AQ4 oxidation. Metabolism was not detected in incubates depleted of NADPH or microsomes. Incubates containing heat denatured microsomes (boiled for 5 minutes before use) failed to support metabolism.

3.3.8 Kinetics of AQ4N and AQM metabolism in untreated rat microsomes

The untransformed kinetic data for initial reaction velocity versus substrate concentration were subjected to observer independent non linear curve fitting analysis as described in section 2.7.3. Using this method, the anaerobic metabolism of AQ4N to both AQ4, AQM and total substrate turnover was found to conform to Michaelis-Menten kinetics (Fig 27). A Hanes-Woolf transform of the kinetic data produced a plot which was linear with respect to both metabolites and total substrate turnover (Fig 28) and allowed kinetic parameters to be established. However, when AQM was used as substrate, plots of initial reaction velocity versus substrate concentration fitted perfectly to sigmoid kinetics as described by the Hill equation (Fig 29). Furthermore, a Hanes- Woolf transform generated a non linear plot (Fig 30) which is consistent with deviation from Michaelis- Menten behaviour. The kinetic parameters for both substrates are shown in table 6.

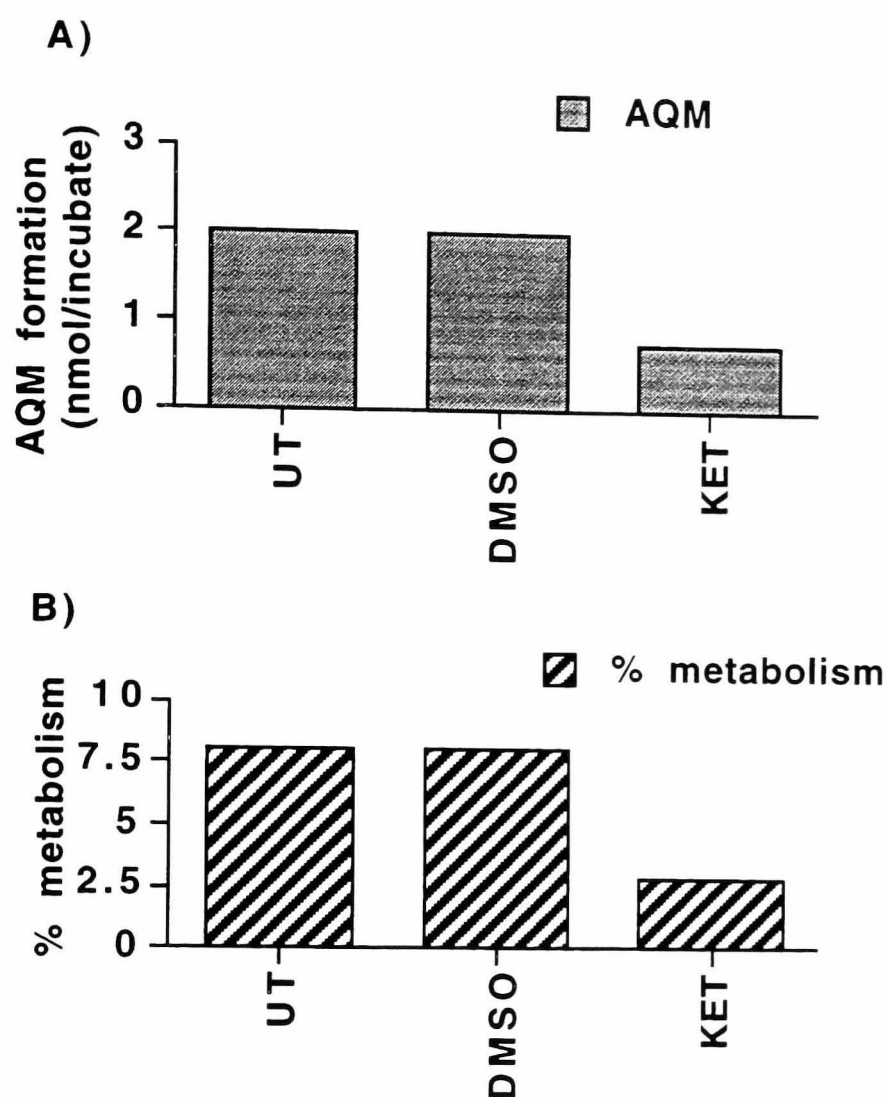


Fig 26. Oxidative metabolism of AQ4 in untreated rat hepatic microsomes.

Data are expressed as in **A)** as the mean of two determinations. Incubates contained 200 μ g of protein and 100 μ M AQ4. Data were collected after 60 min of aerobic incubation. UT= untreated, DMSO= UT+ dimethyl sulphoxide and KET= UT+ ketoconazole (100 μ M).

B) same data expressed as a percentage of metabolism. See section 2.7.2 for experimental conditions.

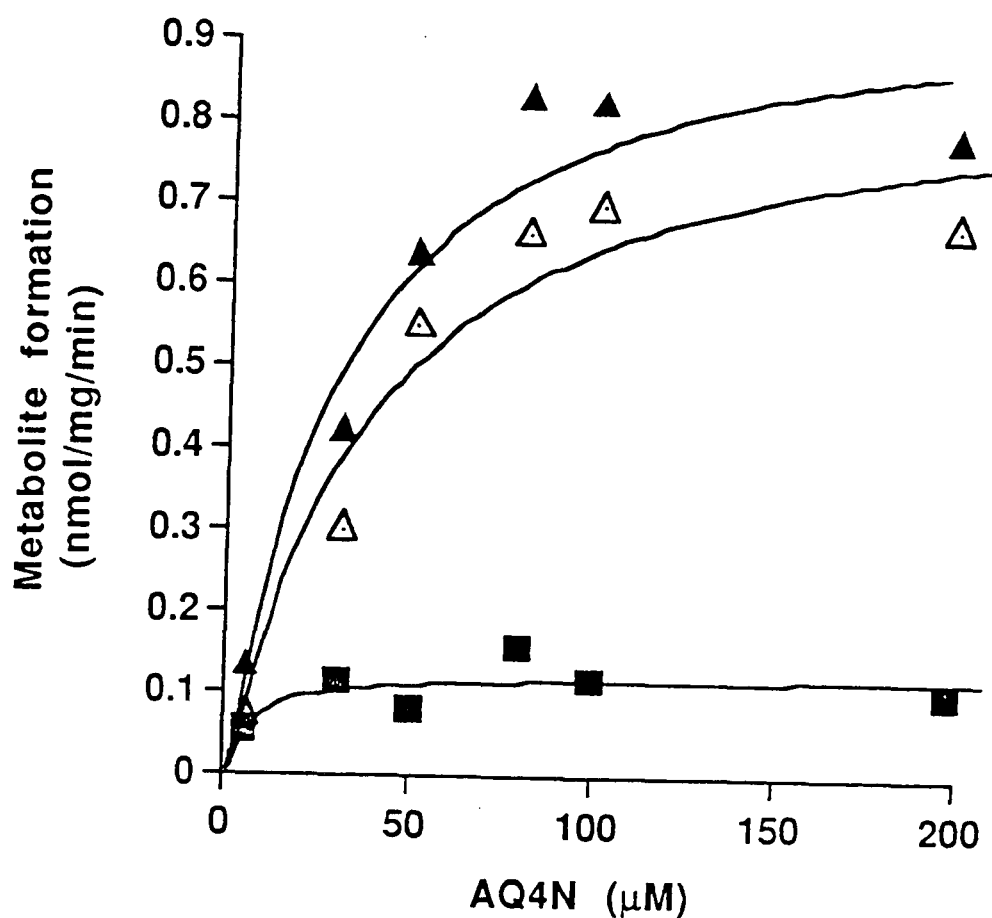


Fig 27. Effect of AQ4N concentration on the initial velocity of anaerobic metabolism.

Incubates contained 200 μg of protein and data are expressed as the mean of three determinations, taken after 40 min incubation. AQ4 formation (black squares), AQM formation (open triangles) and total metabolism (black triangles). Solid lines are curves of best fit. See section 2.7 for experimental conditions and section 2.7.3 for kinetic analysis.

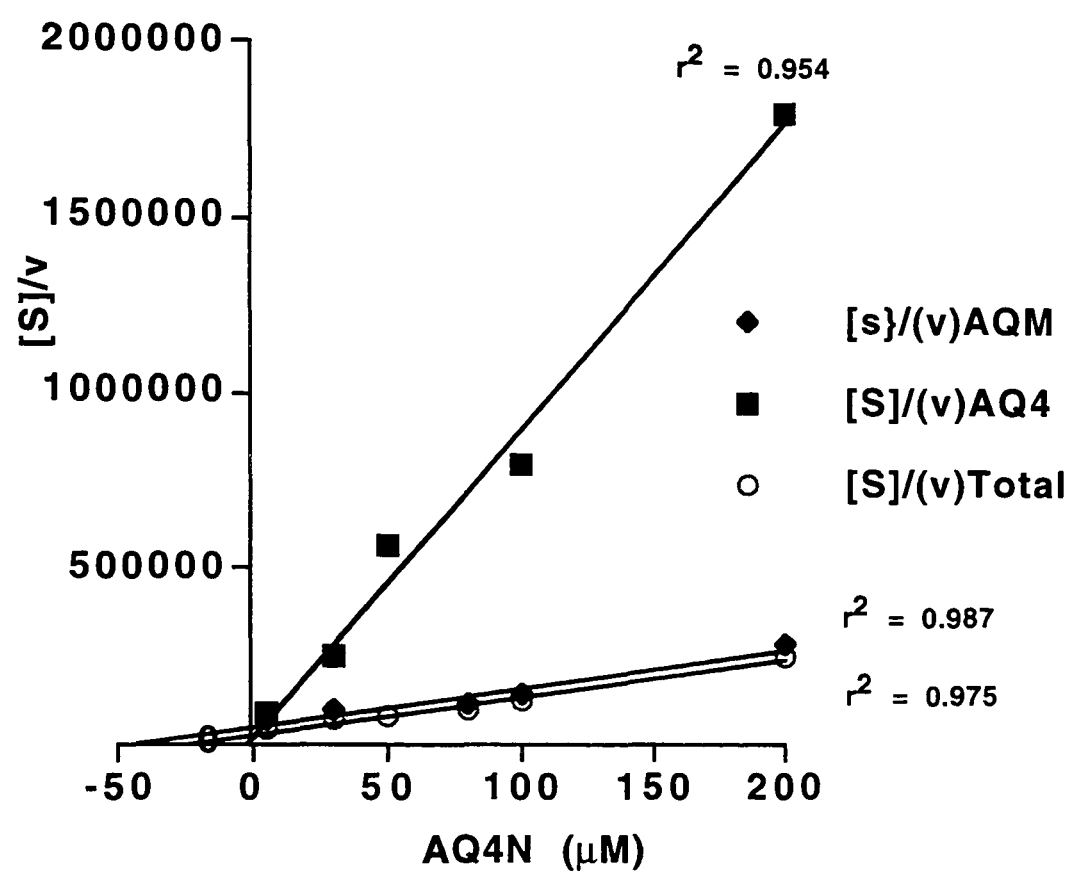


Fig 28. Hanes- Woolf transformation plot of the kinetic data from figure 27 .

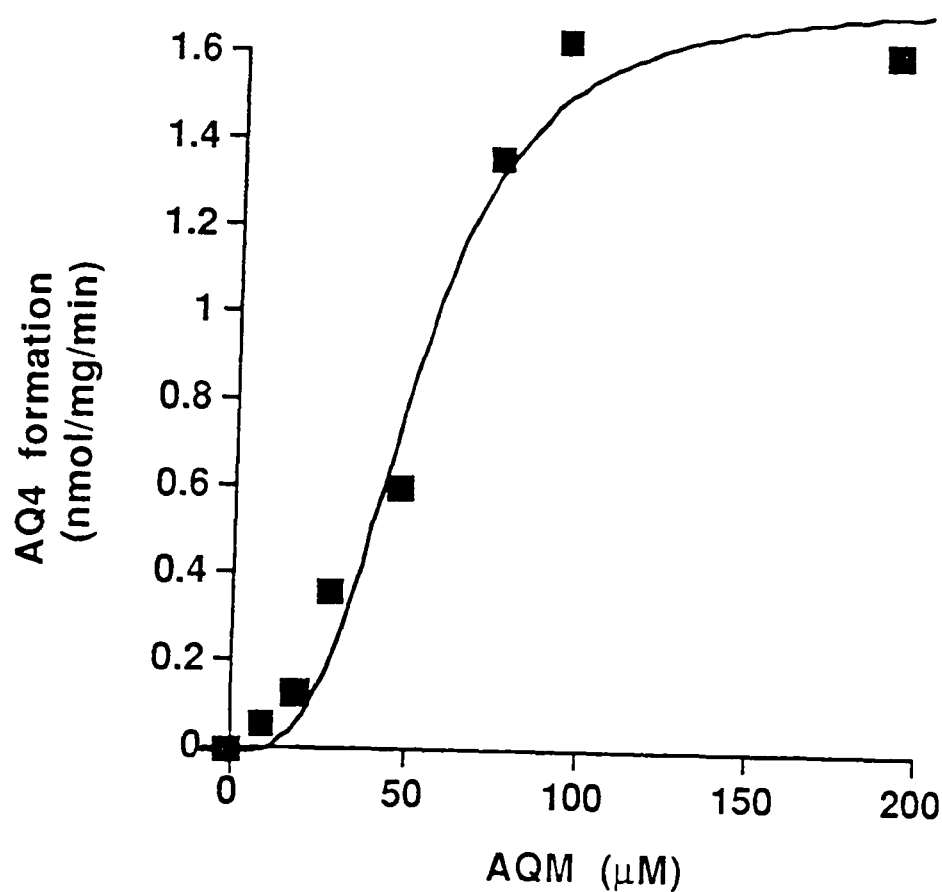


Fig 29. Effect of AQM concentration on the initial velocity of AQ4 formation.

Results are expressed as mean of three determinations (black squares) in incubates containing 200 μg of protein. Data were collected after 40 min of incubation. The solid line represents the curve of best fit as determined by observer independent curve fitting analysis. See section 2.7 for experimental conditions and section 2.7.3 for kinetic analysis.

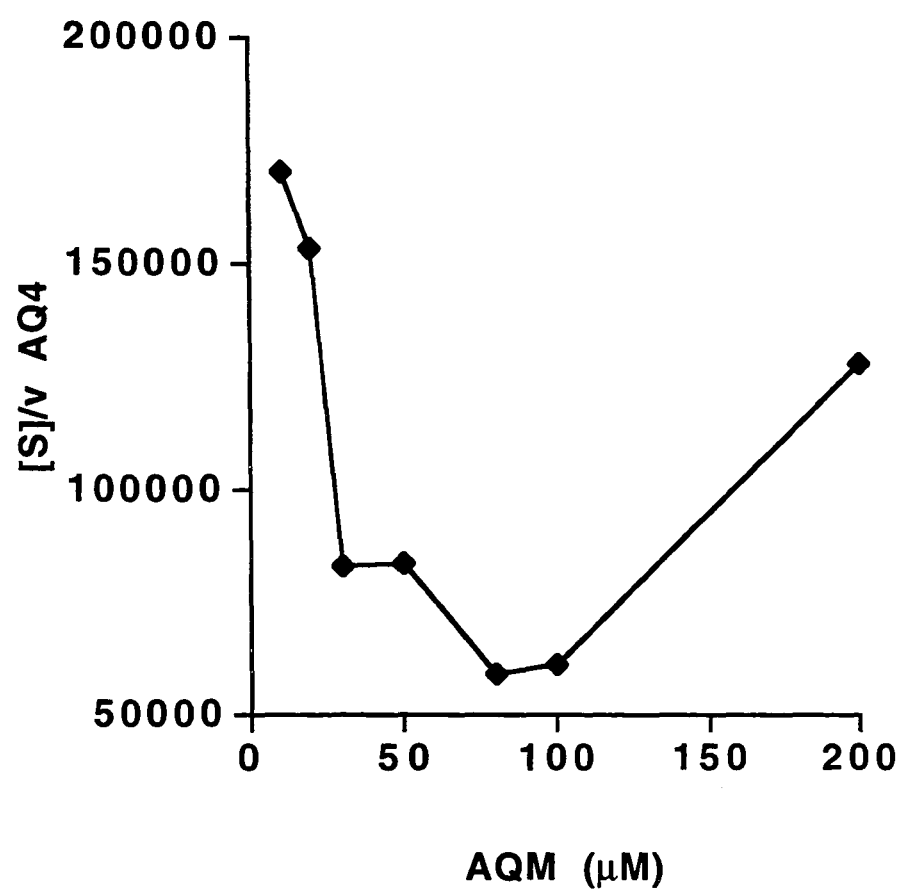


Fig 30. Hanes- Woolf transformation plot of the kinetic data shown in figure 29.

Table 6 Kinetic parameters for AQ4N and AQM metabolism in rat microsomes

Substrate	Metabolite	K_m (μ M)	V_{max}	n^*	CL_{int}
AQ4N	AQM	38.76	0.92	NA	23.7
	AQ4	5.65	0.13	NA	23.0
	Total	30.29	1.05	NA	34.0
AQM	AQ4	27.00	1.72	3	63.0

Results are means of three determinations. n^* = Hill coefficient, CL_{int} (intrinsic clearance) = V_{max}/K_m and NA= not applicable. Units for V_{max} = nmol metabolite formed/mg of protein/min. Units for CL_{int} = μ L/mg/min. Total= sum of metabolites (AQM+AQ4).

3.3.9 SDS- Page characteristics and activities of Purified CPR, HO- 1 and nNOS.

The cytochrome P450 reductase enzyme (CPR) ran to a position corresponding to approximately 80 KD on a 12.5% polyacrylamide SDS gel (Fig 31). This was in good agreement with the published molecular mass of the enzyme (Workman and Walton 1990). However, two other minor bands of unknown identity were also detected at positions corresponding to approximately 66 KD (see figure 31). Despite these minor impurities the preparation was highly active (2.0 μ mol/mg/min) in the reduction of oxidised cytochrome c. The truncated HO-1 protein was found to be a highly purified preparation as only a single band was detected by SDS- PAGE at a molecular weight corresponding to the published molecular weight of the enzyme (Wilks and Ortiz de Montellano 1993). The enzyme had an activity of 93 nmol/ mg/min (mean of two determinations). The activity of nNOS was found to be 0.21 μ mol/mg/min (mean of two determinations).

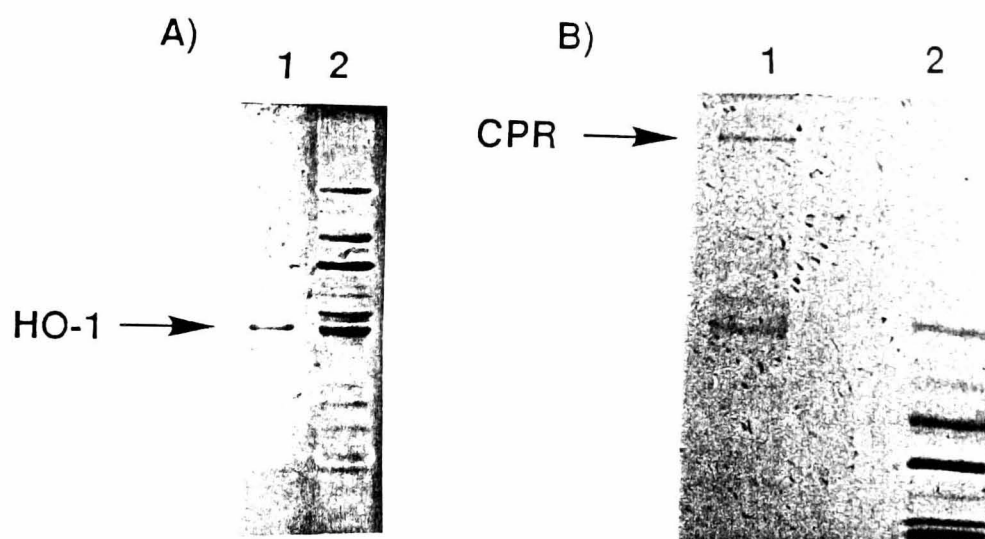


Fig 31. SDS- PAGE for **A)** purified HO- 1 and **B)** partially purified CPR.

Gels were run as described in section. In **A)** 3 μ g of HO- 1 were loaded in lane 1. Molecular mass standards are in lane 2 and are: albumin (66KD), ovalbumin (45 KD), glyceraldehyde 3- phosphate dehydrogenase (36 KD), carbonic anhydrase (29 KD) and trypsinogen (24 KD), . In **B)** 3 μ g of CPR were loaded in lane 1 and the same molecular mass standards as used in A) are in lane 2.

3.4. Metabolism of AQ4N in experiments using recombinant nNOS and the CPR/ HO- 1 system

The results of anaerobic metabolism experiments using nNOS and the CPR/ HO- 1 system are shown in table 7. With respect to incubations containing nNOS, 120 min anaerobic incubation resulted in the generation of both AQ4 and AQM. Aerobic incubations produced both metabolites however, AQ4 and AQM production was 2.3 and 2.7 fold lower respectively than anaerobic incubations. Metabolism was not

detected in incubates without NADPH or nNOS. Although anaerobic metabolism of AQ4N was detected in incubates containing the CPR/ HO-1 system, the presence of HO-1 caused a small, albeit, significant ($P<0.05$) reduction in the amount of AQ4 formed. A peak corresponding to AQM was not detected in incubates containing the CPR/ HO-1 system (with or without HO-1) and metabolism was not detected in aerobic incubates containing the system with or without HO-1. Similarly, metabolites were not detected in incubates minus HO-1 when either NADPH, haemin or when CPR were removed.

Table 7. Anaerobic metabolism of AQ4N by purified nNOS and the CPR/ HO-1 enzyme system

Conditions	AQ4	AQM
nNOS+ NADPH+AQ4N minus air	0.52 ± 0.03	5.9 ± 0.04
CPR+ HO- 1+ haemin+AQ4N +NADPH minus air	2.55 ± 0.33	ND
CPR+ haemin+ AQ4N+NADPH minus air	$3.18 \pm 0.11^*$	ND

Results are expressed as nmol of metabolite formed/incubate after 120 min of anaerobic incubation. Each result is the mean of three independent determinations \pm SE. See sections 2.8.2 and 2.8.4 for experimental conditions. * significantly different ($P<0.05$) from incubates containing HO-1. HO-1=haem oxygenase, CPR= cytochrome P450 reductase and ND= not detected.

3.5. Conclusions

1) In rat hepatic microsomes, the novel anthraquinone di-*N*-oxide prodrug, AQ4N was metabolised under physiological conditions by a process that shows a marked preference for NADPH over NADH as reduced cofactor and was inhibited by air. Furthermore, the anaerobic metabolism of this prodrug did not occur in the cytosol and was inhibited by the general CYP inhibitors ketoconazole (100 μ M) and carbon monoxide. In addition, AQ4 was oxidised to AQM under aerobic conditions in a process inhibited by ketoconazole.

2) Rat hepatic microsomes also mediated the anaerobic metabolism of AQM (the two electron reduced mono-*N*-oxide of AQ4N) to AQ4. The metabolism, like that of AQ4N, was inhibited by air, carbon monoxide and ketoconazole. The metabolism occurred maximally when NADPH was used as reduced co factor and cytosolic metabolism was found to be approximately 10% of that observed in microsomes (see Table 5).

3) Microsomes from rats pre treated with known CYP inducers anaerobically metabolised AQ4N to different extents. Interestingly, when AQM was used as substrate, a similar profile of differential metabolism was obtained to that of AQ4N. Specifically ISO (CYP 2E inducer) and PB (CYP 2B inducer) pretreatment significantly enhanced the metabolism of both compounds. Whereas 3 MC and PCN pretreatments produced microsomes which repressed the metabolism of both AQ4N and, in separate experiments, the mono-*N*-oxide (AQM) compared to uninduced microsomes. Furthermore, inhibition studies confirmed that CYP 2E and CYP 2B were the major rat CYPs involved in the metabolism of AQ4N and AQM.

4) The kinetics of AQ4N metabolism conformed to a classic Michaelis-Menten model. This was true for the generation of AQM, AQ4 and total substrate turnover (sum of metabolites). In contrast, the kinetics of AQM metabolism were found to be better described by sigmoid kinetics.

The kinetic parameters V_{\max} , K_m and CL_{int} were determined for the metabolism of both compounds and demonstrated that AQM was a better substrate (higher V_{\max} , and higher CL_{int}) for rat hepatic microsomes than AQ4N.

5) Preliminary experiments demonstrated that AQ4N was a substrate for purified rat nitric oxide synthase (nNOS) and partially purified cytochrome P450 reductase (CPR). The latter enzyme requiring haem for activity. However, the anaerobic metabolism of AQ4N by CPR with haem was decreased in the presence of human haem oxygenase.

In summary, both AQ4N and the mono-*N*-oxide AQM undergo hypoxia dependent metabolism in the presence of rat hepatic microsomes and NADPH. In addition, AQ4 underwent a small amount of oxidation under aerobic conditions and in the presence of NADPH. Differential metabolism studies and the use of inhibitors demonstrated that rat hepatic CYPs metabolised both of these compounds. Furthermore, both compounds were substrates for rat hepatic CYP 2E and 2B. In addition, preliminary experiments suggested that CPR (in combination with haem) and nNOS were both able to metabolise AQ4N.

Chapter 4

Chapter 4

Metabolism of AQ4N and AQM in human subcellular fractions

4.1 Aims

To investigate the role of the human CYP enzymes in the metabolism of AQ4N and AQM in a variety of human subcellular fractions and in some clinically resected human renal and colonic tumours.

4.2 Materials and Methods

The approach adopted to identify human CYP enzymes responsible for the metabolism of both the prodrug AQ4N and the mono-*N*-oxide AQM have been outlined in detail in section 2.1. Livers of road accident victims or those taken from organ donor patients were kindly provided by Professor M Danny Burke, clinicopathological data for each liver are shown in table 2. Clinically resected human tumours along with the corresponding samples of healthy tissue were provided by Dr G I Murray and the details for each tumour are shown in table 3. Gene transfected human lymphoblastoid cell microsomes were obtained from the source cited in section 2.2.2.

4.2.1 Protein determination

All tissue protein was quantified by the method described in section 2.5.

4.2.2 Metabolism of both AQ4N and AQM in human subcellular fractions

Anaerobic conditions were obtained in an identical manner to that described in the previous chapter and are detailed in section 2.6. Metabolism of AQ4N and, where possible AQM, in human liver, renal, colon and various human tumours was carried out by the method described in section 2.7. CYP specific inhibitors were also used in separate metabolism studies using the method described in section 2.7.1. Oxidative metabolism of AQ4 was determined in two individual livers by the method described in section 2.7.2.

4.2.3 Correlation analysis

Distribution free Spearman Rank correlation between the anaerobic metabolism of both AQ4N and AQM and various CYP activities in human liver microsomes was determined by the method described in section 2.9.1.

4.2.4 Kinetic analysis

The kinetics of AQ4N bioreduction were analysed in an identical manner to that used for the rat mediated metabolism. The observer independent software used allowed for a simultaneous fitting of data to classic kinetic equations and is described in section 2.7.3.

4.2.5 Metabolism of AQ4N in human gene transfected cell microsomes

The CYP 3A and CPR activities of human lymphoblastoid cell microsomes were assayed as described in section 2.8.3. The metabolism of AQ4N by lymphoblastoid cell microsomes transfected with separate cDNA sequences for CYP 3A4, CYP 2B6 and CPR is described in section 2.8.5.

4.2.6 HPLC and Metabolite detection

At appropriate times, all metabolic incubations were terminated and deproteinised (section 2.9). The metabolites of either AQ4N or AQM were analysed and quantified by reverse phase isocratic HPLC as described in detail in section 2.9.

4.3 Results

4.3.1 Metabolism of AQ4N and AQM in human hepatic tissue

Anaerobic metabolism of AQ4N (100 μ M) was supported in all human liver microsomes (HLM) tested. In incubates containing 400 μ g of protein, the range (\pm SE) of total metabolism after 60 min incubation was 14.26 ± 1.43 (highest) to 3.65 ± 1.05 nmol/incubate (lowest) (Fig 32 and 33). In separate experiments where 100 μ M AQM was used as substrate and incubations contained 100 μ g of protein, the range of AQ4 formation (\pm SE) after 60 min incubation was 4.24 ± 0.3 (highest) to 1.42 ± 0.2 (lowest) (Fig 34). Metabolism of both compounds was undetectable in incubates purged with carbon monoxide, depleted of NADPH or in incubates containing heat denatured (boiled for 5 min) microsomes. In air saturated incubates, the metabolism of AQ4N to AQM was routinely less than 4% of anaerobic controls whereas the production of AQ4 was not detected. Metabolism of AQ4N to both metabolites was undetected in cytosolic fractions. When AQM was used as substrate, the anaerobic generation of AQ4 in cytosol was consistently less than 10% of the value obtained in microsomes.

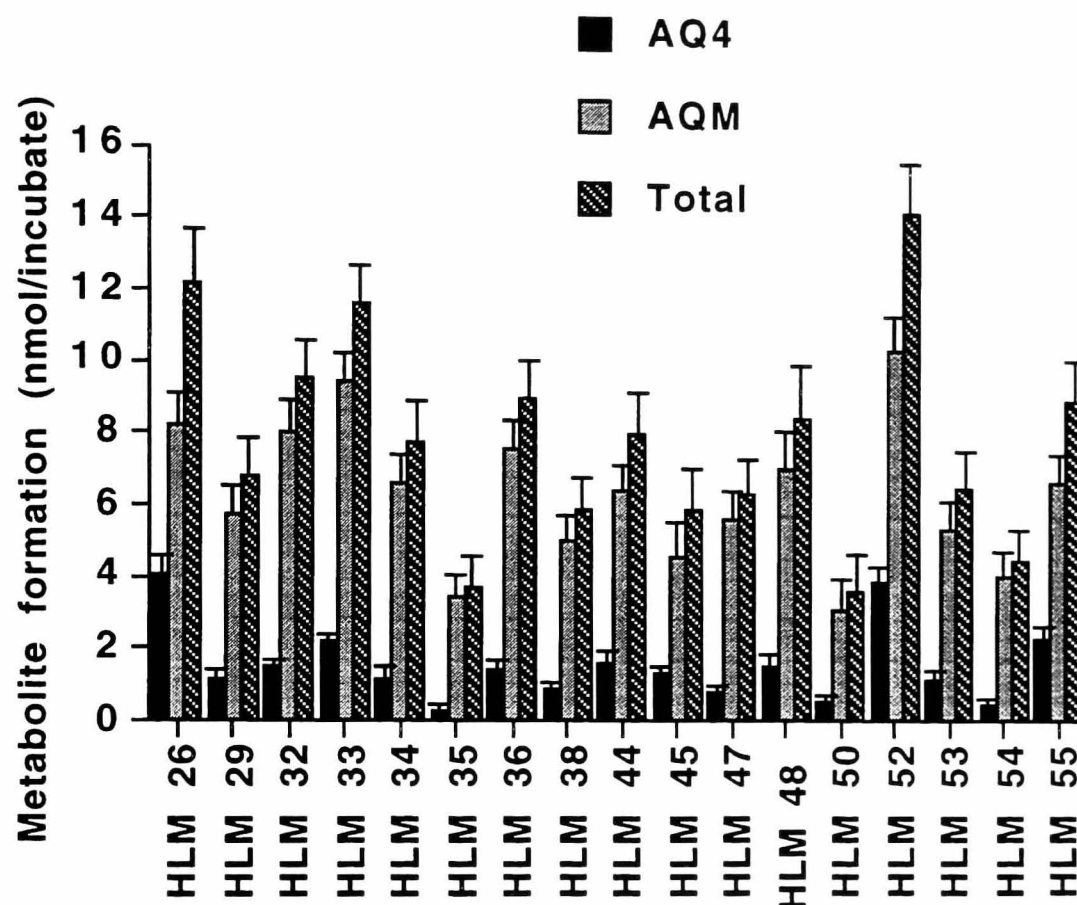


Fig 32. Anaerobic metabolism of 100 μ M AQ4N in a panel of 17 human liver microsomes (HLM's).

Incubations contained 400 μ g of protein and data were obtained after 60 min incubation. Results are expressed as the mean \pm SE for three independent determinations. See section 2.7 for experimental methods.

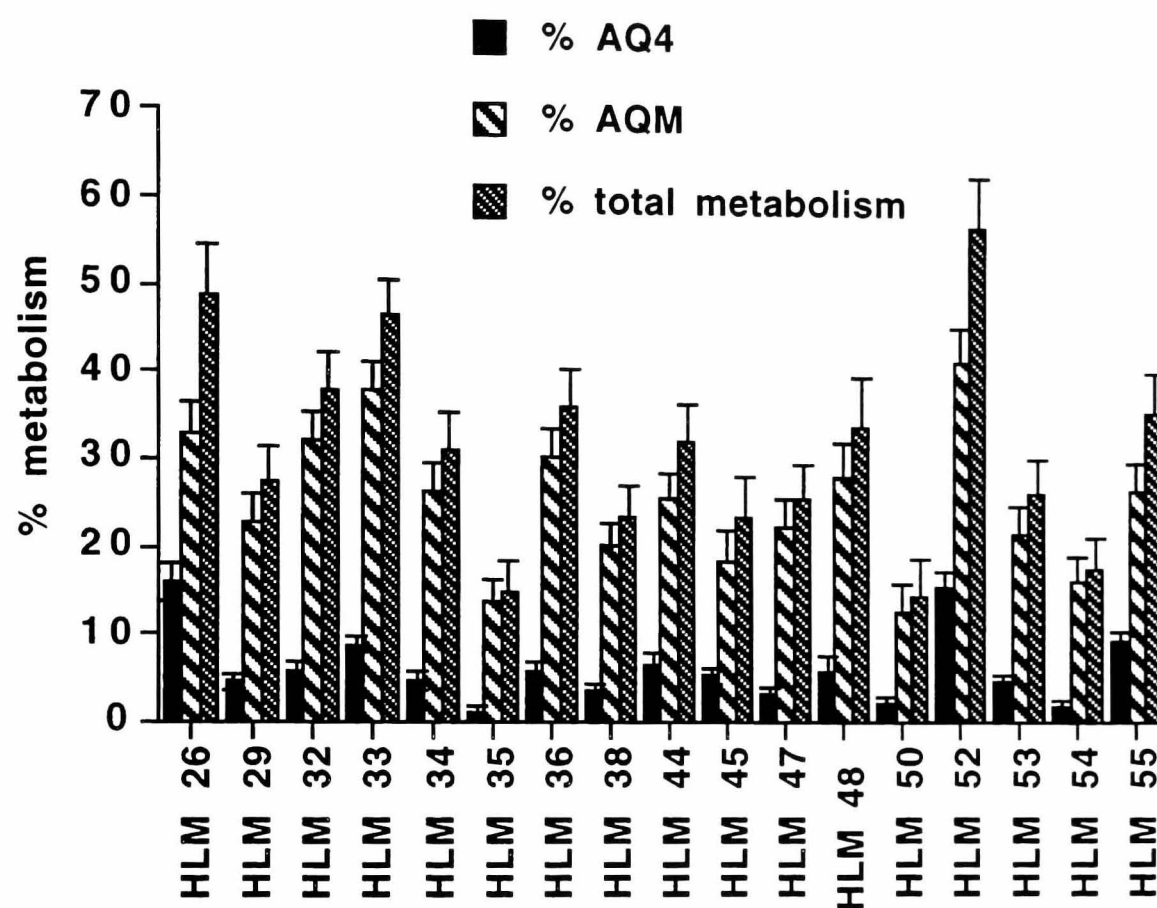


Fig 33. Percentage anaerobic metabolism of 100 μ M AQ4N in a panel of 17 human liver microsomes.

Data are derived from figure 32 and are expressed as the mean percentage metabolism \pm % SE

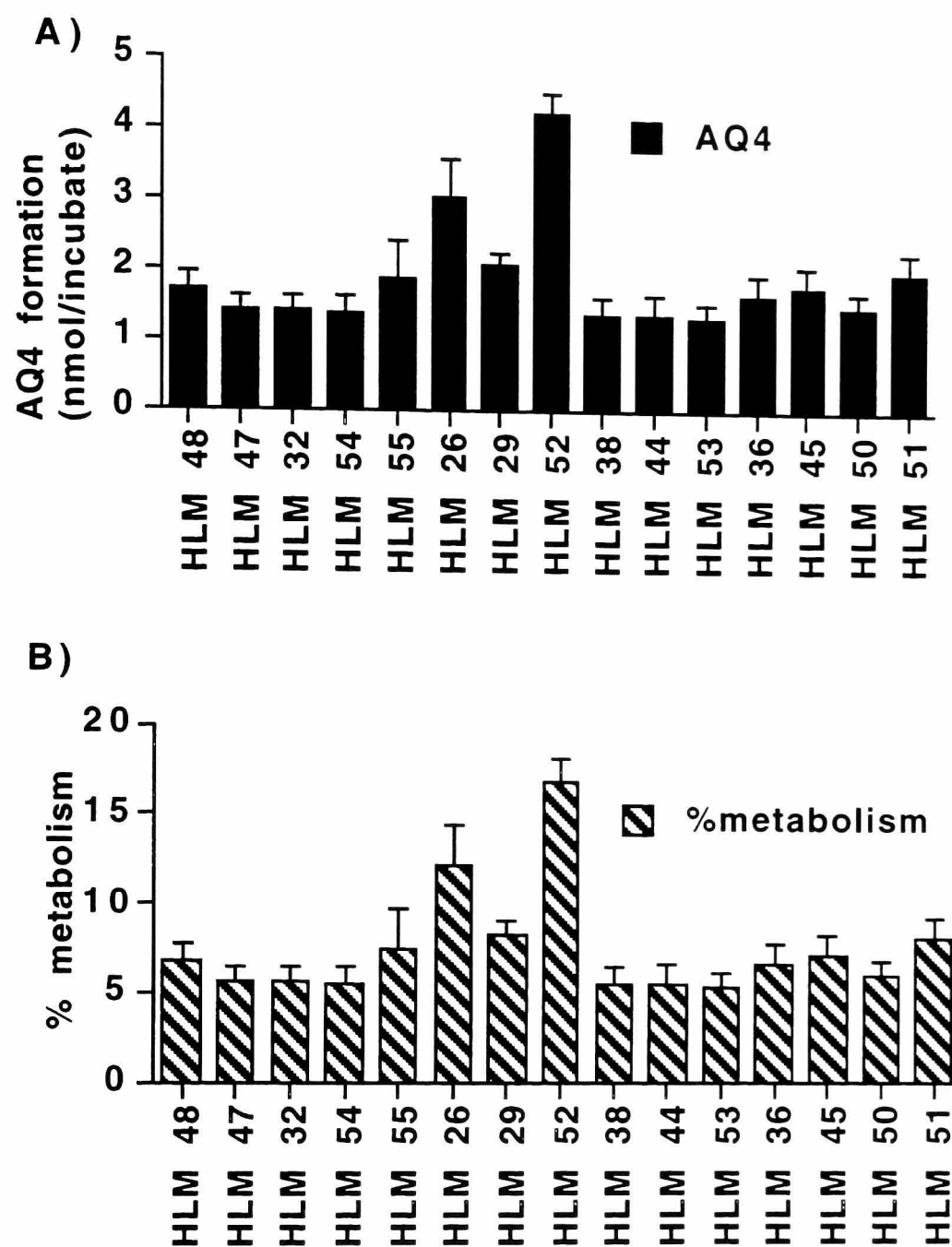


Fig 34. Anaerobic metabolism of AQM in a panel of seventeen human liver microsomes (HLMs).

Incubates contained 100 μ g of protein and 100 μ M AQM. Data were taken after 60 min incubation and are expressed as **A)** the mean \pm SE for three independent determinations or **B)** percentage metabolism. See section 2.7 for experimental conditions.

4.3.2 Correlations between the metabolism of AQ4N and AQM and markers of CYP activity/content

Scattergrams and Spearman rank correlation coefficients (r_s) for the metabolism of both AQ4N and AQM versus various CYP activities/isoform content are shown from Figure 35 through to Figure 37. Significant correlations ($p < 0.01$) were obtained for the metabolism of AQ4N and two CYP 3A markers, namely benzoxyresorufin *O*-deethylation (BROD) and tamoxifen *N*-demethylation (TND). AQ4N metabolism was not significantly correlated with markers of CYP 2C, 1A, 2A or 2D (Table 8). Similarly, the metabolism of AQM correlated strongly ($p < 0.01$) with BROD activity ($r_s = 0.74$, $N = 14$) and to a lesser extent ($p < 0.05$) with tamoxifen *N*-demethylation ($r_s = 0.83$). Interestingly, AQM metabolism also correlated with coumarin 7-hydroxylase activity ($p < 0.05$), a marker of CYP 2A activity (Fig 37 C). The metabolism of AQM to AQ4 correlated strongly with the overall four electron reduction of AQ4N to AQ4 ($p < 0.01$) (Fig 38 A). However, the metabolism of AQM to AQ4 correlated only weakly ($p < 0.05$) with the two electron reduction of AQ4N to AQM and the total metabolism of AQ4N (Fig 38 B and C respectively). Like AQ4N, AQM metabolism did not correlate with markers of CYP 1A/2C or 2D (Table 9).

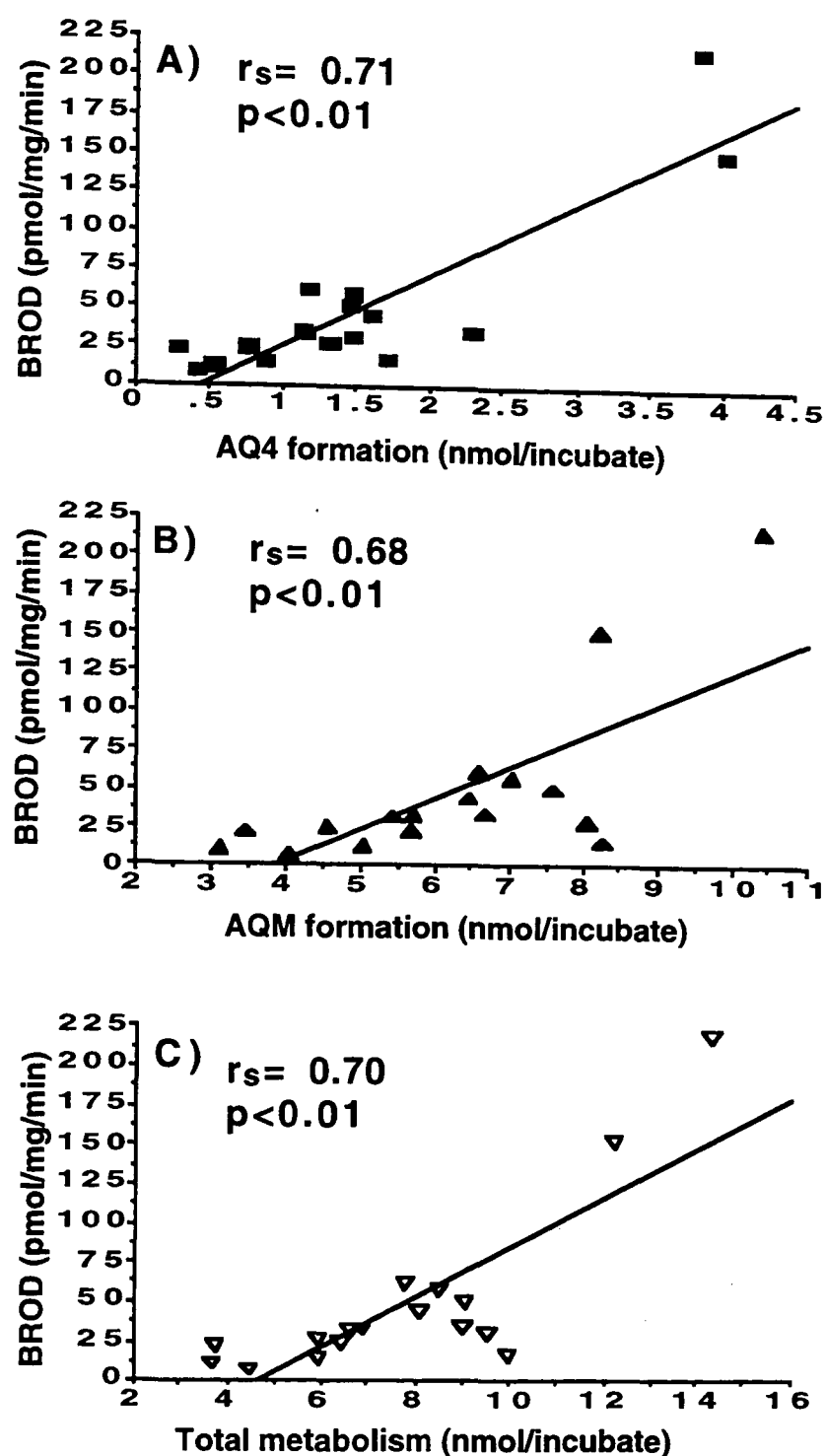


Fig 35. Correlations between Benzyloxyresorufin O-deethylase (BROD) activity and the anaerobic metabolism of AQ4N

Data from figure 30 were subjected to Spearman rank correlation analysis, (N= 17). Regression lines are shown for correlations that reach significance at $p < 0.01$ **A)** AQ4 formation. **B)** AQM formation and **C)** total metabolism. See section 2.7 for experimental conditions and 2.9.1 for analysis.

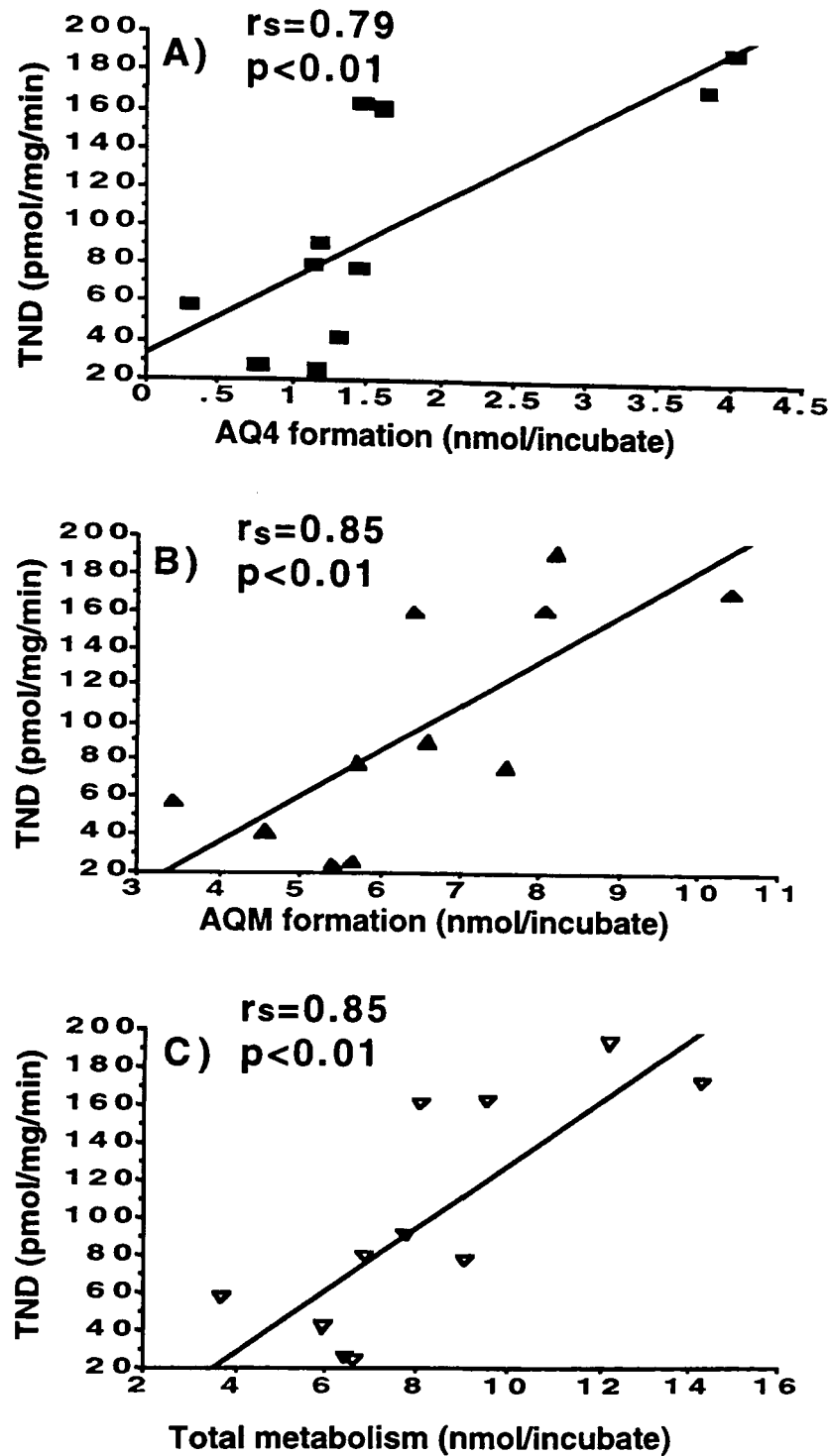


Fig 36. Correlations between tamoxifen N-demethylation (TND) and the anaerobic metabolism of AQ4N.

Data from figure 30 were subjected to Spearman rank correlation analysis, (N=17). Regression lines are shown for correlations that reach significance at $p<0.01$. **A)** AQ4 formation, **B)** AQM formation and **C)** total metabolism. See section 2.7 for experimental methods and 2.9.1 for analysis.

Table 8. Non significant Spearman rank correlations ($p>0.05$) between various CYP activities/ isoform content and the anaerobic metabolism of AQ4N in human liver microsomes.

Metabolite	CYP activity/ content	CYP marker	rs	p value	N
AQ4	tolbutamide hydroxylation	CYP 2C	0.05	0.84	17
AQM	tolbutamide hydroxylation	CYP 2C	0.13	0.59	17
Total	tolbutamide hydroxylation	CYP 2C	0.15	0.65	17
AQ4	CYP 2C content	CYP 2C	0.37	0.12	17
AQM	CYP 2C content	CYP 2C	0.23	0.36	17
Total	CYP 2C content	CYP 2C	0.31	0.20	17
AQ4	coumarin hydroxylation	CYP 2A	0.31	0.31	12
AQM	coumarin hydroxylation	CYP 2A	0.08	0.80	12
Total	coumarin hydroxylation	CYP 2A	0.19	0.53	12
AQ4	CYP 1A content	CYP 1A	-0.13	0.68	12
AQM	CYP 1A content	CYP 1A	-0.02	0.94	12
Total	CYP 1A content	CYP 1A	-0.04	0.89	12
AQ4	DMOD	CYP 2D	-0.08	0.80	12
AQM	DMOD	CYP 2D	0.04	0.90	12
Total	DMOD	CYP 2D	0.07	0.82	12

Correlations were based on the data shown in figure 32. Total= sum of metabolites, DMOD= dextromethorphan O-demethylation, rs= Spearman rank correlation coefficient and N= number of livers tested. CYP 2C and 1A contents were measured by western blotting using polyclonal antibodies (section 2.9.1).

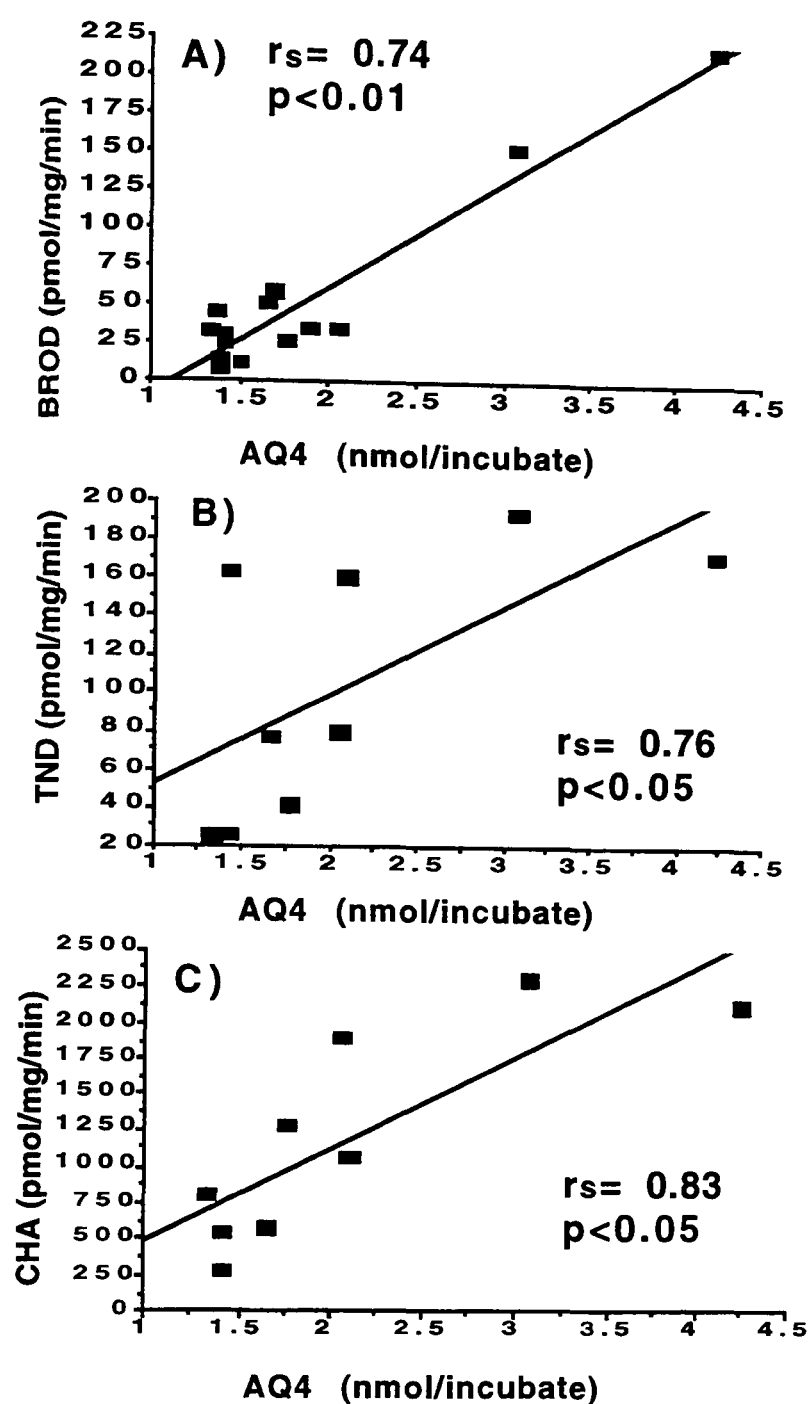


Fig 37. Correlations between the anaerobic metabolism of AQM to AQ4 and various CYP activities.

Data from figure 34 were subjected to Spearman rank analysis. Regression lines are shown for correlations that reached significance at $p < 0.05$ and $p < 0.01$. A) benzyloxyresorufin O-deethylase (BROD) activity (N= 14), B) tamoxifen N- demethylase (TND) activity (N= 9), and C) coumarin 7- hydroxylase (CHA) activity (N= 9). See section 2.7 for experimental conditions and 2.9.1 for analysis.

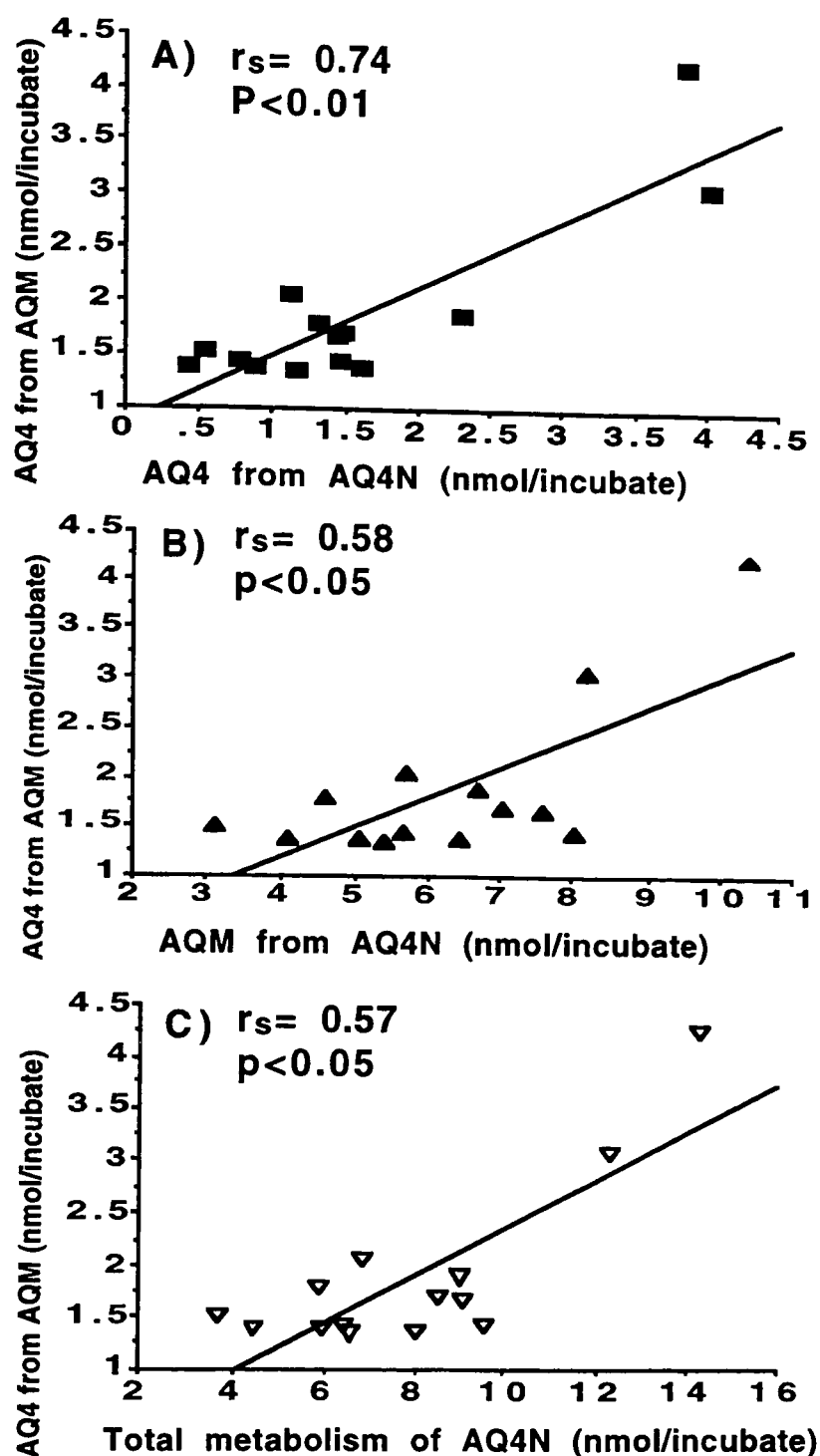


Fig 38. Correlations between the anaerobic metabolism of AQM and the anaerobic metabolism of AQ4N.

Data from figures 32 and 34 were subjected to Spearman rank correlation analysis ($N = 14$). Regression lines are shown for correlations that reached significance at $p < 0.05$. **A)** AQ4 from AQ4N. **B)** AQM from AQ4N and **C)** total metabolism of AQ4N. See section 2.7 for experimental conditions and 2.9.1 for analysis.

Table 9. Non significant Spearman rank correlations ($p>0.05$) between various CYP activities/ isoform content and the anaerobic metabolism of AQM in human liver microsomes.

CYP activity/ content	CYP marker	rs	p value	N
tolbutamide hydroxylation	CYP 2C	0.00	1.00	14
CYP 2C content	CYP 2C	0.43	0.12	14
CYP 1A content	CYP 1A	-0.28	0.38	11
DMOD	CYP 2D	0.42	0.23	9

Correlations were based on the anaerobic production of AQ4 as shown in figure 34. DMOD= dextromethorphan *O*-demethylation, rs= Spearman rank correlation coefficient and N= number of livers tested. CYP 2C and 1A contents were measured by western blotting using polyclonal antibodies (section 2.9.1).

4.3.3 Effect of inhibitors on the metabolism of AQ4N in human liver microsomes

The effect of inhibitors was investigated in three individual liver microsome preparations, HLM 50, HLM 45 and HLM 55. Alpha naphthoflavone (ANF;10 μM) had essentially no effect on the metabolism of AQ4N in all livers tested. Triacetyloleandomycin (TAO;50 μM) inhibited completely the formation of AQ4 in all three HLM preparations. AQM production was inhibited by 71% in HLM 50, 82% in HLM 45 and 100% in HLM 55. KET (100 μM) and carbon monoxide prevented the formation of any detectable metabolites in all three HLM preparations tested (Fig 39 to 41). Typical chromatograms for control and TAO inhibition of AQ4N metabolism are shown for HLM 55 (Fig 42).

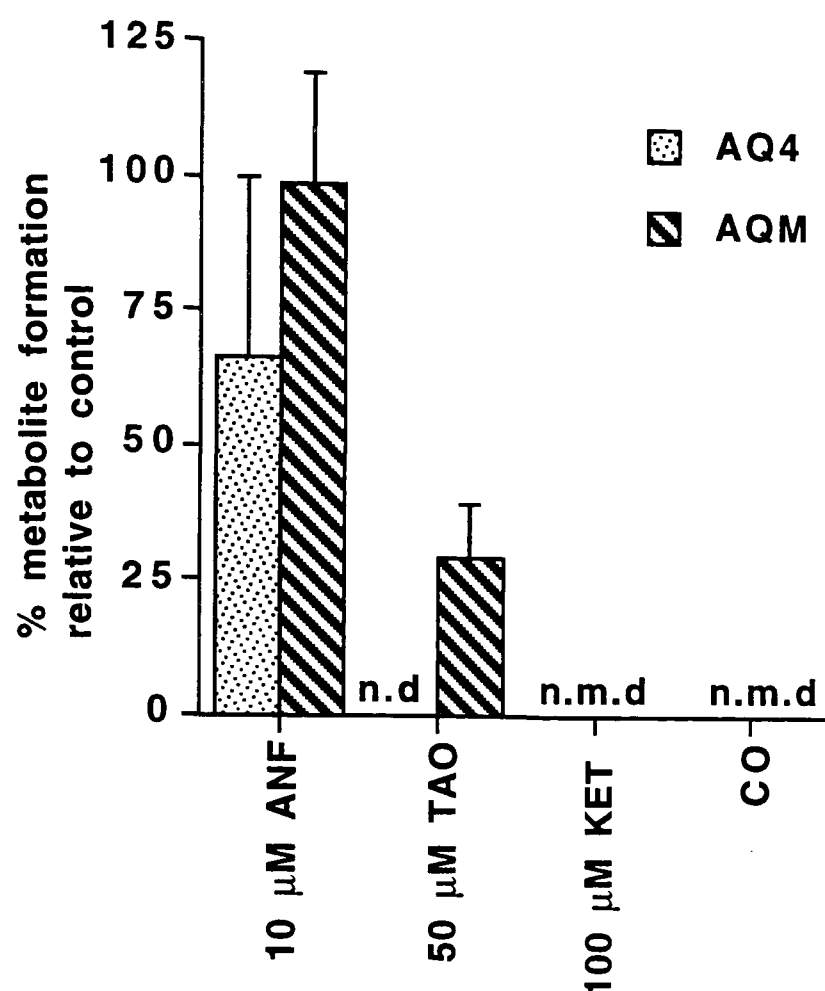


Fig 39. Effect of CYP inhibitors on the anaerobic metabolism of AQ4N in microsomes from HLM 50.

Results are expressed as mean percentage metabolite formation \pm % SE for three determinations relative to control incubations carried out without CYP inhibitor. Each incubate contained 400 µg of protein and 100 µM AQ4N. Data were obtained after 60 min incubation and inhibitors are: alpha- naphthoflavone (ANF), triacetyloleandomycin (TAO), ketoconazole (KET) and carbon monoxide (CO). See section 2.7.1 for experimental conditions. n.d=not detected, n.m.d=no metabolites detected.

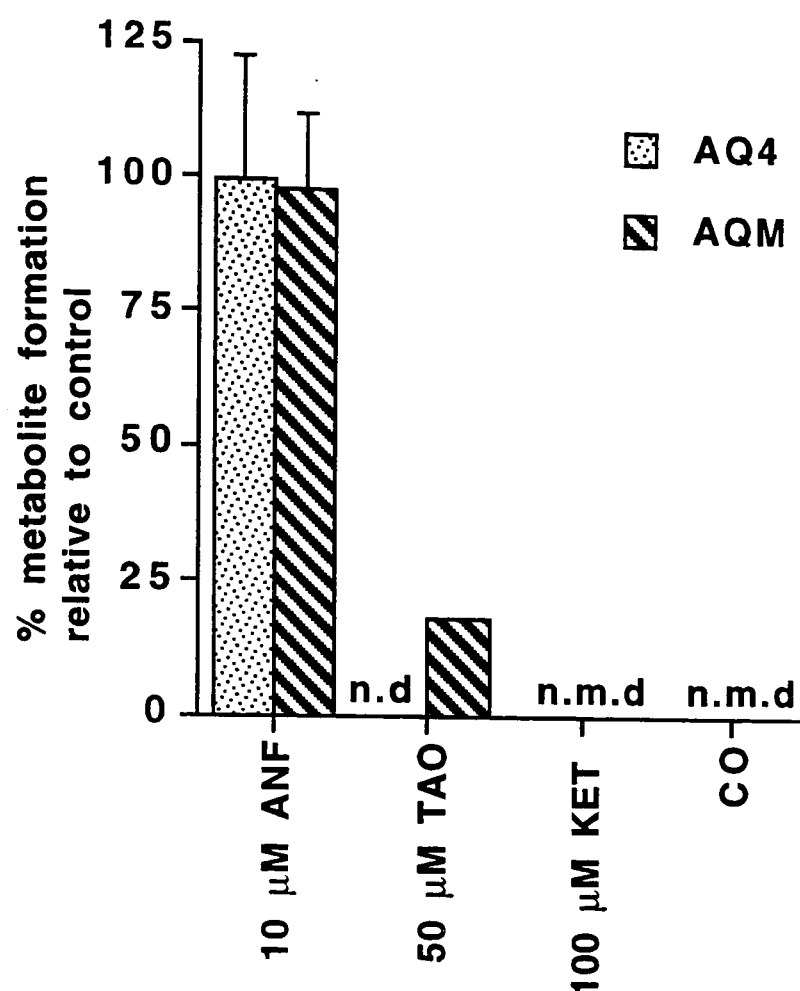


Fig 40. Effect of CYP inhibitors on the anaerobic metabolism of AQ4N in microsomes from HLM 45.

Results are expressed as mean percentage metabolite formation \pm % SE for three determinations relative to control incubations carried out without CYP inhibitor. Each incubate contained 400 µg of protein and 100 µM AQ4N. Data were obtained after 60 min incubation and inhibitors are: alpha naphthoflavone (ANF), triacetyloleandomycin (TAO), ketoconazole (KET) and carbon monoxide (CO). See section 2.7.1 for experimental conditions. n.d=not detected and n.m.d=no metabolites detected.

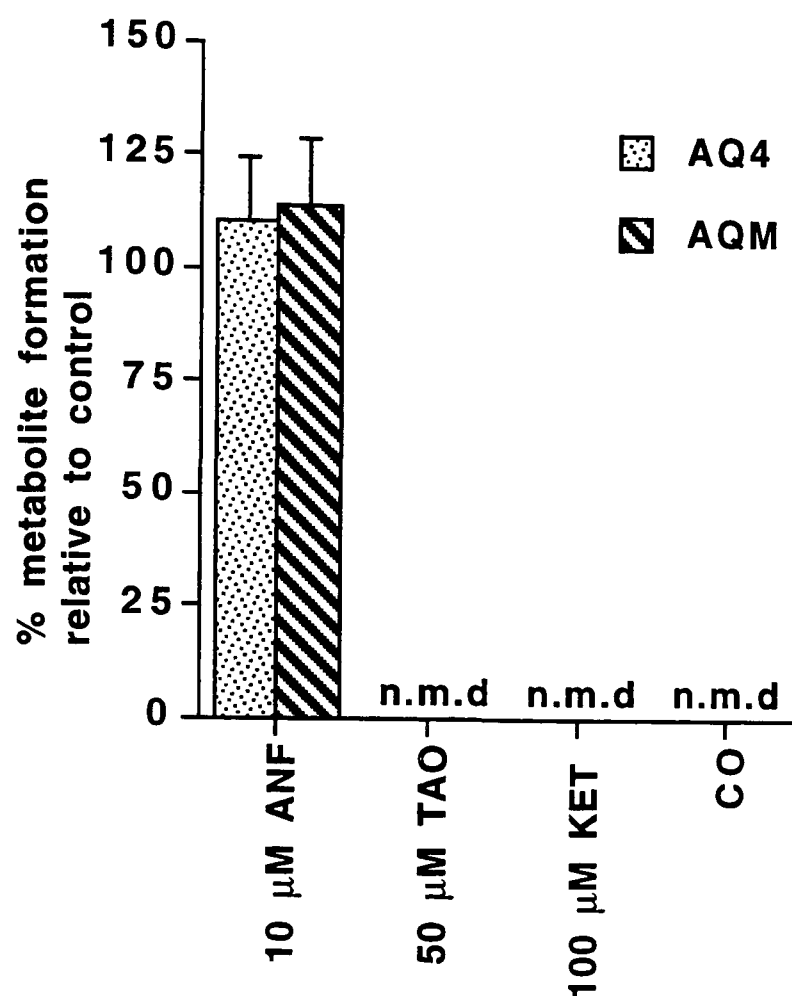


Fig 41. Effect of CYP inhibitors on the anaerobic metabolism of AQ4N in microsomes from HLM 55.

Results are expressed as mean percentage metabolite formation \pm % SE for three determinations relative to control incubations carried out without CYP inhibitor. Each incubate contained 400 µg of protein and 100 µM AQ4N. Data were obtained after 60 min incubation and inhibitors were: alpha naphthoflavone (ANF), triacetyloleandomycin (TAO), ketoconazole (KET) and carbon monoxide (CO). See section 2.7.1 for experimental conditions. n.m.d=no metabolites detected.

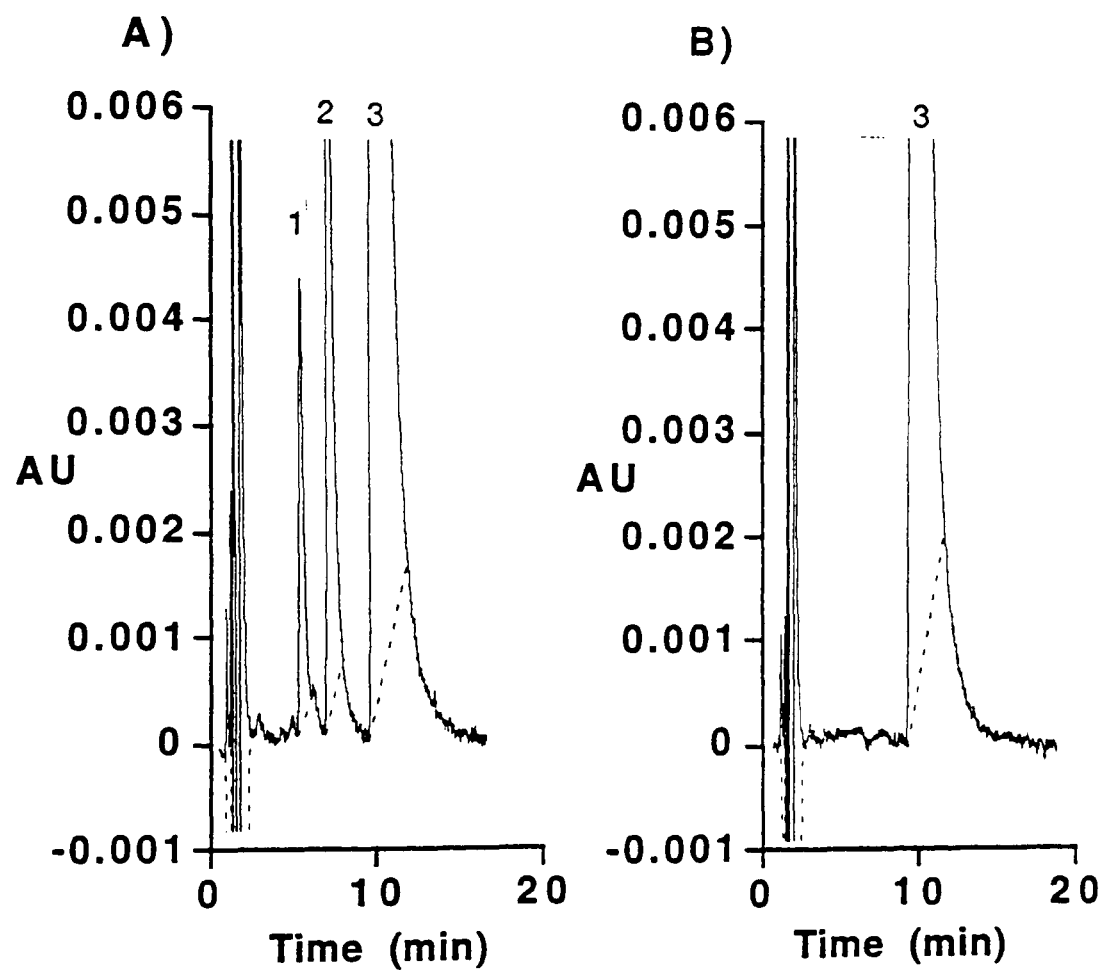


Fig 42. Typical HPLC chromatograms for the anaerobic metabolism of 100 μ M AQ4N in HLM 55. Chromatograms have been taken after 60 min incubation in experiments using 400 μ g of protein and are **A)** incubation in DMSO and **B)** incubation using 50 μ M troleandomycin (TAO). Peaks are 1) AQ4, 2) AQM and 3) AQ4N.

4.3.4 Kinetics of AQ4N metabolism in human liver microsomes

Initial reaction velocities for the anaerobic metabolism of AQ4N in three separate human liver microsome preparations were found to be linear with respect to time from 0 to 40 min (Figs 43 to 45). A slight lag in reaction velocity was observed for HLM 50 and 45 at protein concentrations up to 160 μ g before becoming linear up to approximately 400 μ g (Figs 46 and 47 respectively). HLM 55 kinetics were linear with respect to protein from 0 to 400 μ g (Fig 48). Untransformed kinetic data for the effect of substrate concentration versus initial reaction velocity, for all three individual livers, were subjected to observer independent non linear curve fitting analysis (section 2.7.3) and subsequently shown to conform to Michaelis-Menten kinetics (Figs 49 to 51). Hanes-Woolf transforms of the kinetic data generated linear plots (Figs 52 to 54) from which the kinetic parameters were derived (Table 10).

4.3.5 Oxidative metabolism of AQ4 in human liver microsomes

Oxidative metabolism of AQ4 was investigated in two human liver microsome preparations, HLM 47 and HLM 55. In both preparations 60 min incubation, using 400 μ g of protein, resulted in a single peak with identical chromatographic and spectral properties to AQM (range: (HLM 55) 0.77 nmol- (HLM 47) 0.66 nmol). No metabolism was detected in incubates minus NADPH or microsomes or in incubates containing heat denatured microsomes or the CYP inhibitors KET (100 μ M) or CO. (Figs 55 and 56). Furthermore, no *N*-oxidation occurred under hypoxia

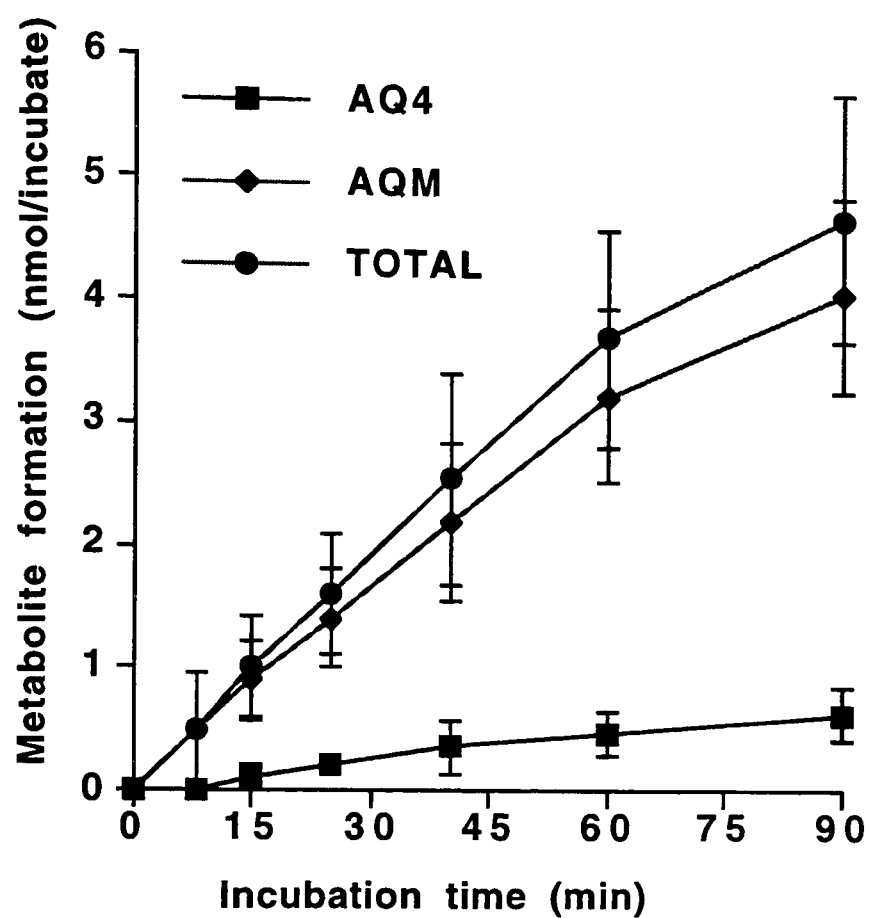


Fig 43. Effect of incubation time on the anaerobic metabolism of AQ4N in microsomes from HLM 50.

Results are expressed as the mean \pm SE for three independent determinations. Each incubate contained 400 μ g of protein and 100 μ M AQ4N. See section 2.7 for experimental conditions.

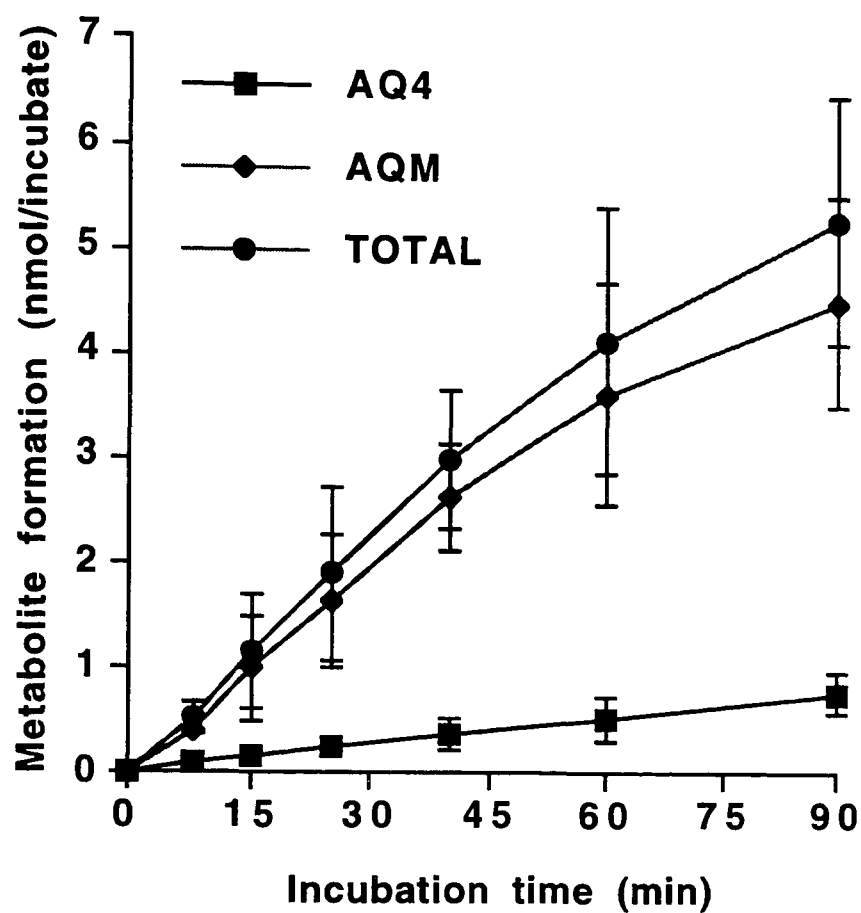


Fig 44. Effect of incubation time on the anaerobic metabolism of AQ4N in microsomes from HLM 45.

Results are expressed as the mean \pm SE for three independent determinations. Each incubate contained 400 μ g of protein and 100 μ M AQ4N. See section 2.7 for experimental conditions.

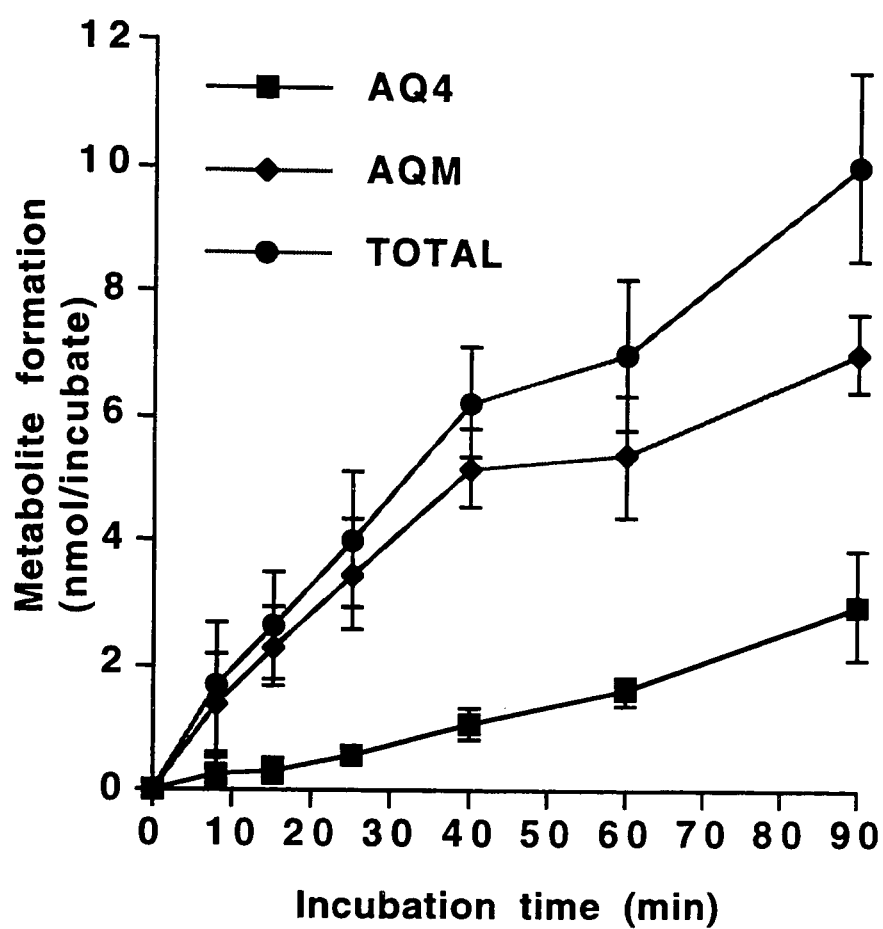


Fig 45. Effect of incubation time on the anaerobic metabolism of AQ4N in microsomes HLM 55.

Results are expressed as the mean \pm SE for three independent determinations. Each incubate contained 400 μ g of protein and 100 μ M AQ4N. See section 2.7 for experimental conditions.

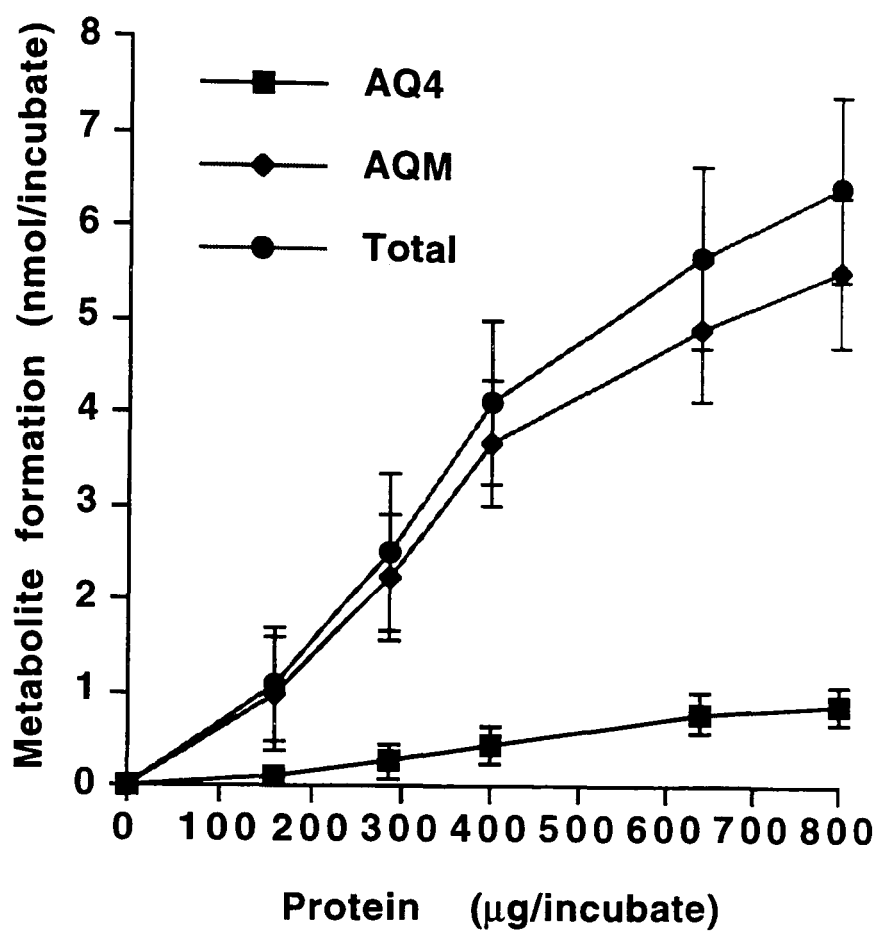


Fig 46. Effect of protein concentration on the anaerobic metabolism of 100 μM AQ4N in microsomes from HLM 50.

Results are expressed as the mean \pm SE for three independent determinations. Data were obtained after 60 min of incubation. See section 2.7 for experimental conditions.

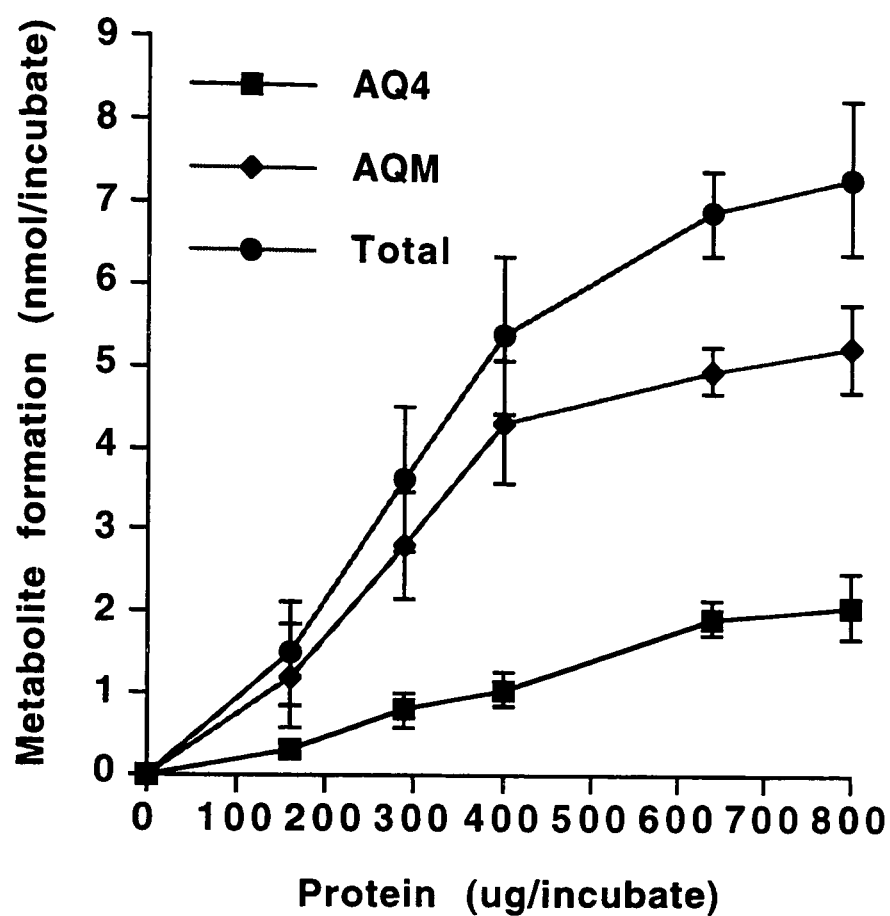


Fig 47. Effect of protein concentration on the anaerobic metabolism of 100μM AQ4N in microsomes from HLM 45.

Results are expressed as the mean \pm SE for three independent determinations. Data were obtained after 60 min incubation. See section 2.7 for experimental methods.

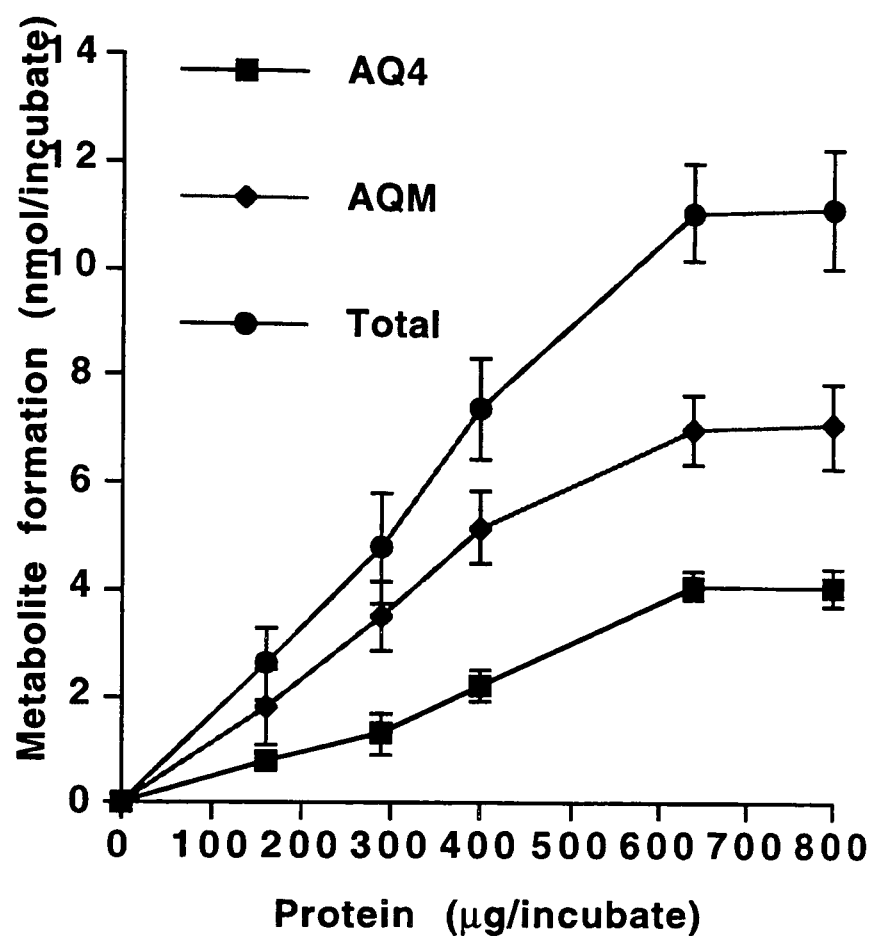


Fig 48. Effect of protein concentration on the anaerobic metabolism of 100 μ M AQ4N in microsomes from HLM 55.

Results are expressed as the mean \pm SE for three independent determinations. Data were obtained after 60 min incubation. See section 2.7 for experimental conditions.

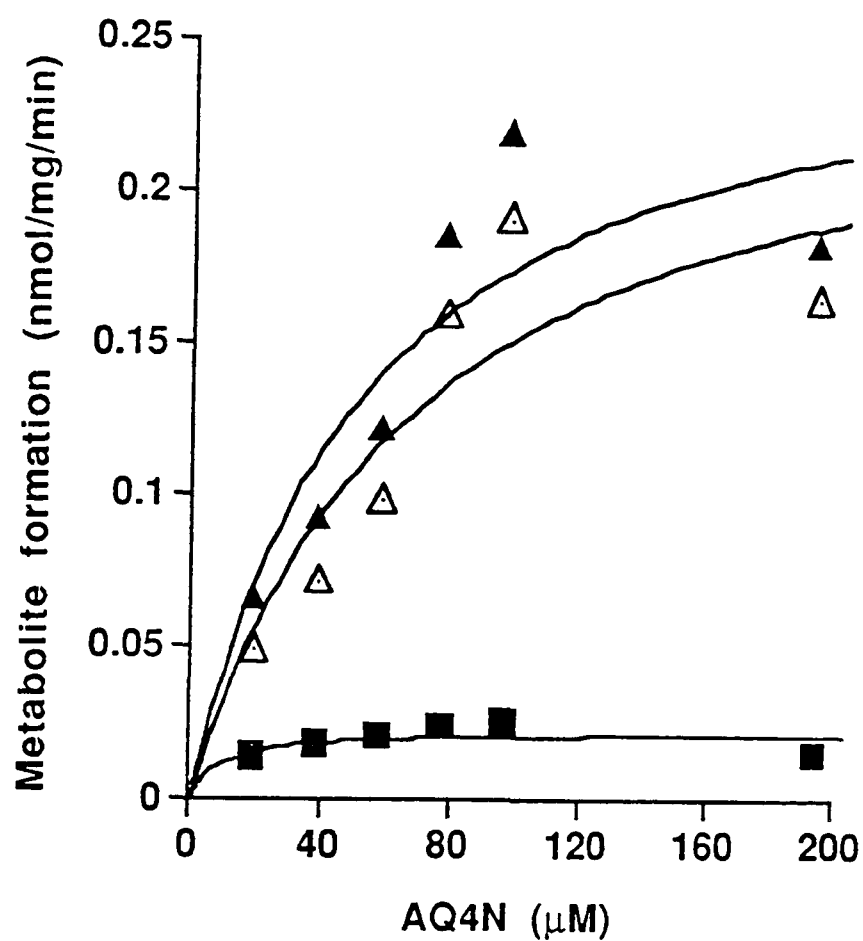


Fig 49. Effect of AQ4N concentration on the initial velocity of metabolite production in HLM 50.

Data are the mean of three incubations and were collected after 40 min of anaerobic incubation. Data are: AQ4 formation (black squares), AQM formation (open triangles) and total metabolism (black triangles). Solid lines are the curves of best fit as determined by observer independent curve fitting (section 2.7.3).

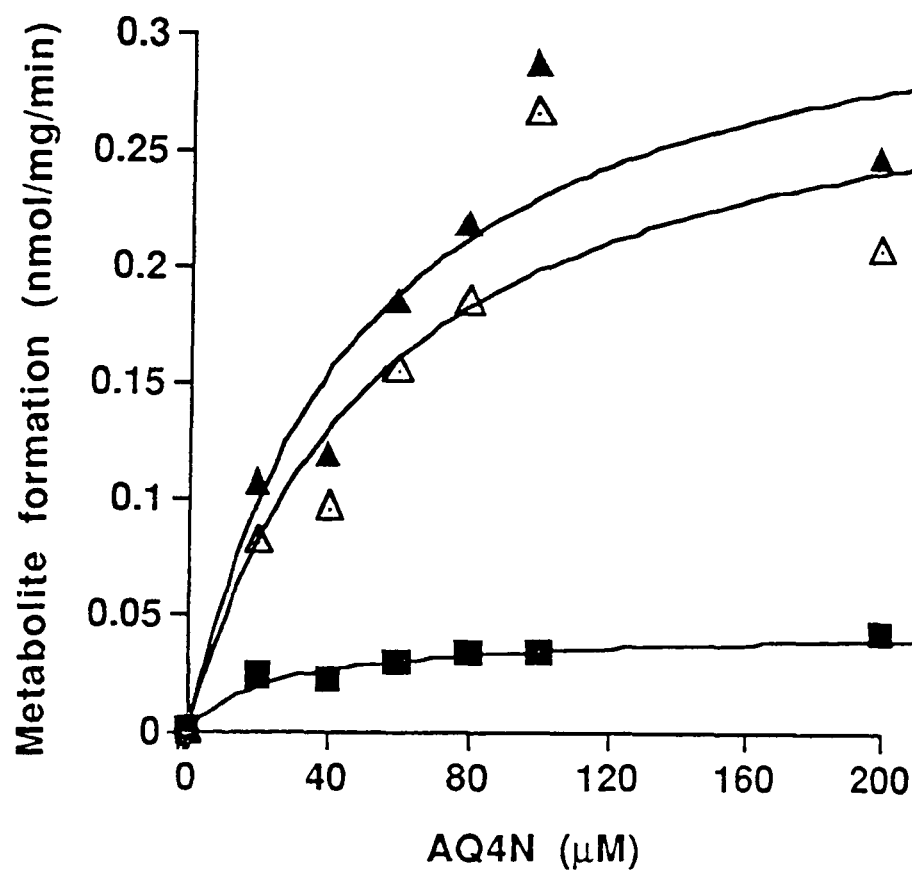


Fig 50. Effect of AQ4N concentration on the initial velocity of metabolite formation in HLM 45.

Data are the mean of three determinations and were collected after 40 min of anaerobic incubation. Data are: AQ4 formation (black squares), AQM formation (open triangles) and total metabolism (black triangles). Solid lines are curves of best fit as determined by observer independent curve fitting (section 2.7.3)

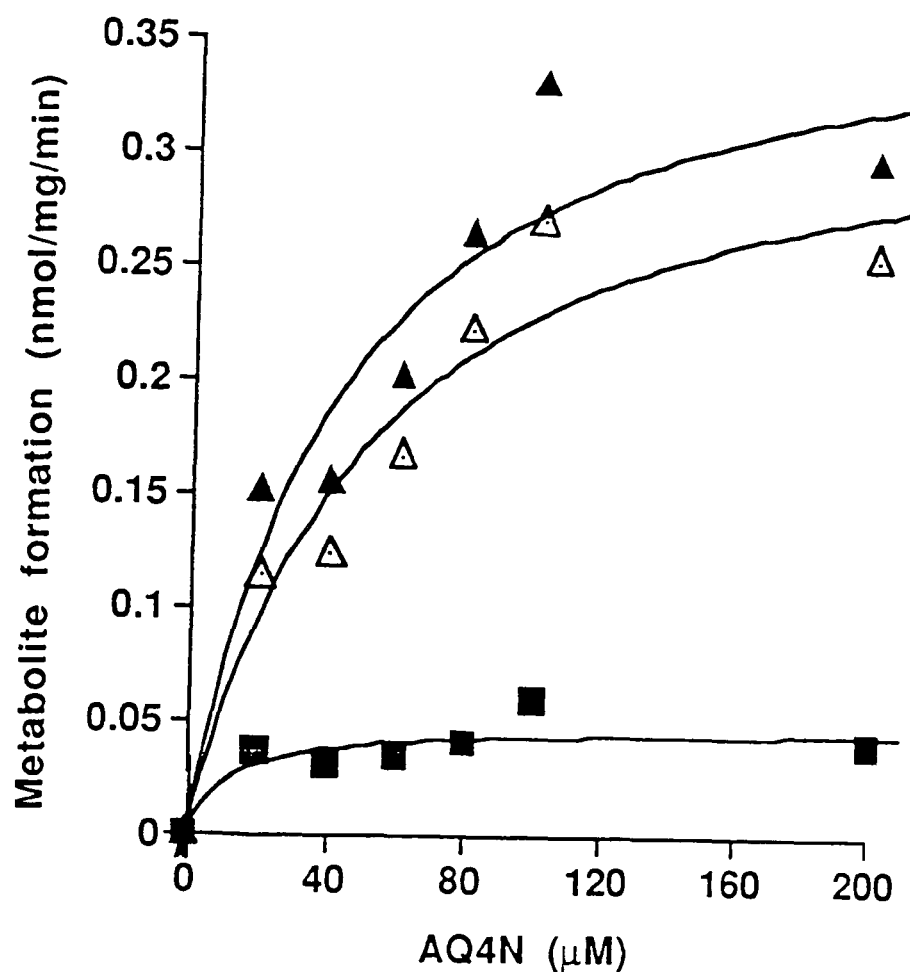


Fig 51. Effect of AQ4N concentration on the initial velocity of metabolite formation in HLM 55.

Data are the mean of three determinations and were collected after 40 min of anaerobic incubation. Data are: AQ4 formation (black squares), AQM formation (white triangles) and total metabolism (black triangles). Solid lines are curves of best fit as determined by observer independent curve fitting (section 2.7.3)

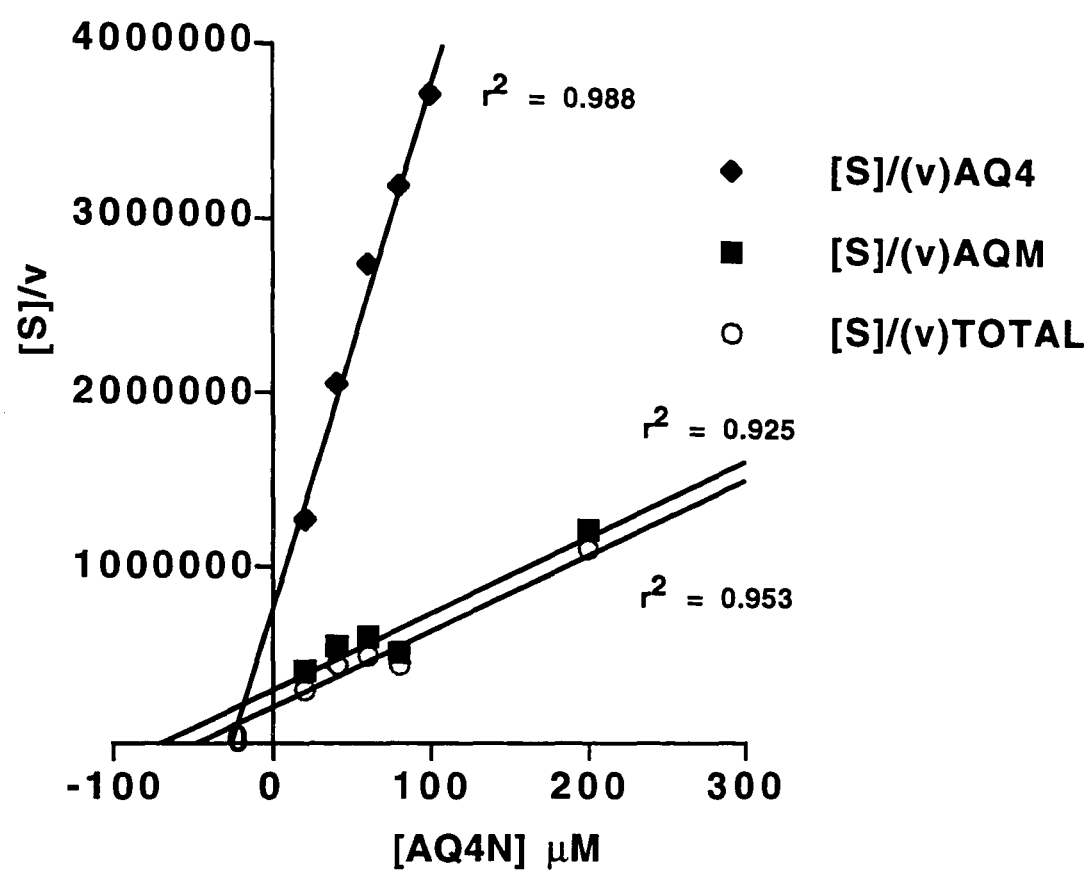


Fig 52. Hanes- Woolf transform of the kinetic data shown in figure 49 for HLM 50.

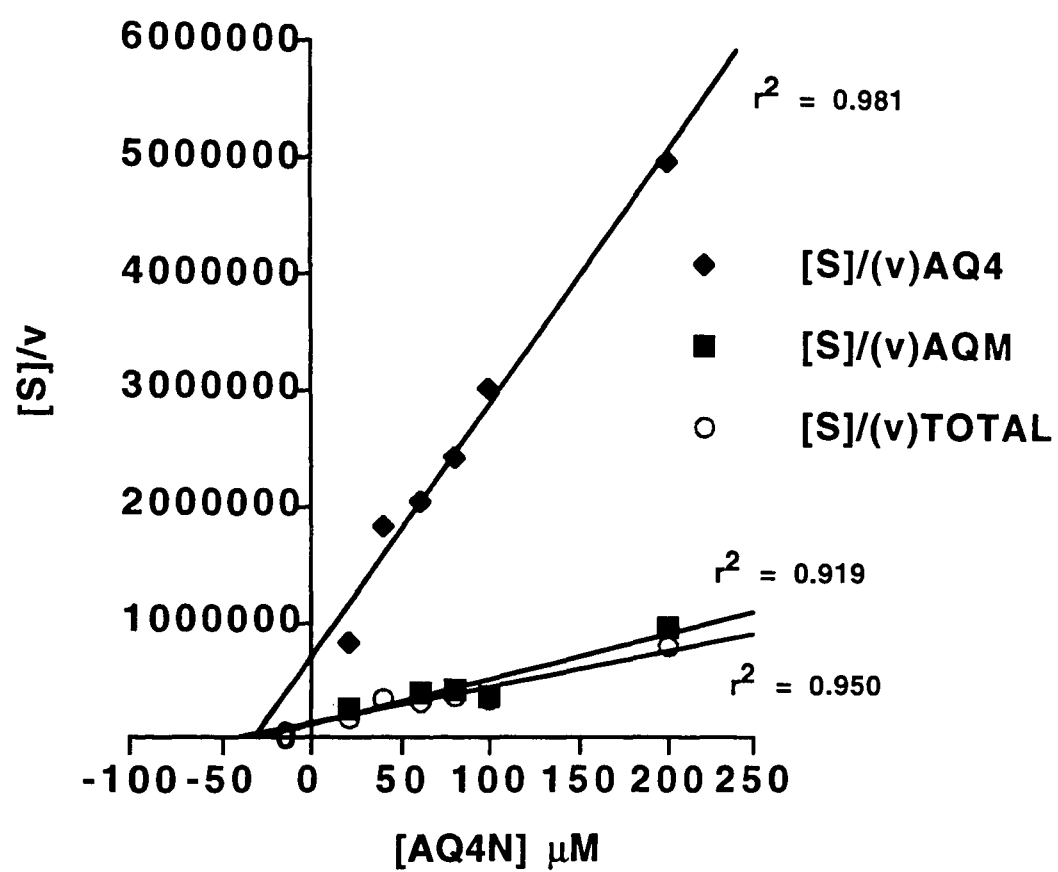


Fig 53. Hanes- Woolf transform of the kinetic data shown in figure 50 for HLM 45.

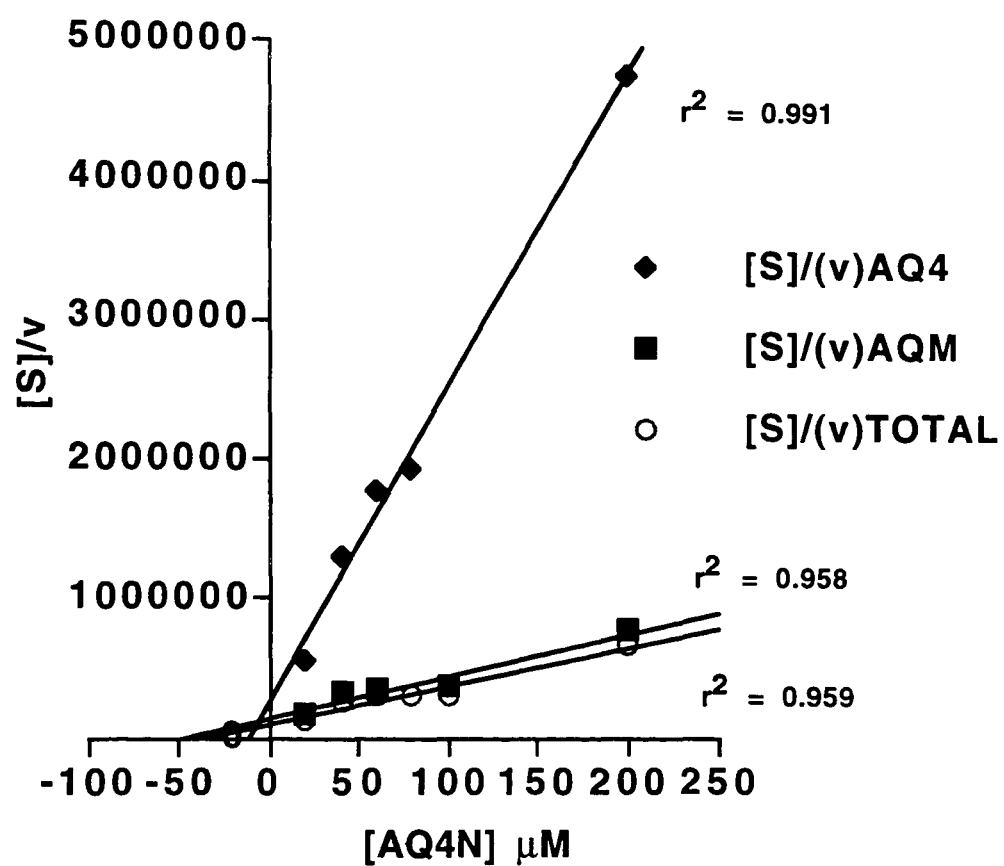


Fig 54. Hanes- Woolf transform of the kinetic data shown in figure 45 for HLM 55

Table 10. Kinetic data for the anaerobic metabolism of AQ4N in three human livers

Liver	Metabolite	K_m (μ M)	V_{max} (nmol/mg/min)	CL_{int}
HLM 50	AQM	70	0.25	3.5
	AQ4	25	0.02	0.8
	total	50	0.27	5.2
HLM 45	AQM	30	0.31	10
	AQ4	22	0.04	1.8
	total	45	0.35	7.7
HLM 55	AQM	48	0.34	7.0
	AQ4	16	0.05	3.2
	total	40	0.40	10

Results are expressed as the mean of three determinations. CL_{int} (intrinsic clearance)= V_{max}/K_m . Units for CL_{int} are μ L/mg/min. Total= sum of metabolites (AQM +AQ4).

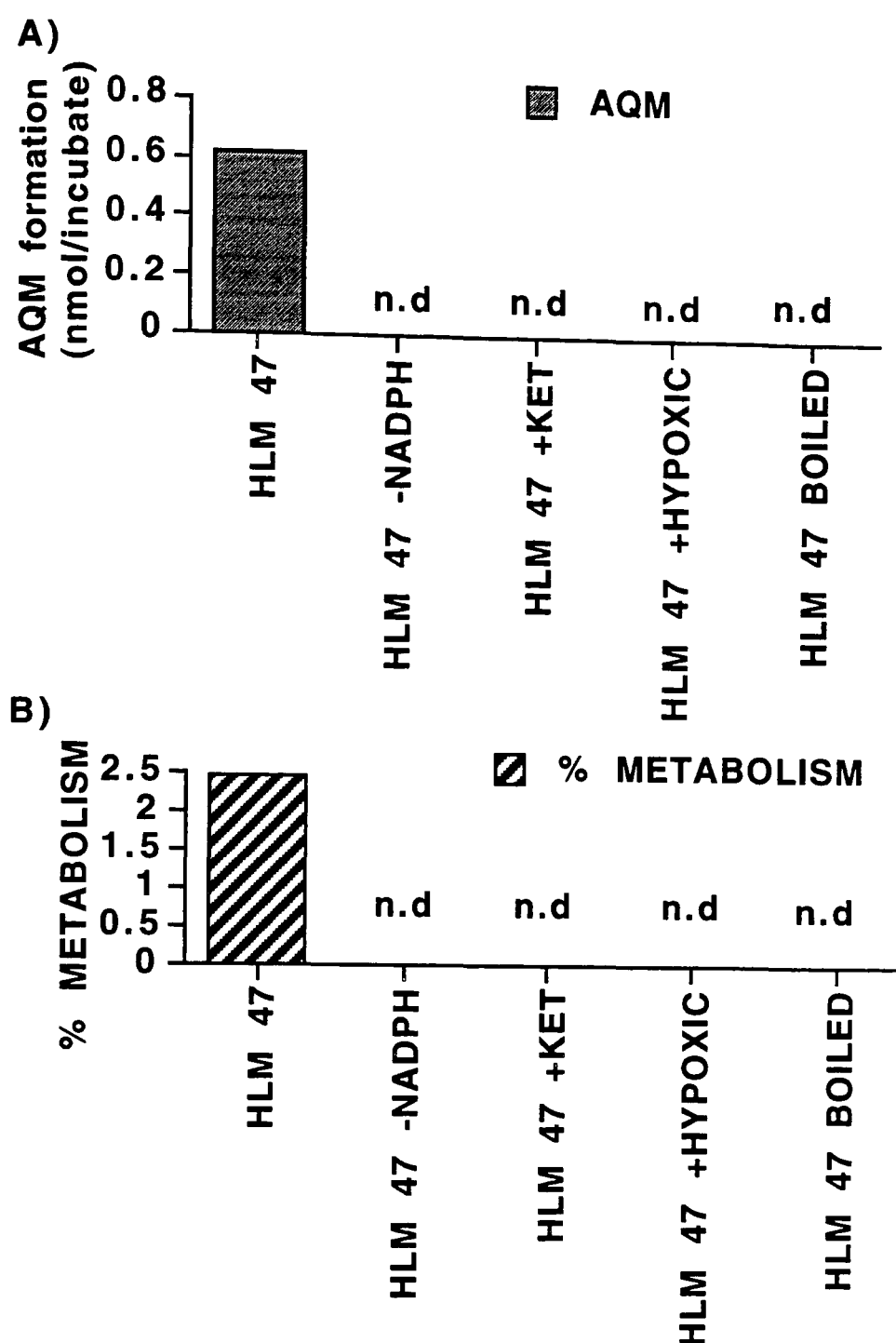


Fig 55. Oxidative metabolism of AQ4 in microsomes from HLM 47.

Data are expressed as in **A)** as the mean of two independent determinations, or **B)** as percentage metabolism. Each incubate contained 400 μ g of protein and 100 μ M AQ4. Data were obtained after 60 min aerobic incubation, n.d.=not detected. See section 2.7.2 for experimental conditions.

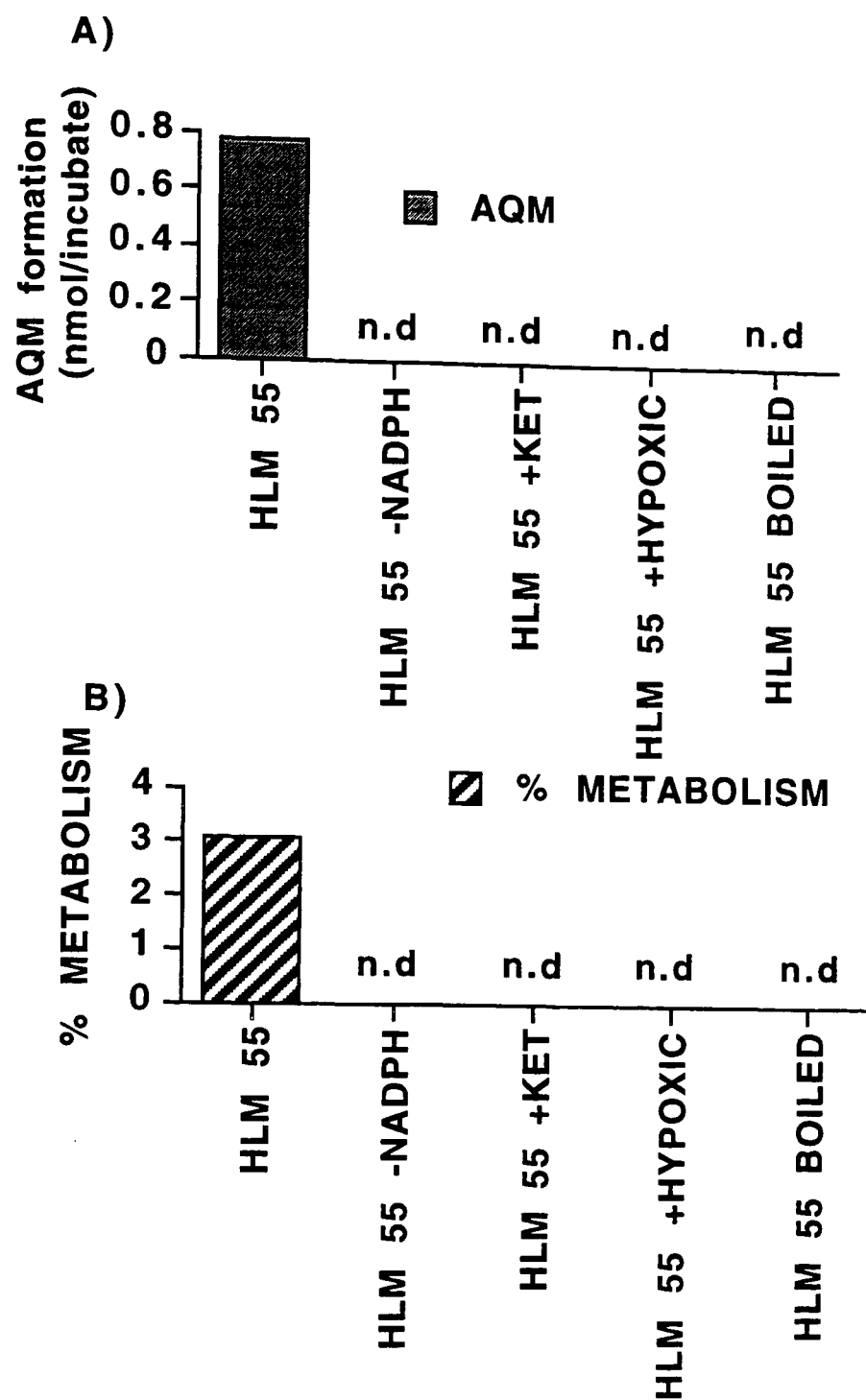


Fig 56. Oxidative metabolism of AQ4 in microsomes from HLM 55.

Data are expressed as in **A)** as the mean of two independent determinations, or **B)** as percentage metabolism. Each incubate contained 400 μ g of protein and 100 μ M AQ4. Data were obtained after 60 min of aerobic incubation, n.d.=not detected. See section 2.7.2 for incubation conditions.

4.3.6 Metabolism of AQ4N in human lymphoblastoid cell microsomes

Human lymphoblastoid cell microsomes containing vector transfected CYP 3A4 protein were found to have a BROD activity of 0.013 nmol/mg/min (mean of two determinations). Activity was undetectable in incubates using the CYP 3A inhibitor TAO (50 μ M). Microsomes from CPR vector transfected cells were found to have a cytochrome c reductase activity of 3.5 μ mol/mg/min (mean of two determinations). Control microsomes (without inserts for CYP 3A4 or CPR) had no detectable activity for either BROD or the reduction of cytochrome c. Microsomes from CYP 3A4 transfectants supported the anaerobic metabolism of AQ4N to both AQM and AQ4 (Fig 57). Metabolism was not apparent in CYP 3A4 transfected microsomes incubated with 50 μ M TAO, in air saturated incubates, or in incubates depleted of NADPH. Similarly, microsomes transfected with CPR or CYP 2B6 were unable to metabolise AQ4N (Fig 57). Metabolism of AQ4N to AQM in control microsomes was 3.5% of CYP 3A4 values whereas AQ4 production was not detected.

4.3.7 Metabolism of AQ4N in human tumour and paired healthy tissue

Metabolism of AQ4N was supported in both normal and neoplastic kidney (Fig 58). In renal cell carcinoma microsomes (HKT5) the anaerobic dependent production of both metabolites was approximately 3 fold less than the corresponding healthy kidney (HK5). However, in a second individual the production of AQ4 in renal cell carcinoma microsomes

(HKT6) was only 1.5 fold less than the paired healthy tissue (HK6). The same individual produced 13 fold less AQM in carcinoma microsomes compared to healthy kidney (Fig 58). AQM was also detected in all colonic tissue (Fig 59). For example the ratio of AQM production in normal versus neoplastic colon was approximately 2.5/1 for both individuals. AQ4 was detected in the healthy colon of one individual only (HC5; Fig 59). Production of AQM was routinely < 5% in normal and neoplastic tissue of kidney and colon in air, NADPH depleted or in incubates containing heat denatured microsomes. Whereas under these conditions, AQ4 was not detected. Furthermore, carbon monoxide purge prevented the formation of either metabolite in normal and neoplastic tissue of both the kidney and colon.

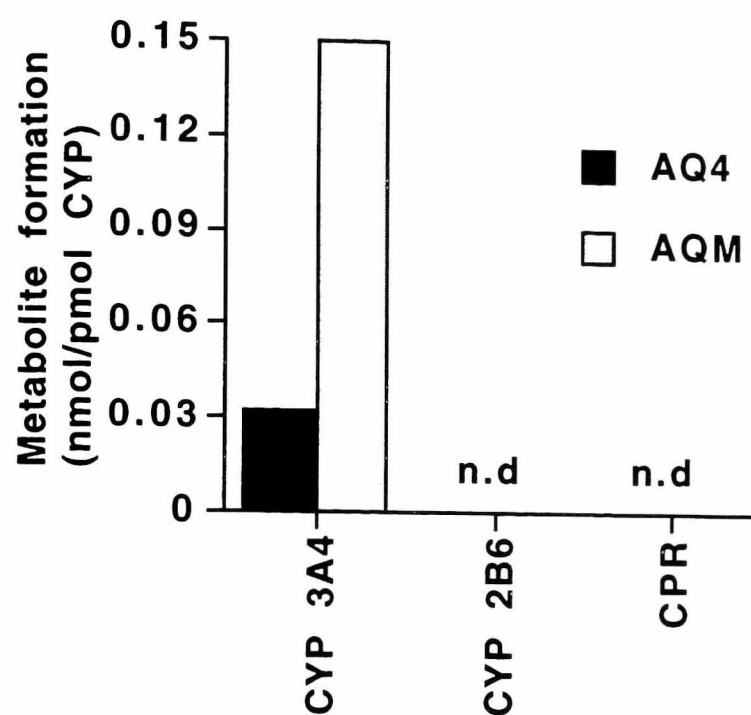


Fig 57. Anaerobic metabolism of AQ4N in human lymphoblastoid cell microsomes transfected with CYP gene inserts.

Results are expressed as the mean of two determinations in incubates containing 400 μ g of protein and 100 μ M AQ4N. Data were collected after 60 min of incubation. See section 2.8.5 for experimental conditions.

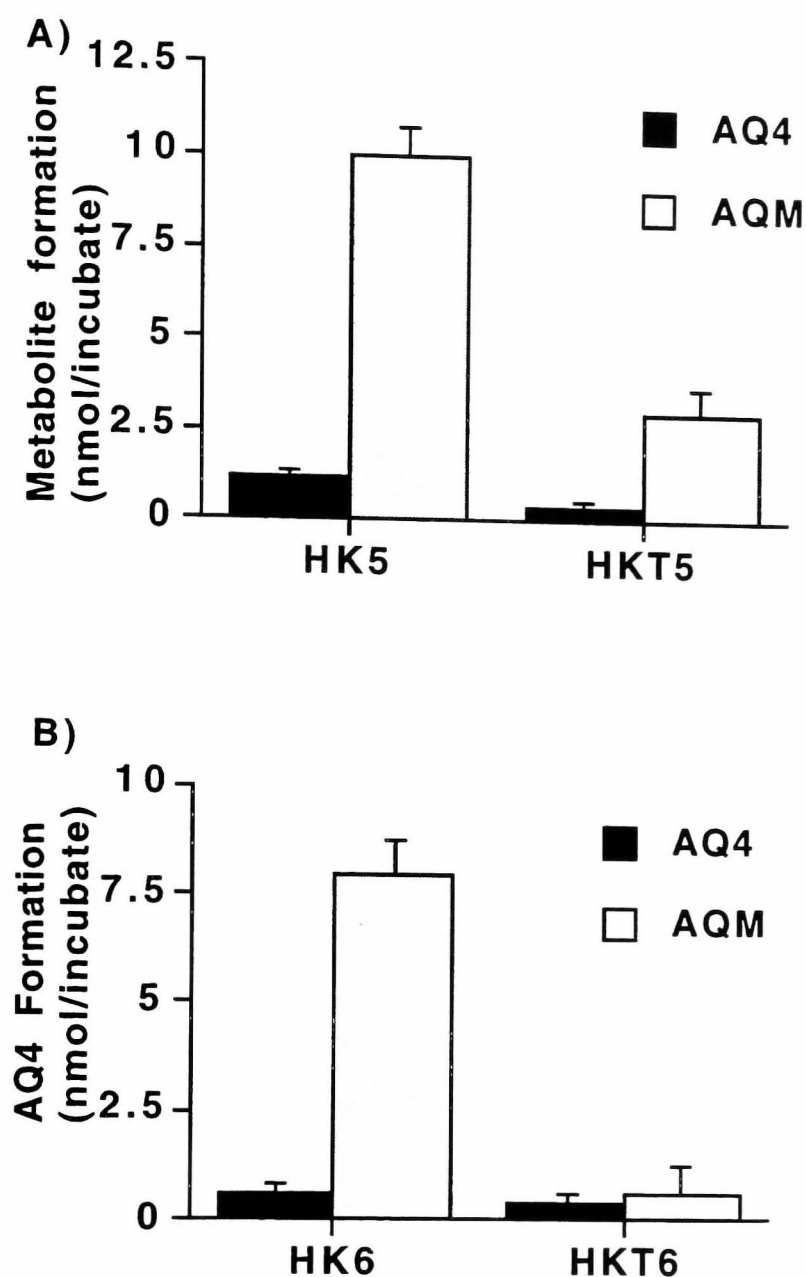


Fig 58. Anaerobic metabolism of 100 μ M AQ4N in microsomes from two patients having undergone surgery for primary renal cell carcinoma. **A)** normal renal microsomes (HK5) and renal carcinoma microsomes (HKT5) from a 62 year old male. **B)** normal renal microsomes (HK6) and renal carcinoma microsomes (HKT6) from a 65 year old female. Data are expressed as the mean \pm SE for three determinations taken after 60 min incubation in incubates containing 800 μ g of protein. See section 2.6 for experimental methods.

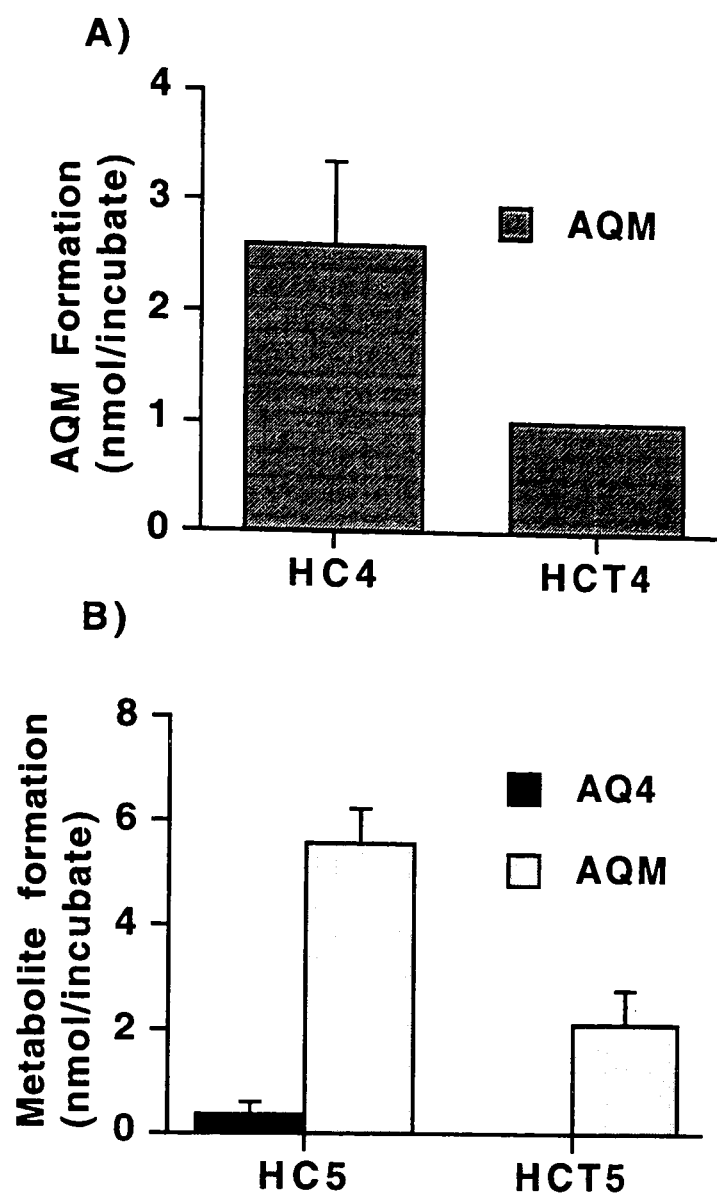


Fig 59. Anaerobic metabolism of 100 μ M AQ4N in microsomes from two patients having undergone surgery for primary adenocarcinoma of the colon. **A)** normal colon microsomes (HC4) and colon adenocarcinoma microsomes (HCT4) from a 66 year old female. **B)** normal microsomes (HC5) and colon adenocarcinoma microsomes (HCT5) from a 52 year old female. Data are expressed as the mean \pm SE for three determinations taken after 60 min incubation in incubates containing 800 μ g of protein. See section 2.6 for experimental methods.

4.4 Conclusions

1) The reductive metabolism of both AQ4N and AQM, were shown to occur under anaerobic conditions by a process that was inhibited by air and requires NADPH as reduced co factor. Furthermore, the metabolism of both compounds was limited to the microsomal fraction and was inhibited by the general CYP inhibitor CO. AQ4 was oxidised to AQM under aerobic conditions in the presence of microsomes and NADPH. However, compared to reductive metabolism the amount of oxidation was very small.

2) The anaerobic metabolism of both compounds was found to correlate strongly with CYP 3A activity but not with the activities of CYPs 1A, 2C or 2D. Interestingly, the anaerobic metabolism of AQM was also found to correlate with CYP 2A activity. The involvement of CYP 3A in the anaerobic metabolism of AQ4N was confirmed, in three individual livers, by the inhibition of metabolism in experiments using the CYP 3A specific inhibitor TAO. No inhibition occurred in anaerobic incubates containing the CYP 1A/2C inhibitor ANF. This finding was consistent with the correlation data and confirmed that CYPs 1A and 2C were not involved in AQ4N bioreduction.

4) Experiments using gene transfected human microsomes demonstrated that CYP 3A4 was capable of AQ4N bioreduction. CYP 2B6 and CPR transfectants were unable to support metabolism.

5) The kinetics of AQ4N metabolism were investigated in three individual livers and were shown to conform to a Michaelis-Menten type model. Although some variation was found between the intra-individual K_m values with respect to the two electron reduction of AQ4N to AQM, the K_m values for the production of AQ4 and total metabolism were similar for each individual and were consistent with the same enzyme in all three individuals metabolising AQ4N. V_{max} values were found to be commensurate with the extent of metabolism so that HLM 50 (lowest v_{max} value) could be described as a poor metaboliser, whereas HLM 55 (highest V_{max}) could be described as a good metaboliser. This trend was also apparent in the calculated CL_{int} values which decreased in the order HLM 55>HLM 45>HLM 50.

6) AQ4N has been shown to be a substrate for human normal and neoplastic kidney and normal and neoplastic colon. The metabolism occurred in both tissue types and was dependent on anaerobic conditions and the presence of NADPH. Furthermore, it appears that CYP enzymes were involved in the tumour mediated metabolism of AQ4N as metabolites were absent in incubates anaerobically purged with the CYP inhibitor CO.

In conclusion, human microsomes supported the anaerobic metabolism of both AQ4N and AQM. The process was inhibited by air and was predominantly catalysed by CYP 3A enzymes. CYP 3A4 has been shown to be at least one member of the CYP 3A family capable of metabolising AQ4N. However, the present findings do not exclude the possibility that CYPs 3A5, 3A3 and 3A7 can anaerobically activate AQ4N. Human

tumours were able to support the anaerobic metabolism of AQ4N and this process was probably mediated by CYP enzymes.

Chapter 5

Chapter five

Preliminary investigation into the *in vivo* metabolism of AQ4N in tumour and non tumour bearing mice.

5.1 Aims

In 1995 Cole and coworkers discovered that administration of AQ4N (250 mg/kg of body weight) in combination with a single dose of 25 Gy to mice bearing a variety of tumours produced some interesting pharmacodynamic results. In particular RIF- 1 and SCCV11 neoplasms were found to be sensitive to the treatment whereas KHT tumours were essentially unaffected. The aims of this preliminary investigation were to 1) Identify AQ4N metabolites in both rodent and human tumours xenografts, namely RIF-1, SCCVII and KHT (rodent) and HT29 (human), freshly excised from mice and so confirm that prodrug metabolism is not restricted to the *in vitro* setting and 2) Establish whether the quantity of cytotoxic AQ4 detected in RIF- 1, SCCV11, and KHT tumours correlated with their *in vivo* sensitivity as determined by Cole *et al* (1995). A third aim was to determine the extent of AQ4N metabolism in non tumour tissue including plasma, liver, gall bladder and hind leg muscle.

5.2 Materials and Methods

C3H female and male nude mice were obtained from Charles River Ltd (Margate, UK). All standard laboratory reagents were obtained from the sources detailed in section 2.2.

5.2.1 Animal dosing procedure*

Animals were dosed by the procedure described in section 2.9.3.

5.2.3 Drug and metabolite extraction

Drug and metabolite extraction were performed as described in section 2.9.4.

5.2.4 Protein analysis

All tissue protein was quantified as described in section 2.5.

* All animal work including the growth of tumours, administration of AQ4N and the resection of tissue for analysis was carried out by members of the technical staff at the MRC Radiobiology Unit, Chilton, Didcot, Oxon, UK.

5.3 Results

5.3.1 Drug and metabolite recovery

The recovery of standards made up in the presence of tissue homogenates was compared to standards made up in the absence of tissue. Typical recoveries over six concentrations were: AQ4N (24.6%), AQM (29.0%) and AQ4 (25.8%).

5.3.2 Tumours

In general, AQ4 was the principle metabolite detected in all tumour samples (Table 11 to 14), and was highest in the HT29 tumour (45.86 pmol/mg) 1 hour after dosing. At the same time point, AQM and AQ4N were 6.8 and 15.5 fold lower respectively. At 48 hours the amount of AQ4 had decreased to 5% of the amount detected at 1 hour and AQM and AQ4N were undetectable at 48 hours. In KHT tumours, AQ4 and AQM were detected 15 minutes after dosing, although by 1 hour the amount of AQ4 had increased approximately 2.5 fold and was undetectable thereafter. AQM was detectable 15 minutes after dosing but was not detected from 1 hour to 48 hours. AQ4N was not detected in KHT tumours at any time point tested. In RIF tumours, AQ4 was present at 24 and 48 hours after dosing, AQM was only detected after 15 minutes and AQ4N, like in KHT tumours, was absent at all time points. In SCCVII tumours, AQ4 was detected after 15 minutes (25.27 pmol/mg) and declined to 6.90 pmol/mg by 48 hours. AQM was present at 0.25 hour but unlike AQ4 was absent at 48 hours. AQ4N was detected at 1 hour only.

Table 11. AQ4N and metabolites in H 29 tumour xenografts excised from nude mice.

Time (hr)	AQ4(pmol/mg \pm SE)	AQM(pmol/mg \pm SE)	AQ4N(pmol/mg \pm SE)
0	ND	ND	ND
0.25	ND	ND	ND
1.00	45.86 \pm 37.47	6.67 \pm 4.00	2.95
24	ND	ND	ND
48	2.27 \pm 0.36	ND	ND

Data have been corrected for % recovery. ND=not detected. Values are pooled mean \pm SE for three mice. Where no SE is given values are means of two.

Table 12. AQ4N and metabolites in KHT tumours excised from C3H mice

Time (hr)	AQ4(pmol/mg \pm SE)	AQM(pmol/mg \pm SE)	AQ4N(pmol/mg \pm SE)
0	ND	ND	ND
0.25	4.80 \pm 3.61	2.73	ND
1.00	11.85 \pm 6.63	ND	ND
24	ND	ND	ND
48	ND	ND	ND

Data have been corrected for % recovery. ND=not detected. Values are pooled mean \pm SE for three mice.

Table 13. AQ4N and metabolites in RIF- 1 tumours excised from C3H mice.

Time (hr)	AQ4(pmol/mg)	AQM(pmol/mg)	AQ4N(pmol/mg)
0	ND	ND	ND
0.25	ND	0.58	ND
1.00	ND	ND	ND
24	3.17	ND	ND
48	2.88	ND	ND

Data have been corrected for % recovery. ND=not detected. Values are mean results from two mice.

Table 14. AQ4N and metabolites in SCCVII tumours excised from C3H mice.

Time (hr)	AQ4(pmol/mg \pm SE)	AQM(pmol/mg \pm SE)	AQ4N(pmol/mg \pm SE)
0	ND	ND	ND
0.25	25.27	11.02	ND
1.00	22.57 \pm 6.00	2.48 \pm 1.71	40.35 \pm 16.22
24	1.83 \pm 0.97	15.47 \pm 15.47	ND
48	6.90 \pm 2.76	ND	ND

Data have been corrected for % recovery. ND=not detected. Values are pooled mean \pm SE for three mice. Where no SE is given values are means of two data points.

5.3.3 Plasma

AQ4N peaked at 1 hour after dosing, with the exception of plasma from the HT29 and NT (non tumour) group which peaked 15 minutes after dosing (Table 15). AQ4N was not detected in any animal, in any group, 1 hour after ip injection. AQM was variable from 15 minutes to 1 hour after dosing and only small amounts of this metabolite were detected in the plasma from

SCCVII and the HT29 groups after 1 hour post ip injection. Interestingly, and unlike the tumours, AQ4 was a minor metabolite in the plasma of C3H mice and the ratio of AQ4/ AQ4N ranged from 0.15- 0.005.

Table 15. AQ4N and metabolites from the plasma of mice (all groups) at various time points after dosing (ip) with 250 mg/kg AQ4N

Animal Group	Metabolite	Time (hr)			
		0.25	1.00	2 4	4 8
NT	AQ4	ND	2.96	NI	ND
	AQM	34.66	31.00±14.34	NI	ND
	AQ4N	717.05	554±231.48	NI	ND
RIF- 1	AQ4	18.20±9.80	ND	ND	ND
	AQM	25.55±21.40	33.93±9.71	ND	ND
	AQ4N	153.51±98.55	680.68±41.30	ND	ND
SCCV11	AQ4	14.69	6.18	17.09±11.59	ND
	AQM	48.92	37.86	1.812	ND
	AQ4N	147.53	378.36	ND	ND
HT29	AQ4	14.82±7.42	6.25	ND	1.26
	AQM	30.72±11.14	23.30	ND	1.31
	AQ4N	152.30±51.11	40.83±21.85	ND	ND
KHT	AQ4	15.08	8.77	ND	ND
	AQM	22.31	92.66±75.96	ND	ND
	AQ4N	240.20	434.60±28.90	ND	ND

Data have been corrected for % recovery. Data are pooled values for three mice and are expressed as pmol metabolite/ mg of tissue protein ± SE. ND=not detected, NI=no information (due to sample damage or absence). Where no SE is given, the values are the mean result from two mice. .

5.3.4 Livers

Both AQ4 and AQM were detected in the livers of all animals (Table 16). Broadly speaking, the amount of AQ4 and AQM declined with time in the livers of the NT and RIF-1 animals. However, this trend was not observed in the livers of mice from the other groups. Interestingly, the amount of hepatic AQ4 only once exceeded the amount of the same metabolite detected in tumours (48 hour value in liver of HT29 mice *versus* 0.25 hour value in HT29 tumour). AQ4N was detected at 0.25 hour in the NT group but absent in all other animals apart from the KHT livers at 24 and 48 hours.

5.3.5 Gall bladders

AQ4N peaked after 15 minutes in KHT and RIF-1 animals and at 1 hour in the gall bladders from NT and HT29 groups (Table 17). From 15 minutes to 1 hour post ip injection all animals, in all groups, showed a qualitatively similar profile of drug and metabolite concentrations in the order AQ4N>AQM>AQ4 (low AQ4/AQ4N ratio). However, this trend was not observed in the data from 1 hour to 48 hour.

5.3.6 Muscle

AQ4 declined in a general fashion from 0.25 hour to 48 hours in all animal groups. With the exception of the KHT mice, AQM levels appeared to increase from 15 minutes to 1 hour (Table 18). From 24 hour onwards, AQM was undetectable or very low in all groups investigated. From 15 minutes to 1 hour metabolite concentrations were consistently detected in the order AQ4N>AQM>AQ4 (low AQ4/AQ4N ratios). AQ4N peaked after 15 minutes in the NT, SCCVII and KHT groups and at 1 hour in the RIF- 1 and HT29

groups. AQ4N was undetectable in all animals, in all groups, from 24 hours onwards.

Table 16. AQ4N and metabolites from the livers of mice (all groups) at various time points after dosing (ip) with 250 mg/kg AQ4N

Animal Group	Metabolite	<u>Time (hr)</u>			
		0.25	1.00	24	48
NT	AQ4	39.00	9.13±2.71	12.14	9.58
	AQM	74.36	3.28±1.71	ND	ND
	AQ4N	17.67	ND	ND	ND
RIF- 1	AQ4	41.27±34.02	11.73	22.00±13.10	9.78±4.72
	AQM	59.63±35.94	3.68	18.42	ND
	AQ4N	ND	ND	ND	ND
SCCV11	AQ4	10.78	8.24	16.79±2.46	25.63±8.20
	AQM	5.53	ND	22.10±11.34	7.90
	AQ4N	ND	ND	ND	ND
HT29	AQ4	28.714±16.66	7.40±0.38	7.81±1.66	110.13±83.47
	AQM	ND	1.62±1.62	18.71±5.05	46.54
	AQ4N	ND	ND	ND	ND
KHT	AQ4	7.96±3.43	1.34	19.89±5.40	10.47±4.51
	AQM	9.58±2.28	7.16	5.46±1.46	29.35±9.20
	AQ4N	ND	ND	1.44	124.40

Data have been corrected for % recovery. Data are pooled values for three mice and are expressed as pmol metabolite/ mg of tissue protein ± SE. ND=not detected. Where no SE is given, the values are the mean result of two mice.

Table 17. AQ4N and metabolites from gall bladder tissue of mice (all groups) at various time points after dosing (ip) with 250 mg/kg AQ4N

Animal Group	Metabolite	<u>Time (hr)</u>			
		0.25	1.00	2.4	4.8
NT	AQ4	9.03	120.15	NI	ND
	AQM	90.48	261.37±42.37	NI	ND
	AQ4N	555.89	1368.95	NI	ND
RIF- 1	AQ4	50.75	2.89	6.76	ND
	AQM	73.30	86.51	1.93	ND
	AQ4N	1415.54	358.85	6.83	ND
SCCV11	AQ4	36.63	NI	81.49	3.41±2.38
	AQM	284.27	NI	135.00	ND
	AQ4N	380.89	NI	NI	ND
HT29	AQ4	66.13	24.69±24.69	18.07	110.49±44.06
	AQM	76.52	103.46±103.4	ND	4.51
	AQ4N	239.05	920.64±577.0	ND	ND
KHT	AQ4	22.28±11.30	59.92	623.25±98.90	9.28±1.45
	AQM	152.11±53.56	107.71	ND	5.16±5.16
	AQ4N	1321.45	497.59	ND	ND

Data have been corrected for % recovery. Data are pooled values for three mice and are expressed as pmol metabolite/ mg of tissue protein ± SE. ND=not detected, NI=no information (due to sample damage or absence). Where no SE is given, the values are the mean result from two mice.

Table 18. AQ4N and metabolites from the hind leg muscle of mice (all groups) at various time points after dosing (ip) with 250 mg/kg AQ4N

Group	Animal Group	Metabolite	0.25	<u>Time (hr)</u> 1.00	2 4	4 8
	NT	AQ4	ND	4.74	NI	ND
		AQM	10.91	19.09	NI	ND
		AQ4N	88.22	56.17	NI	ND
	RIF- 1	AQ4	4.56	1.32	ND	ND
		AQM	9.41	17.12	ND	ND
		AQ4N	53.56	79.52	ND	ND
	SCCV11	AQ4	1.84±1.24	0.50	ND	ND
		AQM	13.89±5.46	89.36	ND	ND
		AQ4N	29.86±23.18	24.26	ND	ND
HT29	AQ4	1.60±0.87	4.59±3.39	ND	1.29	
	AQM	23.07±19.41	62.60±38.40	ND	1.31	
	AQ4N	113.22±78.06	180.79±80.88	ND	ND	
KHT	AQ4	6.06±2.41	ND	ND	4.32	
	AQM	29.50±2.32	6.99±1.07	ND	ND	
	AQ4N	159.77±11.30	53.51±21.16	ND	ND	

Data have been corrected for % recovery. Data are pooled values for three mice and are expressed as pmol metabolite/ mg of tissue protein ± SE. ND=not detected, NI=no information (due to sample damage or absence). Where no SE is given, the values are the mean of two mice.

5.4 Conclusions

1) Both metabolites of AQ4N (AQM and AQ4) were detected in each tumour type assayed and, in general, AQ4 was found to be the predominant metabolite detected. SCCVII tumours showed the most extensive metabolite profile and along with RIF-1 and HT 29 were found to have AQ4 present at 48 hours. However, no clear correlation was found between levels of AQ4 in tumours and the *in vivo* sensitivities of these neoplasms to AQ4N based treatment as published by Cole *et al* (1995).

2) Hepatic tissue from all mice was found to contain both AQ4 and AQM. There was a high degree of within mouse and within group variability. However, the amount of AQ4 in liver rarely exceeded the amount found in tumour material.

3) Plasma was found to contain AQ4N, AQM and AQ4. Unlike tumours, AQ4 was shown to be the minor metabolite detected.

4) Metabolite profiles were found to be highly variable in both gall bladder tissue and muscle. However, the high levels of AQ4N found in gall bladder indicate that liver excretion was a major route of elimination.

In summary, AQ4 and AQM were detected in the rodent and human tumours xenografts of C3H mice, which demonstrated that in the *in vivo* setting the active metabolite of AQ4N (AQ4) was able to reach its cellular target. Metabolites were also found in hepatic and extra hepatic tissues.

Chapter 6

Chapter six

6.1 General Discussion

The HPLC method used throughout the course of this work was a modification of the method originally described by Dr M. Graham (personal communication). The reduction of flow rate from 2 mL/min to 1 mL/min and the acetonitrile concentration from 32% to 30% facilitated an accurate and reproducible assay for the quantitation of AQ4N and the two and four electron reduced metabolites AQM and AQ4, respectively. The quantitation of the two electron reduced mono-*N*-oxide, AQM, proved critical to our understanding of AQ4N metabolism as the generation of this metabolite appeared to be the initial event in the metabolism of AQ4N. An exception to this observation was apparent in the experiment using the CPR/ HO system where AQ4 is produced without any detectable AQM. A possible explanation for this finding is discussed later.

The reductive metabolism of AQ4N and AQM has been shown to be an enzymatic process occurring in microsomes and dependent on hypoxic conditions and the presence of reduced cofactor. There is a marked preference for NADPH over NADH as reduced cofactor, a finding which supports the involvement of cytochrome P450 reductase (CPR) as opposed to NADH cytochrome b₅ in the bioactivation of both AQ4N and AQM. It must be stressed, however, that CPR alone does not seem to be able to metabolise either compound. This is based on the following observations. (1) Semi purified rat hepatic CPR required exogenous haem to support AQ4N metabolism in the presence of NADPH. (2) The general CYP inhibitors ketoconazole (KET) and carbon monoxide (CO) inhibited

completely the metabolism of both AQ4N and AQM. (3) Microsomes from human lymphoblastoid cells containing a gene insert for CPR were unable to metabolise AQ4N. The apparent inability of CPR *per se* to mediate the metabolism of AQ4N may have important clinical implications which may favour the use of this particular prodrug over other bioreductives such as tirapazamine. Indeed, the inability of CPR alone to metabolise AQ4N may explain the lack of systemic toxicity observed in rodents given AQ4N compared to similar doses of tirapazamine (Friery 1997 and McKeown *et al*/ 1996). The molecular basis underlying tirapazamine toxicity may be due to CPR mediated one electron reduction of the drug to a reactive nitroxyl radical followed by redox cycling with the subsequent generation of a systemically damaging reactive oxygen species. Indeed mitoxantrone, a structural analogue of AQ4N, does not appear to undergo detectable redox cycling in MCF-7 cells (Fisher and Patterson 1992). AQ4 has been shown to undergo oxidative metabolism and, in rat and human liver microsomes, the compound is converted to AQM and represents the reverse process of the anaerobic dependent two electron reduction of AQM to AQ4. Oxidative metabolism of AQ4 shows an absolute requirement for NADPH and air. The amount of AQM detected was small compared to the reverse process (two electron reduction of AQM to AQ4) and involvement of CYP is likely based on the fact that oxidative metabolism in rat and human was inhibited in incubates containing the CYP inhibitors ketoconazole and carbon monoxide.

The absence of detectable metabolism of either AQ4N or AQM in human or rat microsomal incubates purged with CO or preincubated with KET, has already been mentioned, and infers a major involvement of the cytochrome

P450 haemoproteins (CYP) in the anaerobic dependent activation of both *N*-oxides. CYP has been shown to metabolise several other *N*-oxides under anaerobic conditions in rodents including tiaramide, imipramine, *N,N*-dimethylamine and tirapazamine *N*-oxides (Sugiura *et al* 1976, Powis and Wincentzen 1980, Walton and Workman 1990 and Riley *et al* 1993). In particular, the statistically significant increase ($p < 0.01$) in metabolism of AQ4N to both metabolites and AQM to AQ4 in microsomes from isoniazid (ISO) pretreated animals compared to untreated control microsomes infers a role for the ethanol inducible CYP 2E subfamily. Furthermore, the involvement of CYP 2E in the metabolism of AQM to AQ4 was confirmed by preincubation, of the mechanism based CYP 2E inhibitor diethyldithiocarbamate (DIE), with ISO pretreated microsomes. Specifically, DIE preincubation abolished the generation of AQ4 from AQM, in experiments using AQ4N as substrate, and reduced the formation of AQ4 from AQM by around 70% in incubates using AQM as substrate. However, a somewhat perplexing finding was that the same CYP 2E inhibitor only reduced the formation of AQM from AQ4N to 43% compared to ISO treated microsomes preincubated with AQ4N in the absence of DIE. These results may suggest that, in addition to CYP 2E induction, ISO treatment may lead to the up regulation of another enzyme that is capable of anaerobically reducing AQ4N to AQM (*via* a two electron reduction) but which is uninhibited by DIE.

AQ4 production was significantly enhanced in experiments using either AQ4N or AQM incubated with microsomes from phenobarbitone (PB) pretreated animals. This observation is consistent with the involvement of CYP 2B. However, CYP 2B seems to catalyse only the two electron

reduction of AQM to AQ4 as AQM production in PB induced microsomes pre incubated with AQ4N was not greater than the generation of the same metabolite in untreated control microsomes. The role of CYP 2B in the metabolism of AQM to AQ4 in BP induced microsomes (whether the initial substrate was AQ4N or AQM) was substantiated by the use of the CYP 2B inhibitor metyrapone (MET). Inhibition of AQ4 from AQM was approximately 80% in incubates preincubated with 10 μ M MET compared to controls. In experiments using AQ4N as substrate for PB induced microsomes, the same concentration of MET inhibited completely the formation of AQ4 and decreased the formation of AQM by 2.5 fold. The latter observation was surprising since PB induction did not enhance the production of AQM compared to untreated microsomes. A possible explanation for this is the involvement of an unidentified enzyme which is inhibited by MET but not increased by PB pretreatment.

Microsomes from male Sprague-Dawley rats pretreated with pregnenolone 16-carbonitrile (PCN) produced a similar quantity of AQM from AQ4N but the production of AQ4 was significantly reduced compared to tween 80 (TWE) controls. In a similar fashion, the metabolism of AQM to AQ4 was reduced in microsomes from PCN induced animals. These results indicate that the rat CYP 3A protein does not contribute to the two electron reduction of AQM to AQ4. Furthermore, this lack of CYP 3A mediated reduction of AQM occurs in experiments where AQ4N is converted to AQ4 *via* AQM or when AQ4 is produced directly from substrate AQM. Repression of AQ4N conversion to both metabolites and AQM to AQ4 was observed also in microsomes from 3-methylcholanthrene (3 MC) pretreated animals, implying a lack of involvement of CYP 1A in the total metabolism of either AQ4N or AQM. The

molecular basis for the repression of AQ4N or AQM metabolism in microsomes from PCN or 3 MC induced animals may involve the availability of cellular haem for newly translated CYP apoprotein. Indeed haem has been identified as a post transcriptional regulating factor in the expression of CYP (Bhat and Padmanaban 1988 and Padmanaban *et al* 1989). In this scenario UT, ISO or PB induced microsomes contain sufficient CYPs 2B and 2E to metabolise either compound. Furthermore, these apoproteins have access to a predetermined amount of haem to synthesise functional haemoproteins. In PCN and 3MC induced microsomes an abundance of CYP 1A and 3A exist respectively and these apoproteins may restrict the availability of haem to the isoforms of CYP known to metabolise both AQ4N and AQM, namely CYP 2B and 2E. Alternatively, the induction of CYP 1A and 3A may interfere with the potential of the cell to produce CYPs 2B/2E by down regulation of transcription, translation or a combination of both. Furthermore, the stability of mRNA or apoprotein for either CYP 2B/2E may become compromised. The net result of these cellular events is a reduction in the metabolism of AQ4N/AQM.

In rat microsomes the kinetics of AQ4N metabolism conformed to a classical Michaelis-Menten type model. This was true for the conversion of AQ4N to the two electron reduced metabolite AQM ($K_m = 38.76 \mu M$, $V_{max} = 0.92$ nmol/mg/min), the four electron reduced cell cytotoxin AQ4 ($K_m = 5.65 \mu M$, $V_{max} = 0.13$ nmol/mg/min) and for the kinetics of total substrate turnover (sum of metabolites) ($K_m = 30.29 \mu M$, $V_{max} = 1.05$ nmol/mg min). However, when AQM was used as substrate the velocity of AQ4 formation versus AQM concentration provided data which were best described by sigmoid kinetics. These findings indicate a cooperative two electron reduction of AQM to AQ4

with a calculated Hill coefficient (n) of 3.0. The calculated value for n infers there are three binding sites for AQM within the enzyme molecule and catalysis is most effective when these molecules are bound to the enzyme. In such a system the binding of these activating molecules may change the three dimensional conformation of the enzyme to a state which favours catalysis. The current findings do not exclude the possibility that AQM molecules may alter the conformation of the CPR molecule and hence make the passage of electrons from CPR to CYP more effective.

Apart from differences in kinetic behaviour, the K_m values for the total metabolism of AQ4N (to AQM and AQ4) or the two electron reduction of AQM to AQ4 are similar, 30.29 μM and 27.00 μM respectively. This is consistent with the findings of the induction/inhibition experiments and suggests the same enzyme system(s) are responsible for the metabolism of both compounds. However, the V_{max} obtained from experiments using AQM as substrate, exceeds the corresponding value for the total substrate turnover of AQ4N. This leads to the conclusion that AQM is a better substrate for rat liver microsomes, characterised by the higher CL_{int} value. It is noteworthy that the kinetic analysis of both AQ4N and AQM produce K_m values which are approximately seventeen fold lower than the published value for indicine *N*-oxide (Powis and Wincentzen 1980) and between approximately two and five fold lower than the corresponding values for imipramine, tiaramide and *N,N*-dimethylaniline *N*-oxide respectively (Sugiura *et al* 1977). Although all six compounds had broadly similar V_{max} values, AQ4N and AQM would appear to be better substrates for CYP reduction as reflected in their higher CL_{int} values.

In human liver microsomes it has been shown unequivocally that the anaerobic dependent metabolism of AQ4N is a process mediated by the CYP 3A subfamily of enzymes. This is based on the following experimental findings. Firstly, the metabolism of AQ4N to the two (AQM) and four (AQ4) electron reduced compounds, as well as total substrate turnover (sum of AQM plus AQ4), correlated significantly ($p < 0.01$) with benzoxyl resorufin *O*-dealkylase (BROD) and tamoxifen *N*-demethylase (TND) activities, both of which are recognised probes for CYP 3A. In experiments using AQM as substrate a similar finding emerged, namely the two electron reduction to AQ4 correlated significantly with BROD activity and with TND activity. Metabolism of both AQ4N or AQM did not however correlate with marker activity for the other human hepatic phase 1 enzymes namely CYP 1A, 2C or 2D. However, when AQM was used as substrate, a significant correlation ($p < 0.05$) between the two electron reduction to AQ4 and coumarin 7-hydroxylase activity (CYP 2A marker) was found. Secondly, the metabolism of AQ4N in microsomes preincubated with 50 μM TAO, a known CYP 3A inhibitor, abolished the production of AQ4 and inhibited the formation of AQM by about 84% (mean of three determinations in three livers). Furthermore, ANF had no significant effect on the metabolism of AQ4N, indicating that CYPs 1A, 2C and 2A were not involved in the metabolism of AQ4N to either the two or four electron reduced metabolites. The results of these inhibitor experiments were entirely consistent with the correlation data. Finally, human lymphoblastoid cell microsomes from cells transfected with a functional CYP 3A4 gene were able to support the anaerobic metabolism of AQ4N to both metabolites. The metabolism was inhibited totally in the presence of 50 μM TAO. By way of comparison, AQ4N

metabolism was not detected in incubates containing human microsomes from cells transfected with an insert for CYP 2B6 or CPR.

The kinetics of AQ4N metabolism in three separate human livers conformed to a classic Michaelis-Menten model. Furthermore, the calculated K_m values for the two electron reduction of AQ4N to AQM, followed by the subsequent two electron reduction of AQM to AQ4 and the total metabolism of AQ4N (sum of AQM and AQ4) were similar, suggesting that the same enzyme was responsible for the metabolism of the prodrug in all three individuals. The V_{max} values obtained reflected the extent of AQ4N metabolism within the three individuals, such that HLM 55 could be described as a good metaboliser of AQ4N having the highest V_{max} and CL_{int} value while HLM 50, a poorer metaboliser, had a lower V_{max} and CL_{int} value accordingly. Furthermore, the K_m value for total AQ4N metabolism in untreated rat microsomes was similar to the corresponding values obtained in the three human livers. However, due to the higher V_{max} obtained in rat, the CL_{int} value for the rat mediated metabolism was found to be between 6.5 and 3.4 fold higher. From these data it was apparent that AQ4N is a better substrate for rat than human liver microsomes.

The results demonstrate, for the first time, that AQ4N can be anaerobically metabolised in human renal and colonic tumours. Furthermore, the metabolism of the prodrug within both renal and colonic neoplasms is consistent with the involvement of CYP, as metabolite production was inhibited completely in the presence of the CYP inhibitor CO.

The anaerobic metabolism of AQ4N by human CYP 3A enzymes provides a rational drug target for AQ4N based treatment regimes. To date, CYP 3A enzymes have been detected in a broad spectrum of human cancers including colon (McKay *et al* 1993), colorectal (de Waziers *et al* 1991), soft tissue sarcomas (Murray *et al* 1993), breast (McKay *et al* 1993 and Chabot *et al* 1997), lung (Kivitso *et al* 1995), oesophagus (Murray *et al* 1994), liver (Fritz *et al* 1993), bladder (Murray *et al* 1995), prostate (Murray *et al* 1995) and stomach (Murray *et al* 1998). Importantly, some of these neoplasms appear to express CYP 3A whereas its presence in the corresponding normal tissue is undetectable (Murray *et al* 1994, Murray *et al* 1995, Murray *et al* 1998 and McKay *et al* 1993). This latter observation presents the possibility of AQ4N undergoing entirely tumour specific bioactivation.

Although the mechanism underlying the reductive activation of AQ4N has not been studied, a number of *N*-oxides including tiaramide *N*-oxide and *N,N*-dimethylaniline have been shown to undergo type II spectral interactions with CYP in the absence of oxygen (reviewed by Lindeke and Paulsen-Sorman 1988). These observations have led Patterson (1993) to speculate on a general mechanism for anaerobic dependent reduction of *N*-oxides by haemoproteins, including CYPs. This mechanism could apply to the anaerobic dependent metabolism of AQ4N and AQM. Initially CYP is one electron reduced by CPR, a process that is a prerequisite for *N*-oxide binding to the haem centre. Secondly, the CYP enzyme and the *N*-oxide form an enzyme/ substrate complex, with the *N*-oxide moiety binding to the Fe²⁺ ion of the porphyrin ring and the rest of the substrate binding to the active site within the CYP molecule. Thirdly, a second one electron reduction by CPR produces the apoprotein/Fe^{IV}=O species and an amine.

Finally, the amine is released and a molecule of water is formed. The sequence is shown in Figure 60.

In addition to *N*-oxide/haem interactions, the ability of a drug to fit snugly into the active site of an enzyme is critical for catalysis. With this in mind, the metabolism of AQ4N and AQM by CYP 3A enzymes is further supported as the most important interaction between an amino acid within the active site of CYP 3A and a newly docked substrate is thought to be the hydrogen bond donor asparagine 74 (Asn 74) and a hydrogen bond acceptor on the substrate molecule (reviewed by Smith *et al* 1997a). Furthermore, the distance between this interaction and the site of metabolism has been proposed to be 6.81 ± 1.27 Ångstroms (reviewed by Smith *et al* 1997a). The distance between the 5 or 8 hydroxy group on AQ4N or AQM and the oxygen atom of the *N*-oxide group is 9 Ångstroms (Teesdale- Spittle, personal communication). However, it is possible that free rotation of the *N*-oxide group around sigma bonds within the alkylamino side arms means the proposed distance of 6.81 Ångstroms between hydrogen bonding and site of metabolism is entirely feasible. Rotation of the *N*-oxide group around a sigma bond can occur without imposing any energetic constraints on the AQ4N molecule (P Teesdale- Spittle, personal communication). Secondly The large active site of CYP 3A4 is very accessible to *N*-alkyl based groups and has been proposed to change conformation in order to account for its broad range of substrate activities (reviewed by Smith *et al* 1997b).

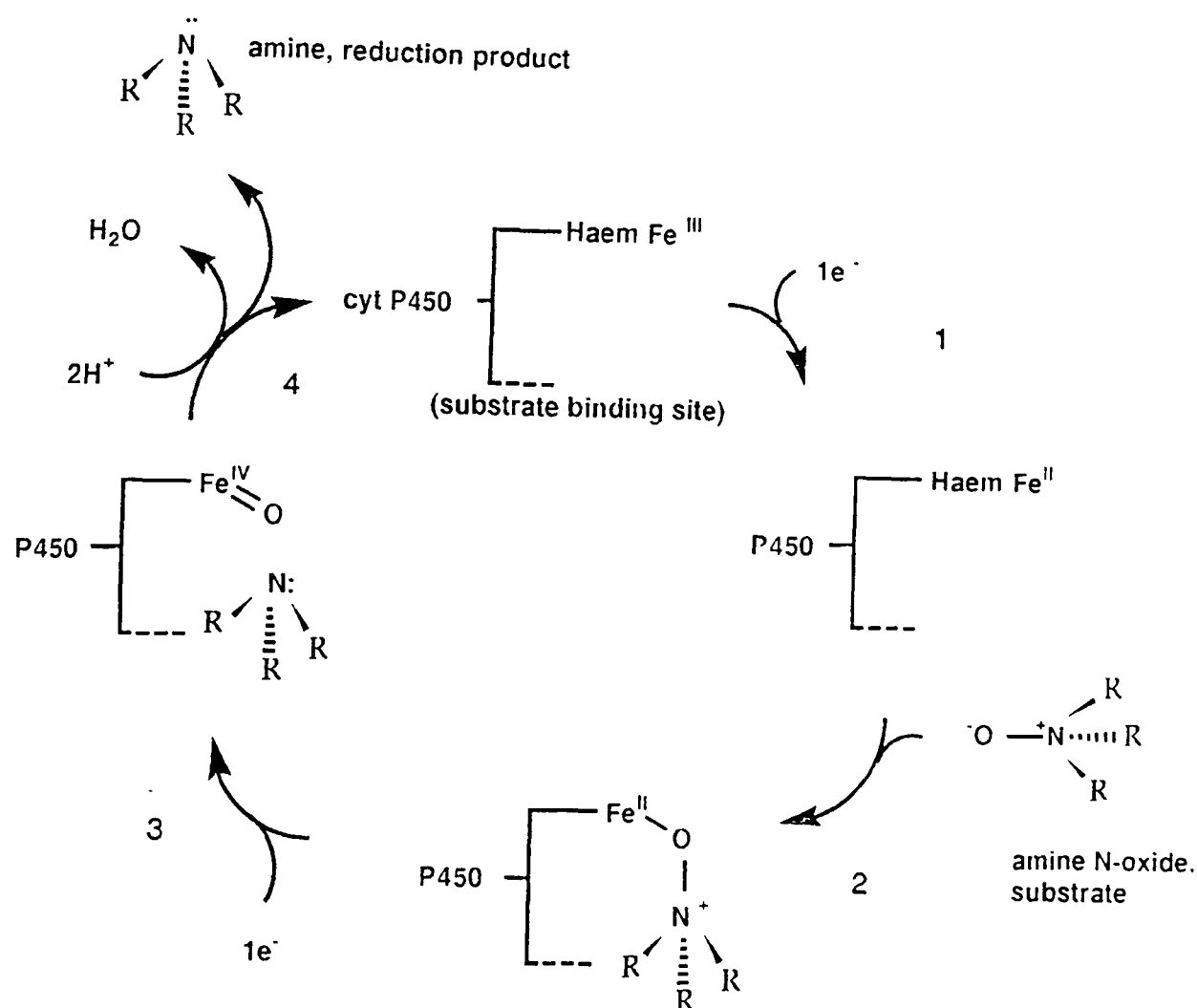


Fig 60. Proposed mechanism of NADPH dependent cytochrome P450 mediated reduction of N- oxides (adapted from Patterson 1993). See text for details. Steps are: **1)** one electron reduction of CYP. **2)** Enzyme substrate complex formation. **3)** second one electron reduction and **4)** amine release

In addition to CYP 3A mediated metabolism of AQ4N, semi purified rat CPR, in combination with haem, was shown to metabolise AQ4N to AQ4, a process dependent on both NADPH and anaerobic conditions. The absence of detectable AQM in this experiment was, at first, hard to rationalise. However, CPR is known to have at least three binding sites for haem (Yoshinaga *et al* 1982) and, in the presence of molecular oxygen,

degrades haem to biliverdin (Docherty *et al* 1982 and Masters and Schacter 1976). Under conditions of hypoxia it is possible that the CPR/ haem complex acts as a makeshift haemoprotein unable to oxidise haem but instead shuttling electrons through the bound haem moieties on to the N-oxide groups of AQ4N with the subsequent oxidation of NADPH. In this scenario both N-oxide groups are simultaneously reduced to tertiary amines, by a similar mechanism to that outlined in Figure 60, and so AQ4 is produced but not AQM. Addition of haem oxygenase (HO) to this system did not enhance AQ4N metabolism but produced a slight, albeit significant ($p<0.05$), repression of metabolism. The reason for this observation is at present unknown. AQ4N was also a substrate for purified nitric oxide synthase (NOS). The appearance of both AQM and AQ4 under hypoxic conditions may not be entirely surprising as NOS is known to be a CYP type haemoprotein (White and Marletta 1992). Indeed the amino acid sequence of NOS enzymes contain a high degree of homology with CPR (Bredt *et al* 1991) and may allow the enzyme to function as a chimeric CPR-CYP enzyme (reviewed by Schmidt *et al* 1993).

So far discussion has focused on the metabolic conversion of AQ4N to its metabolites in subcellular fractions, human tumours *ex vivo* and by semi purified and purified enzyme systems. The *in vivo* metabolism of AQ4N in tumour and non tumour bearing C3H mice was conducted with a view to qualitatively determine whether the metabolites of AQ4N could be identified in the rodent tumours and so confirm metabolism of AQ4N in an *in vivo* model as opposed to an *in vitro* one. Firstly, cytotoxic AQ4 was detected in all rodent neoplasms. The amount of AQ4 detected exceeded the amount of AQM and AQ4N (high AQ4/ AQ4N ratio) in all tumours at all times (with the

exception of one result in SCCVII tumours at 1 hour). Using the same C3H murine model, an early study by Cole *et al* (1995) found that AQ4N was particularly effective in retarding the growth of the RIF- 1 and SCCV11 tumours but had little effect on KHT tumours. Although the present study failed to identify a definite trend between the amount of AQ4 detected in these tumours and the *in vivo* sensitivity of the tumours to AQ4N administration (from the study of Cole and co workers) it is noteworthy that AQ4 is detectable at 48 hours in both the SCCVII and RIF- 1 neoplasms but absent in the KHT tumours from 1 hour onwards. The detection of AQ4N metabolites within the livers of C3H mice is likely to reflect the activity of murine CYPs mediating the reductive metabolism of the anthraquinone in areas of low oxygen tension. Indeed the pericentral region of the liver is known to be hypoxic to some extent (reviewed by Woodrooffe *et al* 1995). In general, the lower AQ4/ AQ4N ratios found in plasma, muscle and gall bladder tissue, compared to tumour and liver, were probably due to the absence of appropriate reductase enzymes, presence of too much oxygen or a combination of both of these factors.

6.2. Future work

The metabolism of AQ4N, and AQM, have been described in detail and the enzymes responsible for the bioreduction of both of these compounds identified. A number of interesting questions have arisen as a result of this work and could be the focus of future research, these are outlined below.

- 1) The specific isoforms of CYP responsible for AQ4N metabolism in the human renal and colonic tumours could be identified by the use of isozyme

specific inhibitors pre incubated with AQ4N and NADPH under hypoxic conditions. Indeed this work could be extended to look at the metabolism of AQ4N in tumours other than those of renal or colonic origin.

2) Although the CYP 3A subfamily as a whole, and in particular the CYP 3A4 isoform, have been shown to bioactivate AQ4N, the individual contribution of CYP 3A5, 3A3 and CYP 3A7 remains to be firmly established. With this in mind, a series of metabolism experiments using cells transfected with cDNA for each isoform would determine which of these CYPs could contribute to the metabolism AQ4N and AQM.

3) The expression of CYP 3A enzymes in many tumours has been investigated by a number of workers. However, correlations between CYP 3A activity and the type, origin, clinical grade, invasiveness, metastatic potential and degree of differentiation of human tumours have not been evaluated. This kind of detailed information would establish which particular tumours are most suitable for AQ4N (or possibly AQM) treatment.

4) The preliminary work with purified rat brain NOS and the CPR/ HO system has shown that these enzymes are capable of AQ4N metabolism. However, further work is required to establish whether these systems have any relevance *in vivo*.

5) Although the results of the preliminary *in vivo* metabolism experiments show some qualitative trends, an in depth pharmacokinetic analysis of AQ4N in rodents, covering a longer time course and using more animals per time point may clarify and enhance the present findings.

6) A detailed investigation into the kinetics of AQM metabolism in human tissue may, like in the rat, show that this compound is a better substrate for human microsomal enzymes than AQ4N. Furthermore, the aerobic toxicity of AQM to cell lines *in vitro* and in rodents *in vivo* should be evaluated as this compound may prove to be a superior prodrug to AQ4N.

6.2 1 Concluding remarks

AQ4N bioreduction has been shown to occur in a variety of rodent and human tissue fractions *in vitro*, in rodent tumours *in vivo* and in *ex vivo* samples of human tumours. Furthermore, CYP and other haem based enzymes specifically contribute to the metabolism of this prodrug. In rats, CYPs 2B and 2E contribute to the reductive activation of AQ4N while in humans, AQ4N is bioreduced by CYP 3A enzymes. These enzymes have been detected in a broad spectrum of human cancers.

Collectively, these findings suggest that AQ4N based prodrug therapy should be considered as an ideal treatment regime for patients bearing solid tumour burdens. Such tumours are known to contain significant numbers of hypoxic cells and express CYP 3A enzymes which, in certain cases, are found in higher amounts than in normal tissue.

References

Adams G E and Stratford I J. Bioreductive drugs for cancer therapy: The search for tumour specificity. *International Journal of Oncology Biology and Physics* 29, 231-238, 1994

Adeagbo A S O. Endothelium- derived hyperpolarising factor: characterisation as a cytochrome P450 1A-linked metabolite of Arachidonic acid in perfused rat mesenteric prearteriolar bed. *American Journal of Hypertension*, 10, 763-771, 1997

Applegate L A, Luscher P and Tyrrell R M. Induction of haem oxygenase: A general response to oxidant stress in cultured mammalian cells. *Cancer Research*, 974-978, 1991

Backes W L. Ch2 in *Handbook of Experimental Pharmacology* (Eds Schenkman J B and Greim H) 105, 1993

Baker M A, Zeman E M, Hirst V K and Brown J M. Metabolism of SR 4233 by Chinese hamster ovary cells: basis of hypoxic cytotoxicity. *Cancer Research*, 48, 5947-5952, 1988

Bassukas I D, Hofmoke G and Maurer- Schutze B. Treatment with tumour necrosis factor alpha and interferon alpha of a human kidney cancer xenograft in nude mice: Evidence for an anticachetic effect of interferon alpha. *Anticancer Research* 14 237-246, 1994

Beall H D, Timothy Mulcahy R, Siegel D, Traver R D, Gibson N W and Ross D. Metabolism of bioreductive antitumour compounds by purified rat and human DT diaphorase. *Cancer Research*, 54, 3196-3201, 1994

Bedford J S. and Mitchell J B. The effect of hypoxia on the growth and radiation response of mammalian cells in culture. *British Journal of Radiology*, 47, 687-696, 1974.

Bergsjö P and Evans J C. Oxygen tension of cervical carcinoma during the early phase of external irradiation. *Scand. J. Clin. Lab. Invest.*, 27, 71-82, 1971

Bickel M H. The pharmacology and biochemistry of *N*-oxides. *Pharmacological Reviews*, 21, 325-355, 1969

Born R, Hug O and Trott K R. The effect of prolonged hypoxia on the growth and viability of chinese hamster cells. *International Journal of Radiation Oncology Biology and Physics*, 1, 687, 1979.

Bradford M. A rapid, sensitive method for the quantitation of microgram quantities of protein using the principle of protein dye binding. *Analytical Biochemistry*, 72, 248-254, 1976

Bredt D S and Snyder S H. Nitric oxide mediates glutamate-linked enhancement of c GMP levels in the cerebellum. *Proceedings of the National Academy of Sciences USA*, 86, 9030-9033, 1989

Bredt D S, Hwang P M, Glatt C E, Lowenstein C, Reed R R and Snyder S H. Cloned and expressed nitric oxide synthase structurally resembles cytochrome P450 reductase. *Nature*, 351, 714-718, 1991

Bremner J C M. Assessing the bioreductive effectiveness of the nitroimidazole RSU 1069 and its prodrug RB 6145: With particular reference to *in vivo* methods of evaluation. *Cancer and Metastasis Reviews* 12, 177-193, 1993

Brown J M and Lemmon M J. Potentiation by the hypoxic cytotoxin SR 4233 of cell killing produced by fractionated irradiation of mouse tumours. *Cancer Research*, 50, 7745-7749, 1990

Burke M D, Thompson S, Elcombe C R, Halpert J, Haaparanta T and Mayer R T. Ethoxy-,pentoxy-and-benzyloxy-phenoxazones and homologues: a series of substrates to distinguish between different induced cytochromes P450. *Biochemical Pharmacology*, 34, 3337-3345, 1985

Burke M D, Thompson S, Weaver R J, Wolf C R and Mayer R T. Cytochrome P450 specificities of alkoxyresorufin *O*-dealkylation in human and rat liver. *Biochemical Pharmacology*, 48, 923-936, 1994

Butler S A, Wood P J, Cole S, Williams C, Adams G E and Stratford I J. Enhancement of bioreductive drug toxicity in murine tumours by inhibition of the activity of nitric oxide synthase. *British Journal of Cancer*, 76, 438-444, 1997

Cancer Research Campaign. Scientific Yearbook, (Edt Walker L), 1996

Chabot G G, Verjus M A and Mathieu M C. Determination of cytochrome P450 isoenzymes of the 3A subfamily in human breast cancer. Proceedings of The American Association for Cancer Research, 38, 562, 1997

Chang T K, Gonzalez F J and Waxman D J. Evaluation of triacetyloleandomycin, alpha-naphthoflavone and diethyldithiocarbamate as selective chemical probes for inhibition of human cytochromes P450. Archives of Biochemistry and Biophysics, 311, 437-442, 1994

Charles I G, Chubb A, Gill R, Clare J, Lowe P N, Holmes L, Page M, Keeting J G, Moncada S. and Riveros- Moreno V. Cloning and expression of rat neuronal nitric oxide synthase coding sequence in a baculovirus/insect cell system. Biochemical and Biophysical Research Communications, 196, 1481-1489, 1993

Cheng S Y, Haung H J Su, Nagane M, Ji X D, Wang D, Shih C C Y, Arap W, Huang C M and Cavenee W K. Suppression of glioblastoma angiogenicity and tumourigenicity by inhibition of endogenous expression of vascular endothelial growth factor. Proceedings of the National Academy of Science, USA, 93,8502-8507, 1996.

Choi A M and Alam J. Haem oxygenase 1: Function, regulation, and implication of a novel stress inducible protein in oxidant- induced lung injury. American Journal of Respiratory Cell and Molecular Biology. 15, 9-19, 1996

Cohen L F, Glaubiger D L, Kann H E and Kohn K W. Protein associated DNA single strand breaks and cytotoxicity of dihydroxyanthracenedione (DHAD) NSC 301739 in mouse 1210 leukaemia cells. Proceedings of The American Association for Cancer Research. 21, 277, 1980

Cole S, Patterson L H, Williams C A, Bowler J D, Raleigh S M and Stratford I J. The activity of AQ4N, a novel bioeductively- activated cytotoxin against KHT, RIF- 1 and SCCVII murine tumours *in vivo*. British Journal of Cancer, 71, (suppl XX1V), 20, 1995

Cooper M R and Cooper M R. American Cancer Society Textbook of Clinical Oncology (first edition) (Eds, Holleb A I, Fink D J and Murphy G P), Ch 5, 47-69, 1991.

Costa A K, Baker M A, Brown J M and Trundell R J. *In vivo* hepatotoxicity of SR 4233 (3-Amino-1,2,4-benzotriazine-1,4-dioxide), a hypoxic cytotoxin and potential antitumour agent. Cancer Research, 49, 952-929, 1989

Crespi C L, Langenbach R and Penman B W. Human cell lines, derived from AHH- 1 TK+/- human lymphoblasts, genetically engineered for expression of cytochromes P450. Toxicology, 82, 89-104, 1993

Crespi C L, Penman B W, Gelboin H V and Gonzalez F J. A tobacco smoke derived nitrosamine 4-(methylnitrosamino)-1-(3-pyridyl)-1-butanone (NNK) is activated by the polymorphic human cytochrome P450 2D6 (CYP 2D6). Carcinogenesis, 12, 1197-1201, 1991

Crespi C L, Penman B W, Leahey A E, Arlotto M P, Stark A, Parkinson A, Turner T, Steimel D T, Rudo K, Davies R L and Langenbach R. Human cytochrome P450 2A3: cDNA sequence, role of the enzyme in the metabolic activation of promutagens, comparison to nitrosamine activation by human cytochrome P450 2E1. *Carcinogenesis*, 11, 1293-1300, 1990

Crespi M D, Ivanier S E, Genovese J and Baldi A. Mitoxantrone effects topoisomerase activities in human breast cancer cells. *Biochemical Biophysical Research Communications*. 136, 521-528, 1986

Cresteil T and Jaiswal A K. High levels of expression of the NAD(P)H:quinone oxidoreductase (NQO₁) gene in tumour cells compared to normal cells of the same origin. *Biochemical Pharmacology*, 42, 1021-1027, 1991

Cresteil T, Monsarrat B, Alvinerie P, Treluyer J M, Viera I and Wright M. Taxol metabolism by human liver microsomes: identification of cytochrome P450 isozymes involved in its biotransformation. *Cancer Research*, 54, 386-392, 1994

Crewe H K, Ellis S W, Lennard M S and Tucker G T. Variable contributions of cytochromes P450 2D6, 2C9 and 3A4 to the 4-hydroxylation of tamoxifen by human liver microsomes. *Biochemical Pharmacology*, 53, 171-178, 1997

Cruse I and Maines M D. Evidence suggesting that the two forms of haem oxygenase are products of different genes. *The Journal of Biological Chemistry*, 263, 3348-3353, 1988

Dayer P, Desmeules J, Leeman T and Striberni R. Bioactivation of the narcotic drug codeine in human liver is mediated by the polymorphic monooxygenase catalysing debrisoquine 4-hydroxylation. *Biochemical and Biophysical Research Communications*. 411-416, 1988

De Waziers I, Cugnenc A, Berger A, Pleroux J and Beaune P H. Drug metabolising enzyme expression in human normal, peritumoural and tumoural colorectal tissue samples. *Carcinogenesis*, 12, 905-909, 1991

Denny W R and Wakelin L P G. Kinetics of binding of mitoxantrone, ametantrone and analogues to DNA: relationship with binding mode and antitumour activity. *Anti- Cancer Drug Design*. 5, 189-200, 1990

Dickins M and Bayliss M K. Toxicology elsewhere. *Human and Experimental Toxicology*, 15, 980-981, 1996

Docherty J C, Masters B S S, Firneisz G D and Shacter B A. Heme oxygenase provides alpha- selectivity to physiological haem degradation. *Biophysical Biochemical Research Communications*, 105, 1005-1013, 1982

Dorie M J and Brown J M. Modification of the anti tumour activity of chemotherapeutic drugs by the hypoxic cytotoxic agent tirapazamine. *Cancer Chemotherapy and Pharmacology*, 39, 361-366, 1997

Dorr R T and William L F, *Cancer Chemotherapy Handbook* (4th Ed), 1982

Dunn C J and Goa K L. Mitoxantrone: A review of its pharmacological properties and use in acute non- lymphoblastic leukaemia. *Drugs and Ageing*. 9, 122-147, 1996

Dushkin M I, Znekov N K, Menshikova E B, Pivovarova E N, Lyubimov G Yu and Volsky N N. Ketoconazole inhibits oxidative modification of low density lipoprotein. *Atherosclerosis*, 114, 9-18, 1995

Eberlein T J and Wilson R E. American Cancer Society Textbook of Clinical Oncology (first edition) (Eds, Holleb A I, Fink D J and Murphy G P), Ch 3, 25-35, 1991.

Edwards Y H, Potter J and Hopkinson D A. Human FAD- dependent NAD(P)H diaphorase. *Biochemical Journal*, 187, 429-436, 1980

Elwell J H, Siim B G, Evans J W and Brown J M. Adaption of human tumour cells to tirapazamine under aerobic conditions. *Biochemical Pharmacology*, 54, 249-257, 1997

Enoch H G and Strittmatter P. Cytochrome b₅ reduction by NADPH cytochrome P450 reductase. *Journal of Biological Chemistry*, 254, 8976-8981, 1979

Ervine C M, Matthew D E, Brennan B and Houston B. Comparison of ketaconazole and fluconazole as cytochrome P450 inhibitors. *Drug Metabolism and Disposition*, 24, 211-215, 1996

Ewing J F, Weber C M and Maines M D. Biliverdin reductase is heat resistant and coexpressed with constitutive and heat shock forms of haem oxygenase in brain. *Journal of Neurochemistry*, 61, 1015-1023, 1993

Fisher G R and Patterson L H. Lack of involvement of reactive oxygen in the cytotoxicity of mitoxantrone, C1941 and ametantrone in MCF- 7 cells: comparison with doxorubicin. *Cancer Chemotherapy and Pharmacology*. 30, 451-458, 1992

Forsythe J A, Jiang B- H, Iyer N V, Agani N, Leung S W, Koos R D and Semenza G L. Activation of vascular endothelial growth factor gene transcription by hypoxia inducible factor- 1. *Molecular Cell Biology*, 16, 4604-4613, 1996

Foye W O, Vajragupta O and Sengupta S K. DNA binding specificity and RNA polymerase inhibitory activity of bis-(alkylamino)anthraquinones and bis-(methylthio)vinylquinolinium iodides. *Journal of Pharmacological Sciences*. 71, 253-256, 1982

Friery O P. An investigation of the interaction of the novel bioreductive drug AQ4N with radiation and cancer chemotherapy drugs. PhD thesis, University of Ulster, 1997

Funae Y and Imaoka S. Chapter in *Cytochrome P450, structure, mechanism and biochemistry* (2nd Edition) (Ed P R Ortiz de Montellano) Plenum Press New York and London, 1995

Gallagher E P, Kunze K L, Stapleton P L and Eaton D L. The kinetics of aflatoxin B1 oxidation by human cDNA- expressed and human liver microsomal cytochromes P450 1A2 and 3A4. *Toxicology and Applied Pharmacology*, 141, 595-606, 1996

Garcia- Closas M, Kelsey K T, Wienke J K, Xu X, Wain J C and Christiani D C. A case control study of cytochrome P450 1A1, glutathione S- transferase M1, cigarette smoking and lung cancer susceptibility. *Cancer Causes and Control*, 8, 544-553, 1997

Garfinkle D. Studies on pig liver microsomes 1, Enzyme and pigment composition of different microsomal fractions. *Archives of Biochemistry and Biophysics*, 77, 493-509, 1958

Geng J and Strobel H W. Identification of inducible mixed function oxidase system in rat glioma C6 cell line. *Journal of Neurochemistry*, 65, 554-563, 1995

Gilman A and Philips F S. The biological action and therapeutic application of the β - chloroethyl amines and sulfides. *Science*, 103, 409-436, 1946

Godwin A K, Meister A, O'Dwyer P J, Huang C S, Hamilton T C and Anderson M E. High resistance to cisplatin in human ovarian cancer cell lines is associated with marked increase in glutathione synthesis. *Proceedings of the National Academy of Science, USA*, 89, 3070-3074, 1992.

Gonzalez F J, Matsunaga T, Nagata K, Meyer U A, Nebert D W, Paslewka J, Kozak C A, Gillette J, Gelboin H V and Hardwick J P. Desbrisoquine-4-hydroxylases: characterization of a new P450 gene subfamily, regulation, chromosomal mapping, and molecular analysis of the DA rat polymorphism. *DNA*, 6, 149-161, 1987

Gonzalez F J. Chapter 16 in *Handbook of Experimental Pharmacology* (Eds Schenkman J B and Greim H) 105, 1993

Gonzalez F J. Molecular genetics of the P450 superfamily. *Pharmacological Reviews*, 45, 1-38, 1990

Gonzalez F J. The molecular biology of cytochrome P450's. *Pharmacological Reviews*, 40, 243-285, 1989

Goodman A I, Choudhury M, Silva J- LD, Schwartzman M L and Abraham N G. Overexpression of the haem oxygenase gene in renal carcinoma. *Proceedings of The Society for Experimental Biology and Medicine*, 214, 54-61, 1997

Groves J T and Han Y- Z. Chapter 1 in *Cytochrome P450, structure, mechanism and biochemistry* (2nd Edition) (Ed P R Ortiz de Montellano) Plenum Press New York and London, 1995

Guengerich F P, Dannan G A, Wright S T, Martin M V and Kaminsky L S. Purification and characterisation of liver microsomal cytochrome P450: electrophoretic, spectral, catalytic and immunochemical properties and

inducibility of eight isozymes isolated from rats treated with phenobarbital and beta-naphthoflavone. *Biochemistry*, 21, 6019-6030, 1982

Guengerich F P, Martin M, Beaune P H, Kremers P, Wolf T and Waxman D. Characterisation of rat and human microsomal P450 forms involved in the nifedipine oxidation- a prototype for genetic polymorphism in oxidative drug metabolism. *Journal of Biological Chemistry*, 261, 5051-5060, 1986

Guengerich F P. Chapter 14 in *Cytochrome P450, structure, mechanism and biochemistry* (2nd Edition) (Ed P R Ortiz de Montellano) Plenum Press New York and London, 1995

Guengerich F P. Destruction of Haem and Haemoproteins mediated by liver microsomal reduced nicotinamide adenine phosphate-cytochrome P450 reductase. *Biochemistry*, 17, 3633-3639, 1978

Gustafson D L and Pritsos C A. Bioactivation of mytomicin C by xanthine dehydrogenase from EMT6 mouse mammary carcinoma tumours. *Journal of the National Cancer Institute*. 84, 1180-1185, 1992

Gustafson D L and Pritsos C A. Kinetics and mechanism of mytomicin C bioactivation by xanthine dehydrogenase under aerobic and hypoxic conditions. *Cancer Research*. 53, 5470-5474, 1993

Hall E J and Roizin- Towle L. Hypoxic cell sensitisers: Radiobiological studies at the cellular level. *Radiology*, 453-457, 1975

Halliwell B. and Gutteridge M.C. Free radicals in biology and medicine (2nd Ed), 1989

Halvorson M, Greenway D, Eberhart D, Fitzgerald K and Parkinson A. Reconstitution of testosterone oxidation by purified rat cytochrome P450 3A1. Archives of Biochemistry and Biophysics, 227, 166-180, 1990

Hellman S. Principles of radiation damage, in: Cancer, principles and practise of oncology, 4th Edition (Eds De Vita V T, Hellman S and Rosenberg S A) J B Lippincott company, Philadelphia, 248-275, 1993

Hendrickson F R and Withers H R. American Cancer Society Textbook of Clinical Oncology (first edition) (Eds, Holleb A I, Fink D J and Murphy G P), Ch 4, 35-47, 1991.

Hewitt L F. Oxidation-reduction potentials in bacteriology and biochemistry. 4th Edn, 19-121, London County Council, London, 1936

Hodnick W F and Sartorelli A C. Reductive activation of mytomyacin C by NADH: cytochrome b₅ reductase. Cancer Research, 53, 4907-4912, 1993

Holleb A I. American Cancer Society Textbook of Clinical Oncology (first edition) (Eds, Holleb A I, Fink D J and Murphy G P), Introduction, Xi- 1, 1991.

Huang L E, Arany Z, Livingston D M and Bunn F. Activation of hypoxia inducible transcription factor depends on primarily upon redox- sensitive

stabilisation of its alpha subunit. The Journal of Biological Chemistry, 271, 32253-32259, 1996

Ikegami T, Natsumeda Y and Weber G. Decreased concentration of xanthine dehydrogenase (EC 1.1.1. 204) in rat hepatomas. Cancer Research. 46, 3838- 3841, 1986

Iyer V N and Szbalski W. Mitomycins and porfiromycin: chemical mechanism of activation and cross linking of DNA. Science, 145, 55-58, 1964

Jacolot F, Simon I, Dreano Y, Beaune P, Riche C and Berthou F. Identification of the cytochromes P450 IIIA family as the enzymes involved in the *N*-demethylation of tamoxifen in human liver microsomes. Biochemical Pharmacology, 41, 1911- 1919, 1991

Jefcoate C. Cytochrome P450. Educational Session 4 given at: 86th Annual meeting of the american association of Cancer Research. Toronto, Canada, 1995

Jiang B-H, Agani F, Passanti A and Semenza G L. V- SRC induces expression of hypoxia- inducible factor 1 (HIF-1) and transcription of genes encoding vascular endothelial growth factor and enolase 1: involvement of HIF-1 in tumour progression. Cancer Research, 57, 5328-5335, 1997

Johnson R K, Zee- Cheng R K- Y, Lee W W, Acton E M, Henry D W and Cheng C C. Experimental antitumour activity of aminoanthraquinones. Cancer Treatments Reports, 63, 425-439, 1979.

Joseph P, Xie T, Yuehang X and Jaiswal A K. NAD(P)H: Quinone Oxidoreductase₁ (DT diaphorase): expression, regulation, and role in cancer. *Oncology Research*, 6, 525-532, 1994.

Kappus H. Overview of enzyme systems involved in bioreduction of drugs and in redox cycling. *Biochemical Pharmacology*, 35, 1-6, 1986

Kennedy K A, Teicher B A, Rockwell S and Sartorelli A C. The hypoxic tumour cell: a target for selective cancer chemotherapy. *Biochemical Pharmacology*, 29, 1-8, 1980

Keyes S R, Alfano J A, Jansson I and Cinti D L. Rat liver microsomal elongation of fatty acids. *Journal of Biological Chemistry*, 254, 7778-7784, 1979

Keyes S R, Francasso P M, Heimbrook D C, Rockwell S, Sligar S G and Sartorelli A C. Role of NADPH cytochrome C reductase and DT diaphorase in the biotransformation of mytomycin C. *Cancer Research*, 44, 5638-5643, 1984

Khan S and O'Brien P J. Molecular mechanisms of tirapazamine (SR4233, WIN 59072) induced hepatocyte toxicity under low oxygen concentrations. *British Journal of Cancer*, 71, 780-785, 1995

Kivisto K T, Fritz P, Linder A, Friedel G, Beaune P, and Kroemer H K. Immunohistochemical localization of cytochrome P450 3A in human

pulmonary carcinomas and normal bronchial tissue. *Histochemistry*, 103, 25-29, 1995

Klingenberg M. Pigments of rat liver microsomes. *Archives of Biochemistry and Biophysics*, 75, 376- 386, 1958

Knowles R G and Moncada S. Nitric oxide synthases in mammals. *Biochemical Journal*, 298, 249-258, 1994

Koch C J, Kruuv J, Frey H E and Snyder J. Plateau phase in growth induced by hypoxia. *International Journal of Radiation Biology*, 23, 67, 1973.

Kolstad P. Intercapillary distance, oxygen tension and local recurrence in cervix cancer. *Scand. J. Clin. Lab. Invest. Suppl.*, 106, 145-157, 1968

Lewis A D, Walker C, Morecroft I, Henderson C and Wolf C R. Role of human NADPH cytochrome P450 CYP 2B6 gene family in the metabolism of the anticancer bioreductive drug tirapazamine (SR 4233). *Proceedings of the American Association for Cancer Research*, 36, 602, 1995

Li A P, Kaminski D L and Rasmussen A. Substrates of human hepatic cytochrome P450 3A4. *Toxicology*, 104, 1-8, 1995

Lin A J, Cosby L A, Shansky C W and Sartorelli A. Potential bioreductive alkylating agents. 1. Benzoquinone derivatives. *Journal of Medicinal Chemistry*. 15, 1247-1252, 1972

Lindeke B, and Paulsen- Sorman U. III Nitrogenous compounds as ligands to haemoporphyrins- The concept of metabolic intermediary complexes. In vol 1: Biotransformation of organic nitrogen compounds. Karger Publ, Basel, 63-102, 1988

Masters B S S and Schacter B A. The catalysis of heme degradation by purified NADPH-cytochrome C reductase in the absence of other microsomal proteins. *Annals of Clinical Research*, 8, 18-27, 1976

Mc Clellan- Green P D, Linko P, Yeowell H N and Goldstein J A. Hormonal regulation of male specific rat hepatic cytochrome P450g (P450 11C 13) by androgens and the pituitary. *Journal of Biological Chemistry*, 264, 18960-18965, 1989

McKay J A, Murray G I, Weaver R J, Ewen S W B, Melvin W T. and M Danny Burke. Xenobiotic metabolising enzyme expression in colonic neoplasia. *Gut*, 34, 1234-1239, 1993

McKeown S R, Friery O P, McIntyre I A, Hejmadi M V, Patterson L H and Hirst D G. Evidence of therapeutic gain when AQ4N or tirapazamine is combined with radiation. *British Journal of Cancer (suppl XXVII)*, 1996

Mekhail- Ishak K, Hudson N, Tsao M S and Batist G. Implications for therapy of drug metabolising enzymes in human colon cancer. *Cancer Research*, 49, 4866-4869, 1989

Miles J S, Mc Laren A W, Forrester L M, Glancey M J, Lang M A and Wolf C R. Identification of the human liver cytochrome P450 responsible for coumarin 7-hydroxylase activity. *Biochemical Journal*, 267, 365-371, 1990

Mimura M, Baba T, Yamazaki Y, Ohmori S, Inui Y, Gonzalez F J, Guengerich F P and Shimada T. Characterization of cytochrome P450 2B6 in human liver microsomes. *Drug Metabolism and Disposition*, 21, 1048-1056, 1993

Miners J O, Coulter S, Tukey R H, Veronese M E and Birkett D J. Cytochromes P450 1A2, and 2C9 are responsible for human hepatic *O*-demethylation of R- and S- naproxen. *Biochemical Pharmacology*, 51, 1003-1008, 1996

Miners J O, Smith K J, Robson R A, Mc Manus M E, Veronese M E and Birkett D J. Tolbutamide hydroxylation by human liver microsomes. *Biochemical Pharmacology*, 37, 1137-1144, 1986

Montgomery J A. Chapter 1 in *Methods in Cancer Research*, XV1, (Eds De Vita V T and Busch H) Academic press, New York, San Francisco, London, 1979

Murphy B J, Laderoute K R, Short S M and Sutherland R M. The identification of haem oxygenase as a major stress protein in chinese hamster ovary cells. *British Journal of Cancer*, 64, 69-73, 1991

Murphy B J, Laderoute K R, Vreman H J, Grant D G, Gill S G, Stevenson D K and Sutherland R M. Enhancement of haem oxygenase expression and

activity in A431 squamous carcinoma multicellular tumour spheroids. Cancer Research, 53, 2700-2703, 1993

Murray G I, McKay J A, Weaver R J, Ewen S W B, Melvin W T. and M Danny Burke. Cytochrome P450 expression is a common molecular event in soft tissue sarcomas. Journal of Pathology, 171, 49-52, 1993

Murray G I, Taylor M C, Burke M D and Melvin W T. Enhanced expression of cytochrome P450 in stomach cancer. British Journal of Cancer, 77, 1040-1044, 1998

Murray G I, Taylor M C, McFadyen M C E, McKay J A, Greenlee W F, Burke M D and Melvin W T. Tumour specific expression of cytochrome P450 CYP 1B1. Cancer Research, 57, 3026-3031, 1997

Murray G I, Taylor V E, Mc Kay J A, Weaver R J, Ewen S W B, Melvin W T and Burke M D. Expression of xenobiotic metabolising enzymes in tumours of the urinary bladder. International Journal of Experimental Pathology, 76, 271-276, 1995

Murray G I, Taylor V E, Mc Kay J A, Weaver R J, Ewen S W B, Melvin W T and Burke M D. Immunological localisation of drug metabolising enzymes in prostate cancer. Journal of Pathology, 177, 147-152, 1995

Murray G I, Weaver R J, Paterson P J, Ewen S W B, Melvin W T. and M Danny Burke. Expression of xenobiotic metabolising enzymes in breast cancer. Journal of Pathology, 169, 347-353, 1993 ^a

Murray M and Reidy G F. Selectivity in the inhibition of mammalian cytochromes P450 by chemical agents. *Pharmacological Reviews*, 42, 85-100, 1990

Naylor M A. Novel *N*-oxides as bioreductive drugs. *Oncology Research* 6, 438-491, 1994

Nebert D W and Gonzalez F J. P450 genes: structure, evolution, and regulation. *Annual Reviews of Biochemistry*, 56, 945-993, 1987

Nedelcheva V and Gut I. P450 in rat and man: methods of investigation, substrate specificities and relevance to cancer. *Xenobiotica*, 24, 1151-1175, 1994

Nelson D W, Kamataki T, Waxman D J, Guengerich F P, Estabrook R W, Feyereisen R, Gonzalez F J, Coon M J, Gunsalus I C, Gotoh O, Okuda K and Nebert D W. The P450 superfamily: update on new sequences, gene mapping, accession numbers, early trivial names of enzymes, and nomenclature. *DNA and Cell Biology*, 12, 1-15, 1993

Nelson D W. Chapter in *Cytochrome P450, structure, mechanism and biochemistry* (2nd Edition) (Ed P R Ortiz de Montellano) Plenum Press New York and London, 1995

O'Dwyer P J, Yao K.S, Ford P, Godwin A K and Clayton M. Effect of hypoxia on detoxifying enzyme activity and expression in HT29 Colon adenocarcinoma cells. *Cancer Research*, 54, 3082-3087, 1994.

Omura T and Sato R. The carbon monoxide binding pigment of liver microsomes, I, Evidence for its hemoprotein nature. *Journal of Biological Chemistry*, 239, 2370-2378, 1964

Ono S, Hatanaka T, Hotta H, Satoh T, Gonzalez F J and Tsutsui M. Specificity of substrate and inhibitor probes for cytochrome P450s: evaluation of in vitro metabolism using c DNA- expressed human P450s and human liver microsomes. *Xenobiotica*, 26, 681-693, 1996

Paine A J. Current status review. The cytochrome P450 gene superfamily. *International Journal of Experimental Pathology*. 72, 349-363, 1991

Patterson A V, Barham H M, Chinje E C, Adams G E, Harris A L and Stratford I J. Importance of P450 reductase activity in determining sensitivity of breast tumour cells to the bioreductive drug, tirapazamine (SR4233). *British Journal of Cancer*, 72, 1144-1150, 1995

Patterson A V, Saunders M P, Chinje E C, Talbot D C, Harris A L and Stratford I J. Overexpression of human NADPH: cytochrome c (P450) reductase confers enhanced sensitivity to both tirapazamine (SR4233) and RSU 1069. *British Journal of Cancer*, 1338-1347, 1997

Patterson L H, Craven M R, Fisher G R and Teesdale- Spittle P. Aliphatic amine N-oxides of DNA binding agents as bioreductive drugs. *Oncology Research*, 6, 533-538, 1994

Patterson L H, Maine J E, Cairnes D C, Craven M R, Bennett N, Fisher G R, Ruparelia K and Giles Y. *N*-oxides of DNA affinic agents as bioreductively activated prodrugs. *Proceedings of The American Association for Cancer Research*. 33, 2571, 1992

Patterson L. H. Rationale for the use of aliphatic N-oxides of cytotoxic anthraquinones as prodrug DNA binding agents: a new class of bioreductive agent. *Cancer and metastasis reviews* 12, 119-134, 1993

Phillips R M. The bioreductive activation of a series of potential quinone based anticancer drugs by human DT diaphorase. 9th NCI- EORTC Symposium on new Drugs in Cancer Therapy. A 376, 1996

Porter T D, Beck T W and Kasper C B. NADPH cytochrome P450 oxidoreductase gene organisation correlates with structural domains of the protein. *Biochemistry*, 29, 9814-9818, 1990

Powers W E and Tolmach L J. Demonstration of an anoxic component in a mouse tumour cell population by *in vivo* assay of survival following irradiation. *Radiology*, 83, 328-336, 1964

Powis G and Wincent L. Pyridine nucleotide cofactor requirements of indicine *N*-oxide reduction by hepatic microsomal cytochrome P450. *Biochemical Pharmacology*, 29, 347-351, 1980

Pritsos C A and Gustafson D L. Xanthine dehydrogenase and its role in cancer chemotherapy. *Oncology Research*. 6, 477-481, 1994

Quattrochi, L C, Vu T and Tukey, R H. The human CYP 1A2 gene and induction by 3-methylcholanthrene. *The Journal of Biological Chemistry*, 269, 6949-6954, 1994

Ram P A and Waxman D J. Thyroid hormone stimulation of NADPH cytochrome P450 reductase expression in liver and extrahepatic tissue. *Journal of Biological Chemistry*, 267, 3294-3301, 1992

Rampling R, Cruickshank G, Lewis A D, Fitzsimmons S A and Workman P. Direct measurement of PO₂ subdistribution and bioreductive enzymes in human malignant brain tumours. *Proceedings of The Eighth International Conference on Chemical Modifiers of Cancer Treatment Part 2* (Eds Wasserman T, Siemann D and Sugahara T), 29, 3, 1993

Relling M V, Aoyama T, Gonzalez F J and Meyer U A. Tolbutamide and mephenytoin hydroxylation by human cytochrome P450s in the CYP 2C subfamily. *The Journal of Pharmacology and Experimental Therapeutics*, 442-446, 1990

Reska K, Hartley J A, Kolodziejczyk P and Lown J W. Interaction of the peroxidase- derived metabolite of mitoxantrone with nucleic acids; evidence for covalent binding of ^{14}C -labelled drug. *Biochemical Pharmacology*. 38, 4253-4260, 1989

Riley R J and Workman P. DT diaphorase and cancer chemotherapy. *Biochemical Pharmacology*. 8, 1657-1669, 1992 a

Riley R J and Workman P. Enzymology of the reduction of the potent benzotriazine-di-*N*-oxide hypoxic cell cytotoxin SR 4233 (WIN 59075) by NAD(P)H: (Quinone acceptor) oxidoreductase (EC 1.6.99.2) purified from Walker 256 rat tumour cells. *Biochemical Pharmacology*, 43, 167-174, 1992^b

Riveros- Moreno V, Hefferman B, Torres B, Chubb A, Charles I and Moncada S. Purification to homogeneity and characterisation of rat brain recombinant nitric oxide synthase. *European Journal of Biochemistry*, 230, 52-57, 1995

Rockwell P, Neufeld G, Glassman A, Caron D and Goldstein. *In vitro* neutralisation of vascular endothelial growth factor activation of flk-1 by monoclonal antibody. *Molecular Cell Differentiation*, 3, 91-100, 1995

Romkes M, Faletto M B, Blaisdell, J A, Raucy J L and Goldstein J A. Cloning and expression of complementary DNAs for members of the human cytochrome P450 11C subfamily. *Biochemistry* 30, 3247-3255, 1991

Ross D, Siegal D, Beall H, Prakash A S, Mulcahy R T M and Gibson N W. DT- diaphorase in activation and detoxification of quinones. *Cancer and Metastasis Reviews*, 12, 83-101, 1993.

Ryan D E, Ramanathan L, Iida S, Thomas P E, Haniu M, Shively J E, Lieber L S and Levin W. Characterisation of the major form of rat hepatic microsomal cytochrome P450 induced by isoniazid. *Journal of Biological Chemistry*, 260, 6385-6393, 1985

Ryan D E, Thomas P E, Korzeniowski D and Levin W. Separation and characterisation of highly purified forms of liver microsomal cytochrome P450 from rats treated with polychlorinated biphenyls, phenobarbital and 3-methylcholanthrene. *Journal of Biological Chemistry*, 254, 1365-1374, 1979

Rygaard K and Spang- Thomsen M. Quantitation and Gompertzian analysis of tumour growth. *Breast cancer research and treatment*, 46, 303-312, 1997

Sartorelli A C, Belcourt M F, Hodnick W F, Keyes S R, Pritsos C A and Rockwell S. Preferential kill of hypoxic EMT6 mammary tumour cells by the bioreductive alkylating agent porfiromycin. *Advances in Enzyme Regulation*, 35, 117-130, 1995.

Sartorelli A.C. The role of mitomycin antibiotics in the chemotherapy of solid tumours. *Biochemical Pharmacology*, 35, 67-69, 1986.

Schacter B A, Nelson E B, Marver H S and Masters BSS. Immunochemical evidence for an association of haem oxygenase with the microsomal

electron transport system. Journal of Biological Chemistry, 247, 3601-3607, 1972

Schacter B A. Haem catabolism by haem oxygenase: physiology, regulation, and mechanism of action. Seminars in hematology, 25, 349-369, 1988

Schmider J, Greenblat D J, Von Moltke L L, Harmatz J S and Shader R I. N-demethylation of Amitriptyline *in vitro*: Role of cytochrome P450 3A (CYP 3A) isoforms and effect of metabolic inhibitors. The Journal of Pharmacology and Experimental Therapeutics, 275, 592-597, 1995

Schmidt H H H W, Lohmann M and Walter U. The nitric oxide and cGMP signal transduction system: regulation and mechanism of action. Biochimica et Biophysica Acta, 1178, 153-175, 1993

Schor N A and Cornelisse C- J. Biochemical and quantitative histochemical study of reduced pyridine nucleotide dehydrogenation by human colonic carcinomas. Cancer Research, 43, 4850-4855, 1983

Seetharam L, Gotoh N, Maru Y, Neufeld G, Yamaguchi S and Shibuya M. A unique signal transduction cascade from flt tyrosine kinase, a receptor for vascular endothelial growth factor VEGF. Oncogene, 10, 135-147, 1995

Sequeira D J and Strobel H W. in vitro metabolism of imipramine by brain microsomes: Effects of inhibitors and exogenous cytochrome P450 reductase. Brain Research, 738, 24-31, 1996

Siim B G, Menke D R, Dorie M J and Brown J M. Tirapazamine induced cytotoxicity and DNA damage in transplanted tumours: relationship to tumour hypoxia. *Cancer Research*, 57, 2922-2928, 1997

Smith D A, Ackland M J and Jones B C. Properties of cytochrome P450 isoenzymes and their substrates Part 1: active site characteristics. *Drug discovery today*, 2, 406-414, 1997a

Smith D A, Ackland M J and Jones B C. Properties of cytochrome P450 isoenzymes and their substrates Part 2: properties of cytochrome P450 substrates. *Drug discovery today*, 2, 479-485, 1997b

Smith G, Harrison D J, East N, Rae F, Wolf H, and Wolf C R. Regulation of cytochrome P450 gene expression in human colon and breast tumour xenografts. *British Journal of Cancer*, 68, 57-63, 1993

Smith P J, Desnoyers R, Blunt N, Giles Y, Patterson L H and Watson J V. Flow cytometric analysis and confocal imaging of anticancer alkylaminoanthraquinones and their *N*-oxides in intact human cells using 647- nm krypton laser excitation. *Cytometry*, 27, 43-53, 1997

Soucek P and Gut I. P450 in rat : structure, functions, properties and relevant human forms. *Xenobiotica*, 22, 83-103, 1992

Spatzenegger M and Jaeger W. Clinical importance of hepatic cytochrome P450 in drug metabolism. *Drug Metabolism Reviews*, 27, 397-417, 1995

Sundseth S S and Waxman D J. Sex- dependent expression and clofibrate inducibility of cytochrome P450 4A fatty acid omega-hydroxylases. Journal of Biological Chemistry, 267, 3915-3921, 1992

Sutherland R M and Franko A J. On the nature of the radiobiologically hypoxic fraction in human tumours. International Journal of Radiation Oncology Biology Physics, 6, 117-120, 1980

Tancock I F and Hill R P. The Basic Science of Oncology (1st Ed), 1987.

Thomlinson R H and Gray L H. The histological structures of some human lung cancers and the possible implications for radiotherapy. British Journal of Cancer, 9, 539-549, 1955

Thomsen L L, Miles D W, Happerfield, Bobrow L G, Knowles R G and Moncada S. Nitric oxide synthase in human breast cancer. 72, 41-44, 1995

Traganos F, Evenson D P, Staiano- Coico L, Darzynkiewicz Z and Melamed M R. Action of dihydroxyanthraquinone on cell cycle progression of a variety of cultured mammalian cells. Cancer Research. 40, 672-681, 1980

Vaupel P, Kallinowski F, and Okunieff P. Blood flow, oxygen supply and metabolic microenvironment of human tumours: a reveiw Cancer research 49, 6449-6465, 1989

Wacher V J, Wu C Y and Benet L Z. Overlapping substrate specificities and tissue distribution of cytochrome P450 3A and P- Glycoprotein: Implications

for drug delivery and activity in cancer chemotherapy. *Molecular Carcinogenesis*, 13, 129-134, 1995

Walton M I and Workman P. Enzymology of the reductive bioactivation of SR 4233: A novel benzotriazine di-*N*-oxide. *Biochemical Pharmacology*, 39, 1735-1742, 1990

Walton M I, Hoban P R, Robson C N, Workman P, Harris A L and Hickson I D. Mytomycin C resistance: Association with decreased NADPH cytochrome P450 reductase activity in chinese hamster ovary (CHO) cells *in vitro*. *British Journal of Cancer*, 60, 474- , 1989

Walton M I, Wolf C R and Workman P. The role of cytochrome P450 and cytochrome P450 reductase in the bioactivation of the novel benzotriazine Di-*N*-oxide hypoxic cytotoxin 3-amino-1,2,4-benzotriazine-1,4-dioxide (SR 4233, WIN 59075) by mouse liver. *Biochemical Pharmacology*, 44, 251-259, 1992

Wang J, Stuehr D J, Ikeda- Saito M and Rousseau D L. Haem coordination and structure of the catalytic site in nitric oxide synthase. *The Journal of Biological Chemistry*, 268, 22255-22258, 1993

Weaver R J, Thompson S, Smith G, Dickins M, Elcombe C R, Mayer R T and M Danny Burke. A comparative study of constitutive and induced alkoxyresorufin O-dealkylation and individual cytochrome P450 forms in cynomolgus monkey (*Macaca fascicularis*), human, mouse, rat and hamster liver microsomes. *Biochemical Pharmacology*, 47, 763-773, 1994

Weber G, Jacson R C, Williams J C, Goulding F J and Eberts T J. Enzymatic markers of neoplastic transformation and regulation of purine and pyrimidine metabolism. *Advances in Enzyme Regulation*. 15, 53- 7, 1977

Weber G, Kizaki H, Tzeng D, Shiotani T and Olah E. Colon tumour: enzymology of the neoplastic program. *Life Sciences*. 23, 729-736, 1978

Wendling P, Manz R, Thews G, and Vaupel P. Inhomogeneous oxygenation of rectal carcinomas in humans. A critical parameter for preoperative irradiation ? *Adv. Exp. Med. Biol.*, 180, 293-300, 1984

White K A and Marletta M A. Nitric oxide synthase is a cytochrome P450 type haemoprotein. *Biochemistry*, 31, 6627-6631, 1992

Wilks A and Ortiz de Montellano P R. Rat liver haem oxygenase: High level expression of a truncated soluble form and nature of the meso-hydroxylating species. *The Journal of Biological Chemistry*, 268, 22357-22362, 1993

Wilson W R, Denny W A, Pullen S M, Thompson K M, Li A E, Patterson L H and Lee H H. Tertiary amine N-oxides as bioreductive drugs: DACA N-oxide, nitracine N-oxide and AQ4N. *British Journal of Cancer*. 73 (Suppl XXII), 1996

Wiseman L R and Spencer C M. Mitoxantrone: A review of its pharmacology and clinical efficacy in the management of hormone resistant advanced prostate cancer. *Drugs and Ageing*. 10, 473-485, 1997

Wolpert M K, Althaus J R and Johns D G. Nitroreductase activity of mammalian liver aldehyde oxidase. *The Journal of Pharmacology and Experimental Therapeutics*, 185, 202-213, 1973

Woodrooffe A J M, Bayliss M K and Park G R. The Effects of hypoxia on drug metabolising enzymes. *Drug Metabolism Reviews*, 27, 471-495, 1995

Workman P and Walton M I. Enzyme-directed bioreductive drug development. *Selective Activation of Drugs by Redox Processes* (Eds Adams G E, Breccia A, Wardman P and Fielden E M), 173-191, Plenum Press, New York, 1990

Workman P, Walton M I, Powis G and Schlager JJ. DT diaphorase: questionable role in mytomycin resistance, but a target for novel bioreductive drugs. *British Journal of Cancer*, 60, 800-802, 1989

Workman P. Bioreductive mechanisms. *International Journal of Radiation Oncology Biology Physics*, 22, 631-637, 1992

Yang C S, Yoo J S, Ishizaki H and Hang J. Cytochrome P450 2E1: Roles in nitrosamine metabolism and mechanism of regulation. *Drug metabolism Reviews*, 22, 147-159, 1990

Yoo J S, Guengerich F P and Yang C S. Metabolism of *N*-nitrosodiakylamines by human liver microsomes. *Cancer Research*, 88, 1499-1505, 1988

Yoshinaga T, Sassa S and Kappas A. A comparative study of heme degradation by NADPH cytochrome c reductase alone and by the complete heme oxygenase system. *Journal of Biological Chemistry*, 257, 7794-7802, 1982

Zeman E M, Brown J, M, Lemmon M, J, Hirst V K and Lee W W. SR 4233: a new bioreductive agent with high selective toxicity for hypoxic mammalian cells. *International Journal of Radiation Oncology, Biology and Physics*, 12, 1239-1242, 1986

Publications

Papers

Patterson, L H and **Raleigh, S M**. Reductive metabolism: Application to prodrug activation. Chapter in 'Drug metabolism towards the next millennium', Gooderham N, Jenner P and Patterson LH (Edt). IOS press. 1998

Raleigh S M, Wanogho E, Burke M D, McKeown S R and Patterson L H. Involvement of human hepatic cytochromes P450 (CYP's) in the reductive metabolism of AQ4N, a novel anthraquinone based antineoplastic prodrug. Accepted for publication in: International Journal of Radiation Oncology Biology and Physics, 1998.

Abstracts

Raleigh S M, Murray M M, Robson T, Gallagher R, McKeown S and Patterson L H. Involvement of human and murine tumour cytochromes P450 (CYPs) in the bioreduction of AQ4N. Accepted for publication in: Annals of Oncology, 1998.

Raleigh S M, Burke M D, Murray G I and Patterson L H. Involvement of renal cell carcinoma cytochrome P450 in the metabolism of AQ4N, a hypoxia activated topoisomerase II inhibitor. Published in Annals of Oncology 7, (suppl 1), 1996 .

Raleigh S M, Tien P and Patterson L H. Involvement of haem and cytochrome P450 reductase in the bioreduction of the anthraquinone di N-oxide AQ4N. Published in Proceedings of the American Association of Cancer Res, 36, abstract no 3584, 1995.

Cole S, Patterson L H, Williams C A, Bowler, J D, Townsend K M S, Hacker, T M, **Raleigh S M** and Stratford I J. The activity of AQ4N, a novel bioreductively activated cytotoxin against KHT, RIF- 1 and SCCV11 murine tumours. Published in British Journal of Cancer, 71, (suppl XX1V), 20, 1995

Presentations

Raleigh S M, Murray M M, Robson T, Gallagher R, McKeown S and Patterson L H. Involvement of human and murine tumour cytochromes P450 (CYPs) in the bioreduction of AQ4N. To be presented at the 10th NCI-EORTC Symposium on New Drugs in Cancer Therapy, Amsterdam, The Netherlands, June, 1998.

Raleigh S M, Wanogho E, Burke M D, McKeown S R and Patterson L H. Involvement of human hepatic cytochromes P450 (CYP's) in the reductive metabolism of AQ4N, a novel anthraquinone based antineoplastic prodrug. Oral communication at the 10th International Conference on Chemical Modifiers of Cancer Treatment. Clearwater, Florida, USA, January 1998.

Raleigh S M, Burke M D, Murray G I and Patterson L H. Involvement of renal cell carcinoma cytochrome P450 in the metabolism of AQ4N, a hypoxia activated topoisomerase II inhibitor. Poster presentation given at the 9 th EORTC Symposium on New Drugs in Cancer Therapy, Amsterdam, The Netherlands, March, 1996.

Raleigh S M, Tien P and Patterson L H. Involvement of haem and cytochrome P450 reductase in the bioreduction of the anthraquinone di N-oxide AQ4N. Poster presentation at the 86th Annual meeting of the American Association for Cancer Research, Toronto, Canada, March, 1995.

Cole S, Patterson L H, Williams C A, Bowler J D, Townsend K M S, Hacker, T M, **Raleigh S M** and Stratford I J. The activity of AQ4N, a novel bioreductively activated cytotoxin against KHT, RIF- 1 and SCCV11 murine tumours. Poster presentation at the British Association of Cancer Research, Nottingham, April, 1995.